

©Copyright 1998

Virginia Polytechnic Institute & State University

All Rights Reserved

A Numerical Model of a Microwave Heated Fluidized Bed

by

Florent P. Faucher, B.S.

Thesis submitted to the Faculty of the
Virginia Polytechnic Institute and State University
in partial fulfillment of the requirements for the degree of

Master of Science

in

Mechanical Engineering

APPROVED:

Dr. James R. Thomas Jr., Chairman

Dr. William A. Davis

Dr. Curtis H. Stern

11 December, 1998
Blacksburg, Virginia

A Numerical Model of a Microwave Heated Fluidized Bed

Florent P. Faucher, M.S.

Virginia Polytechnic Institute and State University, 1998

Advisor: J.R. Thomas Jr.

ABSTRACT

This thesis proposes a model for a microwave heated fluidized bed by ceramic catalyst pellets to highlight the possibility to obtain a temperature gradient between the gas and the pellets. After a review of the recent work on microwave effects on chemical reactions, a short description of the fluidization is given for a better understanding of the phenomena, followed by a development of a model of the heat transfer processes taking place in the fluidized bed. A parameter study describes the trends that should be expected despite the numerous restrictions and assumptions. Also, a set of parameters is proposed for optimal conditions that are close to the real conditions often encountered in practice. Numerous figures and tables are added, completing the main argument advanced in this thesis: it is possible to obtain a temperature difference between the gas and the pellets of a chemical bed reactor heated by microwaves by carefully choosing the following parameters: pellet diameter, bed height, gas velocity, pellet density and electric field.

Acknowledgments

This Master's degree research was conducted at Virginia Polytechnic Institute & State University in the Mechanical Engineering Department. I would like to express my gratitude to my advisor, Dr. James R. Thomas Jr., for his confidence, patience and assistance in the difficult aspects of this project. I would like to thank Dr. J.R. Mahan and Mrs. Jaffrin, that made possible the exchange program between Virginia Tech and Université de Technologie de Compiègne (France). I would like to thank Dr. C.H. Stern and Dr. W.A. Davis for serving on my committee. I am very grateful to my family for its help and encouragement during my studies. I would like to thank the National Science Foundation and Electric Power Research Institute whose funding supported this work.

FLORENT P. FAUCHER

Virginia Polytechnic Institute and State University

December 1998

Contents

Abstract	iii
Acknowledgments	iv
List of Tables	ix
List of Figures	xi
Chapter 1 Introduction	1
1.1 Prelude	1
1.2 Selective Heating Hypothesis	2
1.3 Objectives	3
1.4 The Numerical Model	4
Chapter 2 Literature Review	6
2.1 Enhanced Catalytic Reactions	6
2.1.1 The Thermal Activation of Microwave Radiation	6
2.1.2 Microscopic and Non-thermal Interaction of Microwave Radiation	7
2.2 Electromagnetism Review	9
2.2.1 The Electromagnetic Waves	9
2.2.2 The electric field intensity and the current density	10
2.2.3 The Permittivity	10
2.2.4 The Permeability	10
2.2.5 The Electrical Conductivity	11
2.2.6 The Waveguide	11
2.2.7 The Microwave Applicator	12

2.3	Material Interaction With Microwaves	12
2.3.1	The Dielectric Materials	12
2.3.2	The Polarization	13
2.3.3	The Metallic Catalyst Particles	13
2.4	Fluidization	15
2.4.1	The Geldart Classification	18
2.4.2	The Various Fluidization Types	20
2.4.3	More on Fluidization	23
2.5	Heat Transfer Mechanisms in a Fluidized Bed	23
Chapter 3 Heat Transfer Modeling		28
3.1	Heat Generation	29
3.2	The Convection Inside The Bed	29
3.3	Energy Equations for the Gaseous and Solid Phases	32
3.3.1	The Gaseous Phase Differential Equation	32
3.3.2	The Solid Equation	33
3.4	The Temperature Distribution Inside a Pellet	34
3.5	Description of the FORTRAN Program	37
3.5.1	The Coupled Differential Equations	37
3.5.2	The Pellet Temperature Distribution	37
Chapter 4 Study of the Parameters		39
4.1	Influence of the Nature of Aluminum Oxide.	42
4.2	Influence of the Pellet Diameter.	45
4.3	Influence of the Gas Velocity.	50
4.4	Influence of the Pellet Density	54
4.5	Influence of the Pulsation of the Electrical Field	57
4.5.1	Influence on the Heat Generation	57
4.5.2	Influence of the Period Length	60
4.5.3	Influence of the Duty Cycle	63
4.6	Comparison of the Temperature Rise for Different Heights of Pellets in the Fluidized Bed.	70

Chapter 5 Design of an Optimized Fluidized Bed	74
5.1 Constant Electric Field with Respect to the Axial Direction	75
5.2 Constant Pellet Temperature Through the Bed	77
5.3 A Compromise Between Two Requirements	79
Chapter 6 Conclusions and Recommendations	81
6.1 Conclusions	81
6.2 Limitations and recommendations	83
Bibliography	84
Appendix A Thermophysical Properties	89
A.1 Gas Mixture Formulae	90
A.2 Thermal Conductivities	90
A.2.1 Alumina	90
A.2.2 Butane	91
A.2.3 Helium	92
A.2.4 Platinum	92
A.3 Heat Capacities	93
A.3.1 Alumina	93
A.3.2 Butane	93
A.3.3 Helium	94
A.3.4 Platinum	94
A.4 Dynamic Viscosities	95
A.4.1 Butane	95
A.4.2 Helium	95
A.5 Electric and dielectric properties	96
A.5.1 Electrical Conductivity of Bulk Platinum	96
A.5.2 Dielectric Loss	97
A.5.3 Dielectric Constant	98
Appendix B Fortran code	99
B.1 Subroutine and Variable Description	99

B.2	Parameter File	104
B.3	Subroutines	105
B.4	Main Programs	124
B.4.1	Version One	124
B.4.2	Version Two	127
B.4.3	Version Three	131
Vita		149

List of Tables

4.1	Representative values for the heat generation within 3.3mm pellets: effect of the steady and uniform electromagnetic field on ΔT , T_{pel} and T_{gas} for α - and γ -alumina without metallic catalyst particles.	43
4.2	Effect of the pellet diameter at the minimum fluidization velocity on ΔT , for 700 kg/m ³ pellets. The electric field strength is set such that $T_{\text{pel}}= 300^{\circ}\text{C}$ at the exit of the one inch bed.	49
4.3	Effect of the gas velocity on ΔT for 0.5mm pellets . The electric field strength is set such that $T_{\text{pel}}= 300^{\circ}\text{C}$ at the exit of the one inch bed.	53
4.4	Effect of the gas velocity on ΔT for 3.3mm pellets. The electric field strength is set such that $T_{\text{pel}}= 300^{\circ}\text{C}$ at the exit of the one inch bed.	53
4.5	Effect of the pellet density at the minimum fluidization velocity, and for 0.5mm pellets, on ΔT . The electric field strength is set such that $T_{\text{pel}}= 300^{\circ}\text{C}$ at the exit of the one inch bed.	56
4.6	Effect of the pellet density at the minimum fluidization velocity, and for 3.3mm pellets, on ΔT . The electric field strength is set such that $T_{\text{pel}}= 300^{\circ}\text{C}$ at the exit of the one inch bed.	56
4.7	Effect of the pellet density, using the minimum fluidization velocity for the 3.3mm, 3200 kg/m ³ pellets (2.12 m/s), on ΔT . The electric field strength is set at 52095 V/m.	56
4.8	Effect of the steady electric field strength on the steady-state gas temperature and pellet temperature at $x=1$, for γ -alumina.	58
4.9	Effect of the pulsed electric field strength on the steady-state gas temperature and pellet temperature, for a duty cycle of 0.5.	58

4.10	Ratio of the temperature difference between the gas and the pellets for a steady electromagnetic field to the temperature difference between the gas and the pellets for a pulsed electromagnetic field	59
4.11	Effect of the bed height on ΔT for 0.5mm pellets. The electric field strength is set such that the pellets located at the exit have a temperature of $T_{pel} = 300^{\circ}\text{C}$	73
4.12	Effect of the bed height on ΔT for 3.3mm pellets. The electric field strength is set such that the pellets located at the exit have a temperature of $T_{pel} = 300^{\circ}\text{C}$	73
5.1	Effect of the particle diameter, the bed height, the gas velocity and the electric field strength on ΔT , for a constant electric field with respect to the axial direction, such that $T_{pel} = 300^{\circ}\text{C}$ at the exit of the bed. The 0.5mm pellets belong to the group B of the Geldart classification whereas the 1.4 and 2.3mm pellets belong to the group D.	76
5.2	Effect of the particle diameter, the bed height, the gas velocity and the electric field strength on ΔT , for a varying electric field such that $T_{pel} = 300^{\circ}\text{C}$ at any location. The 0.5mm pellets belong to the group B of the Geldart classification whereas the 1.4 and 2.3mm pellets belong to the group D.	78
5.3	Effect of the particle diameter, the bed height, the gas velocity and the electric field strength on ΔT , for a pellet temperature rising constantly through the bed (300°C to 350°C). The 0.5mm pellets belong to the group B of the Geldart classification whereas the 1.4 and 2.3mm pellets belong to the group D.	80
A.1	Thermal Conductivity of Aluminum Oxide (59)	90
A.2	Thermal Conductivity of Butane	91
A.3	Thermal Conductivity of Helium (60)	92
A.4	Thermal Conductivity of Platinum (59)	92
A.5	Heat Capacity of Aluminum Oxide (59)	93
A.6	Heat Capacity of Platinum (59)	94
A.7	Dynamic Viscosity of Butane	95
A.8	Dynamic Viscosity of Helium (60)	95
A.9	Dielectric loss of α -alumina (63)	97
A.10	Dielectric loss of γ -alumina (63)	97
A.11	Dielectric constant of γ -alumina (65)	98

List of Figures

1.1	Illustration of a fluidized bed, a ceramic pellet and a catalyst particle.	5
2.1	Effect of the pellet diameter and the pellet density on the minimum fluidization velocity	17
3.1	Comparison of correlations for the Nusselt number. The correlations used for our problem are the Kothari formula, for Reynolds number between 0.1 and 100 and the formula adapted from Ranz, for Reynolds number bigger 100.	31
4.1	Effect of the particle diameter on the convection coefficient, calculated for each particle diameter at the minimum fluidization velocity, as a function of the particle diameter, and at three temperatures.	40
4.2	Ratio, for each particle diameter, of the gas velocity necessary to reach a Reynolds number of 0.1 to the minimum fluidization velocity calculated at this pellet diameter.	40
4.3	Effect of a steady electromagnetic field on steady-state ΔT for γ -alumina. The dashed line represents the pellets with a 5% mass fraction in Pt, whereas the solid line represents the pellets without any Pt.	43
4.4	Effect of the presence of metallic particles of Pt on ΔT for α -alumina ceramic support and for various platinum mass fractions.	44
4.5	Effect of the pellet diameter on the gas and on the pellet temperatures. For each plot, the upper curve is the pellet temperature and the lower curve is the gas temperature.	47
4.6	The dashed line represents the fluidization velocity calculated by the approximation and the solid line the fluidization velocity calculated by the quadratic equation.	48

4.7 Effect of the gas velocity on the gas and on the pellet temperatures for 3.3mm pellets. For each plot, the upper curve is the pellet temperature and the lower curve is the gas temperature. 52

4.8 Effect of the pellet density on the gas and on the pellet temperatures for 3.3mm pellets. For each plot, the upper curve is the pellet temperature, the lower curve is the gas temperature, and the gas velocity is equal to the minimum fluidization velocity corresponding to the pellet diameter and pellet density. 55

4.9 Effect of pulsing on the steady-state temperature differences between the gas and the pellets at $x=1$. For the pulsed case, the duty cycle has a value of 0.5. The right hand side figure is the ratio of the temperature difference between the gas and the pellets for a steady electromagnetic field to the temperature difference between the gas and the pellets for a pulsed electromagnetic field. 59

4.10 Effect of the period of the pulsations on the gas and on the pellet temperatures. For each plot, the upper curve is the pellet temperature, and the lower curve is the gas temperature. The duty cycle is 0.5, while the electric field has a value of 54550 V/m. 61

4.11 This plot shows how a steady electric field can achieve a ΔT equal to the pulsed electric field case. $E_{rms} = 3.806 \cdot 10^4$ V/m. The upper curve of this plot is the pellet temperature and the lower one is the gas temperature. This comparison is made with the upper left hand side plot of figure 4.5.2. 62

4.12 Effect of the duty cycle value on the gas temperature and on the pellet temperature. The period of the pulsation is one second and $E_{rms} = 6 \cdot 10^4$ V/m. 64

4.13 The left side of this figure shows a electric field varying by means of a third order polynomial, $E(z) = 3.75 \cdot 10^4(-0.1x^3 + 1.15x^2 - 2x + 1)$ V/m, with the temperature profile of the gas and the pellet above. On the right side, the electric field is uniform, yielding almost constantly rising gas and pellet temperature. $E_{rms} = 3.75 \cdot 10^4$ V/m. 66

4.14 Gas and pellet temperature profiles, with their respective electric field underneath, for a one-inch bed (right hand side) and for a five-inch bed (left hand side). For the temperature profiles, the pellet temperature is the upper curve and the gas temperature is the lower curve. For the two cases, $d_p = 3.3$ mm and $v_g = u_{mf}$ 67

4.15 Gas and pellet temperatures for a few shapes. For each plot, the pellet temperature is the upper curve and the gas temperature is the lower curve. 68

4.16	These electric field give the temperature profiles of figure 4.5.3.	69
4.17	Effect of the bed height on the temperature profiles. For each plot, the pellet temperature is the upper curve and the gas temperature is the lower curve. $E_{\text{rms}} = 2.5 \cdot 10^4$ V/m.	71
4.18	Effect of the bed height on the steady-state temperature rise of the pellets and of the gas, as a function of time. $E_{\text{rms}} = 2.5 \cdot 10^4$ V/m.	72

Nomenclature

a	Factor used for convection coefficient expression
Ar	Archimedes number
b	Factor used for ΔT expression
\vec{B}	Magnetic flux density (Wb/m ²)
c	Speed of light in a given medium (m/s)
C_{pg}	Gas heat capacity (J/kg.m ³)
C_{ps}	Solid heat capacity (J/kg.m ³)
\vec{D}	Electric flux density (C/m ²)
D	Bed diameter (m)
d_b	Effective bubble diameter (m)
d_{bm}	Maximum bubble diameter (m)
d_{b0}	Bubble diameter just above the distributor (m)
d_p	Pellet diameter (m)
d_{par}	Metallic particle diameter (m)
d_{sph}	Equivalent pellet diameter (m)
\vec{E}	Electric field (V/m)
E_0	Electric field outside a pellet (V/m)
E_2	Electric field inside a pellet (V/m)
\dot{E}_{gen}	Energy generated within a control volume (W/m ³)
\dot{E}_{in}	Energy entering a control volume (W/m ³)
\dot{E}_{out}	Energy leaving a control volume (W/m ³)
\dot{E}_{st}	Energy stored within a control volume (W/m ³)
E_{rms}	Root-mean-square electric field (V/m)
$\overline{E_{rms}}$	Average root-mean-square electric field through the bed (V/m)
f	Electromagnetic wave frequency (hz)
Fe	Federov number
g	Acceleration of gravity (m/s ²)
h	Overall convection coefficient (W/m ² .°C)
H_{bc}	Heat transfer coefficient between bubble and cloud (W/m ³ bubble.°C)
h_{bc}	Heat transfer coefficient between bubble and cloud (W/m ² .°C)

H_{total}	Total volumetric heat transfer coefficient between gas and bed ($\text{W}/\text{m}^2\cdot^\circ\text{C}$)
\vec{H}	Magnetic field intensity (A/m)
\vec{J}	Conduction current density (A/m^2)
L	Height of pellets (m)
L_{mf}	Height of pellets at the minimum fluidization (m)
L_{fb}	Height of pellets of a fixed bed (m)
l_{or}	Space, in a perforated plate, between adjacent holes (m^2)
N_{or}	Number of orifice per unit area (m^{-2})
N'_{or}	Fictitious orifice spacing corresponding to touching bubbles (m^{-2})
Nu	Nusselt number accounting for the particle mixing and the gas convection
Nu^*	Nusselt number evaluated for a single particle in cross flow
$P_{0.5}$	Power generated by an electromagnetic field with a duty cycle value of 0.5 (W)
P_1	Power generated by a steady electromagnetic field (W)
Pr	Prandtl number
$\dot{q}, \dot{q}(t)$	Heat generation per unit volume (W/m^3)
R	Overall resistance to heat transfer ($^\circ\text{C}\cdot\text{m}^2/\text{W}$)
$R_{g.c.}$	Resistance to heat transfer due to gas convection ($^\circ\text{C}\cdot\text{m}^2/\text{W}$)
$R_{p.c.}$	Resistance to heat transfer due to mixing ($^\circ\text{C}\cdot\text{m}^2/\text{W}$)
Re_p	Reynolds number
t	Time (sec)
t_p	Pulsation time (sec)
t_r	Rest time (sec)
T_0	Base temperature ($^\circ\text{C}$)
T_g	Gas temperature ($^\circ\text{C}$)
T_p	Pellets temperature ($^\circ\text{C}$)
u_{br}	Bubble rise velocity (m/s)
u_{mb}	Minimum bubbling velocity (m/s)
u_{mf}	Minimum fluidization velocity (m/s)
u_{ms}	Minimum slugging velocity (m/s)
v	Electromagnetic wave frequency (Hz)
V	Volume of a pellet (m^3)

v	Volumetric flow rate of gas (m^3/s)
v_g, u_0	Inlet gas velocity, or superficial velocity (m/s)
v_{or}	Volumetric flow rate from an orifice
x	Nondimensionalized axial direction
z	Axial direction (m)
z_{max}	Freeboard height of the fluidized bed (m)
α	Resistivity coefficient ($^{\circ}\text{C}^{-1}$)
α_p	Ratio of effective diameter of the wake to diameter of the bubble
ΔT	Average steady-state temperature difference between the gas and the pellets through the bed ($^{\circ}\text{C}$)
ΔT_{exit}	Steady-state temperature difference between the gas and the pellets at the exit ($^{\circ}\text{C}$)
ϵ	Porosity or void fraction or voidage
ϵ_0	Permittivity of free space (F/m)
ϵ_1	Complex electrical permittivity of Al_2O_5
ϵ_2	Complex electrical permittivity of Pt
ϵ_e	Voidage in the emulsion phase
ϵ_f	Averall voidage in a fluidized bed
ϵ_m	Complex electrical permittivity of a mixture Al_2O_5 -Pt
ϵ_m''	Electrical permittivity of a mixture Al_2O_5 -Pt
ϵ_{mf}	Voidage at the minimum fluidization
ϵ_{mr}	Relative complex electrical permittivity of a mixture Al_2O_5 -Pt
ϵ_{mr}''	Relative electrical permittivity of a mixture Al_2O_5 -Pt
ϵ'	Dielectric constant (F/m)
ϵ''	Dielectric loss (F/m)
ϵ_r'	Relative dielectric constant
ϵ_r''	Relative dielectric loss
γ_b	Volume of solids dispersed in bubbles divided by the volume of bubbles
δ	Bubble fraction in a fluidized bed
η_h	Heat transfer efficiency factor
λ	Wavelength (m)
λ_g	Gas conductivity ($\text{W}/\text{m}\cdot^{\circ}\text{C}$)
μ	Gas viscosity ($\text{Pa}\cdot\text{s}$)

μ	Complex magnetic permeability (H/m)
μ'	Real magnetic permeability (H/m)
μ''	Magnetic loss (H/m)
ϕ_s	Sphericity coefficient
Φ	Volume fraction of the platinum spherical particles in the pellet
ρ_0	Resistivity of platinum (m/S)
ρ_g	Gas density (kg/m ³)
ρ_s	Pellet density (kg/m ³)
σ_b	Bulk electrical conductivity of platinum (S/m)
σ_{eff}	Effective electrical conductivity of the platinum particles (S/m)
σ_0	Bulk electrical conductivity of the platinum at 20°C (S/m)
σ_2	Effective electrical conductivity of the platinum (S/m)
ω	Angular frequency of the electromagnetic waves (rotation/sec)
Ω	Surface area of the bed section (m ²)

Chapter 1

Introduction

1.1 Prelude

Heating by microwaves provides several advantages for promoting chemical reactions: the energy is brought directly into the matter, the losses are diminished noticeably while the processing times are reduced by the disappearance of the classical intermediate steps (heat exchangers, combustion devices). Thus, the microwave heating is sometimes seen as an alternative to classical heating, and has been also used for freeze-drying and sterilizing.

From another point of view, the simple fact that most organic chemicals do not absorb microwaves appreciably has led scientists to use suitable materials that strongly absorb the microwave radiation, are able to transfer the energy to the reactants adsorbed on the surface of the material and thus initiate the chemical reactions. At a recent conference, Wan and Depew (1) summarized well the advantages of using microwaves in the catalytic chemical reactions: the primary step of a catalytic chemical reaction usually consists of a bond-breaking requiring a high temperature. Unfortunately, back and side reactions occur almost simultaneously and require the use of high mass flow rate to avoid this phenomenon, which gives a low efficiency to the chemical reaction. Therefore, the application of microwave energy in short pulses should increase the selectivity and the efficiency.

Consequently, after several researchers reported enhanced chemical reactions by using microwave heating, in comparison with the classical methods, many conjectures were proposed to describe the local phenomena. However, there is a lack of understanding at the microscopic level, mainly because of the difficulty of performing physical measurements (temperatures, electromag-

netic fields).

Because of these uncertainties, two *a priori* incompatible concepts were developed: the presence of “thermal effects” which are the consequence, for instance, of temperature or pressure increases in the chemical reactor. The thermal effect designation also includes some heat generation effects due to an electromagnetic field, like the local concentrations of electromagnetic field, which give birth to local “hot spots”, with a size of a nanometer order of magnitude. Basically, this theory assumes that the microwaves contribution resides only in heating and eventually in increasing of the efficiency without acting on the molecules, electrons and so forth.

On the contrary, the “non-thermal” effects concept suggests particular phenomena specific to microwaves. For instance, some explanations have advanced the possibility of the microwave field coupling with the desired molecules and thus altering their rotations, leading to increased yield. However, these explanations were disputed by Stuerger and Gaillard (2) who argued the implausibility of such effects. Despite this, one can agree on the existence of non-thermal effects, given the increasing number of papers devoted to it and the number of experiments showing undoubtedly and successfully these particular effects. One also could think that the enhancement in yields and reaction rates reported in the literature could be the consequence of the simultaneous contribution of the two phenomena, given the peculiar conditions necessary to perform the chemical reactions.

The measurement difficulties quoted above makes the modeling of the non-thermal effects difficult, because the parameters that characterize them have not been quantified. As a consequence, the very transient nature of the non-thermal effects cannot be represented. Furthermore, by assuming the metallic catalyst particles as spherical, the model proposed in this thesis simplifies the problem and probably underestimates the effect of the metallic catalyst shape irregularities.

Therefore, this work can be classified as a study of the thermal effects, since this is going to be an analysis of the effect of a simple heat generation source inside a solid which is fluidized, and cooled, by a gas.

1.2 Selective Heating Hypothesis

Under influence of an electromagnetic field, ceramic pellets are heated due to the lossy nature of the material: a fraction of the electromagnetic energy is converted into heat. The adjunction of metallic catalyst particles in ceramic pellets increases the overall heat generation. More specifically, metallic particles dissipate the electromagnetic energy more easily, and local “hot spots”

are assumed to appear at the surface of the particles. Thus, despite the measurement difficulties reported previously, some peculiar effects have been identified at the nanometer scale: the reduced electrical conductivity of metal particles because of the three-dimensional quantum confinement (3), the temperature discontinuity at the metal-support interface due to the Casimir limit (5), and temperature discontinuity at the metal-gas interface due to kinetic theory effects (6).

1.3 Objectives

This study of the thermal effects in a fluidized bed follows the one performed for the fixed bed by J. Lanz (7). The fluidized bed brings the advantage of mixing effects; the high flow rates enhance the transfer coefficients, which can be useful in our case since there exists a potential overheating. Thus, J. Lanz was facing unsteady temperatures, and obtained steadily rising temperatures well above 1000°C.

The first goal of this work is to study the influence of the numerous parameters on the temperature difference between the gas and the pellets in a fluidized bed used for experiments on the isomerization of butane, a chemical reaction that occurs at around 300°C. Figure 1.1 shows the ceramic pellets with the microscopic particles dispersed throughout the ceramic support and attached to it, both heated by the electromagnetic field. Such a heating method can yield pellet temperature higher than the gas temperature, which can be interesting when considering the thermodynamics of a chemical reaction. Indeed, this temperature difference can be thought as being one of the reasons for the enhanced chemical reactions observed, knowing that the chemical reaction rates are temperature dependent, and that reactions occur in the immediate vicinity of the pellets. Thus, Mingos recently quoted the involvement of important temperature differences (300 to 400K), through a literature investigation, consistent with reaction rates and product distributions (8). By unpublished results, he also reports changes in chemical equilibrium constants for the gas phase decomposition of H₂S catalysed by metal sulfides on γ -alumina support (9).

Another goal is to show, for each parameter, the conditions necessary to obtain a pellet temperature higher than the gas bulk temperature in the fluidized bed. The temperature profiles of both gas and pellets also have to be known to insure that the reactor remains in desirable temperature ranges.

Finally, a logical objective is to seek the conditions most conducive to enhancing the chemical reaction by achieving a desired temperature difference between the pellets and the gas during a

further experiment. These conditions are subject to the constraints identified in the literature review section and in the study of the parameters.

1.4 The Numerical Model

The objective of the numerical model is to determine the temperature distribution of both gas and pellets, in terms of the dimensionless axial location in a fluidized bed. It will take into account the presence of the platinum catalyst metallic particles in the overall heat generation term, but the modelling of the local “hot spots” due to local concentration of the electromagnetic field is not included. Indeed, Thomas showed (10), with the scarce knowledge available in the area and for similar assumptions to the ones used in this model (i.e. the metallic particles are perfect spheres), but under a gas pressure of only 0.01 MPa, that the temperature difference between the metallic particles and the ceramic matrix is very low. For atmospheric pressures and for higher gas velocities, this temperature difference would probably be barely noticeable.

Upon request, the model will also give the temperature distribution inside a single pellet at a location and at a time specified by the user.

The input/output aspect of this model will allow the modification of any parameter and the storage of the data. However, a set of parameters are proposed in the program statements to guide the user. More specifically, it will be possible to adapt the electromagnetic field to the experimental conditions; the minimum fluidization velocity will be computed, for the given conditions, in order to help the user in selecting meaningful parameters.

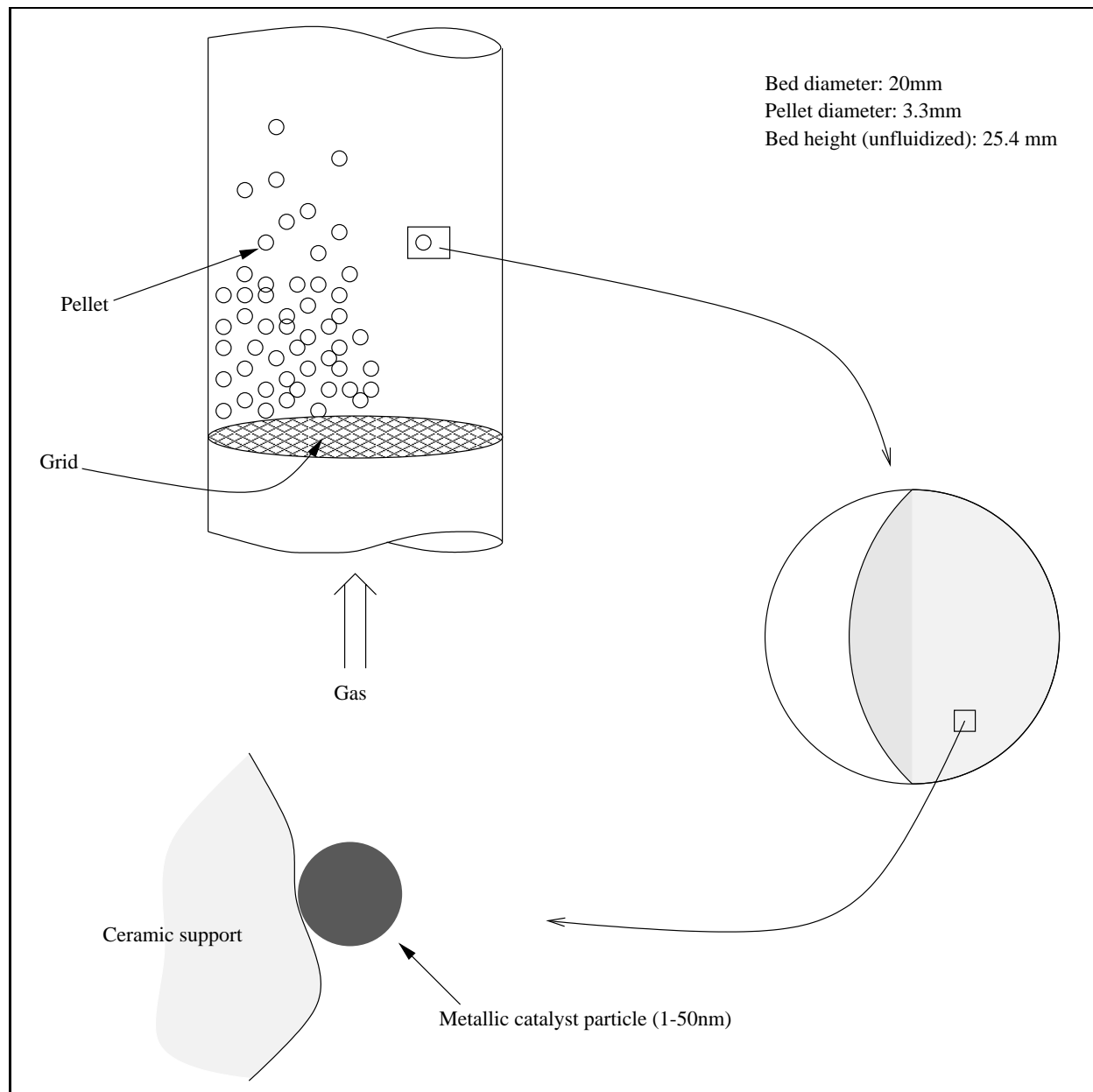


Figure 1.1: Illustration of a fluidized bed, a ceramic pellet and a catalyst particle.

Chapter 2

Literature Review

2.1 Enhanced Catalytic Reactions

Chemical reactions enhanced by microwaves have been studied since the 1970s. Microwave heating has the advantage of bringing the energy directly and rapidly into the chemical reactor by interacting with the catalyst, compared with conventional heating where the energy has to be brought through a heat exchanger located either inside or outside the reactor, meaning delay, inertia and wasted heat. However, one of the limitations of a wider use of microwaves is a lack of fundamental understanding of the heat generation at the microscopic level.

Nevertheless, a growing number of studies simply showed microwaves as a way to heat a reactor although some highlighted enhanced chemical reactions. Thus, Jacob et Chia (11) sum up the two concepts proposed to describe the behavior of materials exposed to electromagnetic fields: the thermal activation of microwave radiation, and the non-thermal interaction of microwave radiation.

2.1.1 The Thermal Activation of Microwave Radiation

This theory basically says that microwave irradiation does not bring any fundamental change in comparison with classical ways of heating the reactors. The studies supporting this conclusion point out the difficulties of the temperature measurement due to the interaction of the electromagnetic field with the probes, leading to inaccuracy, and misleading the researchers who assumed reactions were occurring at lower temperatures than in conventional reactors. Three effects are evoked: the electromagnetic interference, direct heating of the sensor, and perturbation of the field by the

thermometer, though the problem of electromagnetic interference can be solved by placing the sensor perpendicular to the field.

Gedye et al. (12) observed impressive reaction rate enhancement of 10 to 1200 times compared to conventional methods, but the reaction rate enhancement was linked to the pressure increase in the vessel. Similarly, Baghurst et al. (13) showed a reduction in synthesis time of organometallic compounds, but they thought that the rate enhancement was an effect of pressure and temperature rises.

2.1.2 Microscopic and Non-thermal Interaction of Microwave Radiation

Many papers have been devoted to this theory, and several physical phenomena have been conjectured or shown to explain enhancements of yields, rates of reaction, selectivities: selectivity modification due to irradiation, presence of localized heating effects, or improved transport properties of the molecules. However this theory remains very controversial since non-thermal effects would imply, for instance, the alteration at the atomic scale of food or any biological substances heated by microwaves.

Increased Selectivity Due to Microwave Irradiation

Among these published papers, Wan (14) demonstrates the transformation of water and carbon to hydrocarbons, i.e. methane, acetylene and minor products (ethane and ethylene). He remarks that the selectivity depends on the type of microwave catalysts used. Furthermore, he observes the dual functions of metal catalysts, i.e. enhancing chemical reactivity, as well as the influence of the nature of the metal catalyst.

Using radio-frequency and microwave irradiation, Ioffe et al. (15) could produce acetylene from methane and hydrogen over an activated carbon catalyst with higher efficiency and selectivity than classical methods, at temperatures between 1200K and 1400K. They state that, in microwave-induced catalysis, the heat is liberated on the surface of the catalyst for a low conducting material, which is probably the case for the activated carbon he uses. He emphasizes the importance of the irradiation time, as being a factor increasing the selectivity of acetylene (the selectivity is a ratio which shows how oriented a reaction is toward the production of a given specie). However, these experiments are particular since the activated carbon participates both as a reactant and as a catalyst.

Roussy et al. (16) emphasize the importance of the preparation of the catalyst, which basically consists in microwave irradiation before use in a chemical reactor. Thus, they obtain a selectivity in isomerization of 2-methylpentane twice as great than when no preparation is used. They also point out the importance of the nature of the metallic catalyst particle added to the γ -alumina.

Reaction Rate Enhancement Due to Hot Spots

Hot spots have two key aspects: they have both thermal and non-thermal effects. Thermal effects result in locally higher temperatures while non-thermal effects such as local concentrations of electric field, that give birth to them, have been suspected to break chemical bonds.

By studying the isothermal polymerization of epoxy materials, Marand et al. (17; 18) suggest that microwaves heat the molecules directly, because of the cross-linking rate improvement they observed. They evoke also a reactivity enhancement in secondary amines due to molecular inversion.

Thomas (10) showed with many reservations the possibility to selectively heat metallic catalyst particles imbedded in catalyst ceramic pellets of Al_2O_3 , i.e. to heat metallic particles at higher temperatures than the bulk temperature of the ceramic. Thus, the difference in temperature between the catalyst and the ceramic is shown to be size- and frequency-dependent, with an optimum for each particle diameter being a function of the microwave frequency.

In a liquid phase chemical reaction heated by microwaves, Chemat et al. (19) inferred the existence of a temperature difference of 9°C to 18°C between the reactant bulk temperature and the catalyst pellet temperature, the catalyst being made with 3 to 5mm montmorillonite clay spherical pellets with $\text{Fe}_2(\text{SO}_4)_3$ as the metallic particles within the clay. By doing a set of experiments, they clearly linked the microwave heating of the catalyst to the temperature difference and the increase in ester yields. However, these temperature differences were not measured, but deduced by thermodynamics considerations

In another paper, Roussy et al. (20) modeled a temperature profile of a microwave heated fluidized bed. After having achieved experiments using different TE_{0n3} cavity modes, they determined reduced parameters characterizing the bed. They showed how an equal gas and solid temperature was a good assumption, but they had not such a good agreement assuming the general case that the gas temperature is different than the solid temperature. Given the low gas flow

rate sufficient to fluidize the bed and the small bed diameter (a short calculation gives a gas velocity of about $3.93 \cdot 10^{-3} \text{m/s}$), they probably used very small catalyst pellets. This is consistent with the study of the parameters done farther in this summary. It can be noticed that they used a second-order derivative to account for the mixing of the particles, probably considering the phenomenon as a kind of thermal conductivity, whereas Molerus uses more simple terms for the mixing contribution (21; 22) in the heat transfer between a fluidized bed and the cooling or the heating surfaces placed within it.

Improvement of Molecular Transport Properties

In a chemical reaction, the slowest step is the diffusion of reactants through an unreactive medium, therefore this step determines the rate of reaction. Research on microwave processing of ceramic component materials suggest that the diffusion is enhanced by microwave irradiation. Thus, Gibson et al. (23), by studying the desorption of ethylene oxide from polyvinyl chloride, showed the active disruption of hydrogen bonding between the two components.

Hedrick et al. (24) also suggested an increase in diffusion after they reported a shorter heating duration needed to obtain a given percentage of gelation in comparison with classical heating.

2.2 Electromagnetism Review

2.2.1 The Electromagnetic Waves

Electromagnetic waves are defined by a frequency and an amplitude. Frequency and wavelength are linked together, according to:

$$\nu = \frac{c}{\lambda}. \quad (2.1)$$

The effects of the electromagnetic waves differ depending on their frequency. The high frequency waves are dangerous for life whereas low frequency waves are harmless in general. Below are the ranges of wavelengths for several species of rays:

X-rays:	$6 \cdot 10^{-12} \text{m} - 4 \cdot 10^{-8} \text{m}$
Ultraviolet:	$1 \cdot 10^{-7} \text{m} - 4 \cdot 10^{-7} \text{m}$
Visible rays:	$4 \cdot 10^{-7} \text{m} - 8 \cdot 10^{-7} \text{m}$

Infrared rays: $8 \cdot 10^{-7}\text{m} - 10^{-3}\text{m}$

Microwaves: $1\text{mm} - 1\text{m}$

The microwaves used in the model have a wavelength of 0.122m ($2.45 \cdot 10^9$ Hz).

2.2.2 The electric field intensity and the current density

The electric field intensity is defined as the vector force on a unit positive test charge:

$$\vec{E} = \frac{Q}{4\pi\epsilon_0 R^2} \vec{a}_R. \quad (2.2)$$

The current density, \vec{J} , measured in amperes per square meter (A/m^2), is a vector representing the quantity of current crossing a surface area. The current through a closed surface is obtained from:

$$I = \oint_S \vec{J} d\vec{S}. \quad (2.3)$$

2.2.3 The Permittivity

Three fundamental physical properties characterize the heat generation inside a material under the effect of an electromagnetic field. The permittivity relates the electric flux density, \vec{D} , to the electric field, \vec{E} :

$$\vec{D} = \epsilon \vec{E}. \quad (2.4)$$

The permittivity can be written in complex notation:

$$\epsilon = \epsilon' - j\epsilon''. \quad (2.5)$$

The real part, the dielectric constant, represents the energy stored in the material, and the imaginary part, the dielectric loss, represents the ability of the material to dissipate the electric field into heat.

2.2.4 The Permeability

The permeability relates the magnetic flux density, \vec{B} , to the magnetic field intensity, \vec{H} :

$$\vec{B} = \mu \vec{H}. \quad (2.6)$$

The permeability can also be written in complex notation:

$$\mu = \mu' - j\mu'' \tag{2.7}$$

The real part represents the magnetic energy stored in the material, and the imaginary part, the magnetic loss, represents the ability of the material to store the magnetic field as heat.

However, the permeability does not contribute directly in the relationships for the calculation of the heat generated inside the solid by microwaves.

2.2.5 The Electrical Conductivity

The electrical conductivity relates the conduction current density, \vec{J} , to the electric field, \vec{E} :

$$\vec{J} = \sigma \vec{E} \tag{2.8}$$

The electrical conductivity represents the ability of a material to pass an electric current. It can be described as the net translational motion of free charge under the influence of an electrical field. The range of values the electrical conductivity can have is very wide: silver has a conductivity of $6.1 \cdot 10^7$ S/m, but fused quartz has a conductivity of only $4.0 \cdot 10^{-18}$ S/m.

2.2.6 The Waveguide

Electromagnetic waves are characterized by a frequency and an amplitude. For the ones of interest in electric devices, especially the radio frequency waves (RF) and the microwaves, the devices used are composed of the same parts: the generator, the transmission line and the applicator. The generator is the power source for the system and establishes the frequency of operation. The transmission line couples the generator to the applicator, and the applicator is designed to create favorable electromagnetic field distributions around the material to be irradiated. For microwaves, waveguides are used instead of the transmission lines used for the radio frequency waves, because the latter yields too many losses.

A waveguide is any long hollow conductor of constant cross-sectional dimension such that its dimensions are at least $\lambda/4$. The size is considerably larger than the comparable transmission line. The dimensions of the waveguide are determined by electrical field considerations.

2.2.7 The Microwave Applicator

The applicator is an important part of the system design. The dimensions of the object or the volume to be treated with the electromagnetic field are significant factors in the design of the applicator. This means that large objects are better treated by radio frequency waves, whereas smaller ones are better treated by microwaves. Therefore, the design of the applicator will be a compromise of how the electromagnetic field interacts with the material to be heated and the examination of the applicator-workpiece combinations with respect to the advantages and disadvantages.

2.3 Material Interaction With Microwaves

The state-of-the-art for this topic is well summarized by Roussy and Pearce (26). Jacob and Chia (11) also give a good overview of the effect of microwaves in matter. Thus, the behavior of material under the influence of an electric field will be briefly described.

2.3.1 The Dielectric Materials

The electrons around the nuclei of the atoms can exist in only discrete energy levels. In order to pass from a certain level of energy to another, they have to emit or absorb a precise quantity of energy or quanta. The electrons with the highest energy levels, the valence electrons, belong to the valence band, a band consisting of very numerous, closely spaced, discrete levels of energy.

In a crystalline solid, such as a diamond or a metal, the atoms are very well packed, so there exist more permissible energy levels. If there are higher-energy levels in the valence band, or if the valence band merges smoothly into the conduction band, then any additional kinetic energy given to the valence electrons by an external field results in an electron flow. Then the material is called a metallic conductor.

On the contrary, if the electrons with the greatest energy occupy the top level in the valence band and a gap still exists between the valence band and the conduction band, the electrons can not accept small amounts of energy. Then the material becomes an insulator. However, if a sufficiently large amount of energy is provided to the valence electrons, then they skip to the conduction band becomes possible: the material is called a semi-conductor.

Dielectric materials are not perfect insulators, since they conduct electricity somewhat.

2.3.2 The Polarization

The electric field component of microwaves exerts a force on the charged particles found in the compound. If the particles can move freely through the electric field, a current is induced. If they are bound in the compound, i.e. restricted in their movements, they merely reorient themselves in phase with the electric field. This is named the dielectric polarization.

The dielectric polarization can be made up of four components (27), based on the different types of charged particles in matter: electrons, nuclei, permanent dipoles and charges at interfaces

$$\alpha_t = \alpha_e + \alpha_a + \alpha_d + \alpha_i. \quad (2.9)$$

where α_t is the total dielectric polarization,

α_e is the electronic polarization due to polarization of electrons surrounding the nucleus,

α_a is the atomic polarization due to polarization of the nuclei,

α_d is the dipolar polarization due to polarization of permanent dipoles in the material,

and α_i is the interfacial polarization due to polarization of charges at interfaces.

Both atomic and electronic polarization do not contribute to the dielectric heating effect, due to a much faster reversal than the electric field. On the contrary, both conduction and dielectric polarization allow microwave heating in matter. Thus, orientation and disorientation of permanent dipoles occur (dielectric polarization) on the same time scale as the electric field reversal, allowing heat generation by friction with other atoms. Conduction polarization, which in fact corresponds to the interfacial polarization, contributes to dielectric heating when conducting particles are suspended in a non-conducting medium in an homogeneous material.

2.3.3 The Metallic Catalyst Particles

The insertion of metallic catalyst particles of platinum or other conductors modifies the physical properties responsible for the heat generation inside the ceramic support. Several formulae account for this effect. Thus, the Rayleigh formula calculates the complex electrical permittivity for a mixture of metallic particles inside a dielectric material, which is adequate for our problem, but there exist other relationships that quantify the presence of metallic materials.

The Size-dependent Conductivity

The size of the metallic particles used in the ceramic is an important factor modifying the conductivity. Nimitz et al. (3) have studied the effects of the particle size on the conductivity and showed that the conductivity decreases significantly for particles smaller than a micrometer. Thus, the effective conductivity of a metallic particle smaller than a micron is given approximately by:

$$\sigma_{eff} = \left(\frac{d_{par}}{5 \cdot 10^{-6}} \right)^3 \sigma_b, \quad (2.10)$$

where σ_{eff} is the effective electrical conductivity of the platinum particles, d_{par} is the diameter of the metallic particles and σ_b is the bulk conductivity of platinum.

The Permittivity

An estimate of the complex electrical permittivity of any small spherical inclusions within a material is given by (4):

$$\epsilon = \epsilon' - j \frac{\sigma_2}{\omega}, \quad (2.11)$$

whereas the complex electrical permittivity for small conducting spheres is given by:

$$\epsilon = \epsilon_0 - j \frac{\sigma_2}{\omega}. \quad (2.12)$$

The Rayleigh Formula

This asymmetric relationship, because indices 1 and 2 can not be switched, gives the complex effective electrical permittivity for a material which is comprised of a continuous medium (material 1), with small, isolated spherical particles (material 2), dispersed throughout(4):

$$\epsilon_m = \frac{\epsilon_1(2\epsilon_1 + \epsilon_2) + 2\Phi\epsilon_1(\epsilon_2 - \epsilon_1)}{2\epsilon_1 + \epsilon_2 - \Phi(\epsilon_2 - \epsilon_1)}. \quad (2.13)$$

The Böttcher Formula

The Böttcher formula also describes a distribution of particles dispersed in a homogeneous phase with the quadratic formula (4)

$$\frac{\epsilon_m - \epsilon_1}{3\epsilon_m} = \Phi \frac{\epsilon_2 - \epsilon_1}{2\epsilon_m + \epsilon_2}, \quad (2.14)$$

where Φ is the volume fraction of the platinum spherical particles in the pellet, 1 is the index for the continuous medium, 2 is the index for the isolated particles,

$$\epsilon_1 = \epsilon_1' - j\epsilon_1'' \tag{2.15}$$

and

$$\epsilon_2 = \epsilon_0 - j\frac{\sigma_2}{\omega} \tag{2.16}$$

The Maxwell-Wagner Effect

The Maxwell-Wagner effect describes the effect of the presence of conducting impurities within a dielectric material: the application of an external electric field generates a non-uniform charge distribution around it.

The perfectly conducting sphere produces a surface charge immediately, since its surface charge time constant approaches 0. The surface charge time constant can be defined as:

$$\tau = \frac{\epsilon}{\sigma} \tag{2.17}$$

For a semiconducting spherical inclusion, the internal field is a function of the dimensions of the sphere and the frequency of the external electric field, in addition to the electric properties. For a semiconducting sphere suspended in a perfect dielectric and exposed to an instantaneous step external electric field at $t = 0$, at $t = 0^+$ the surface charge is zero everywhere on the sphere since charge has not had time to respond to the external field. Inside the sphere, the electric field is:

$$E_2 = \frac{3\epsilon_1}{2\epsilon_1 + \epsilon_2} E_0 \tag{2.18}$$

The free charge in the semiconductor will move in response to the internal field since $\vec{J} = \sigma \vec{E}$. Thus, a surface charge will be induced arising from the available free charge in the semiconductor. For a step electric field, charge will move until, as t becomes large and steady state is reached, the internal electric field is zero. Consequently, for a static external field, the ideal conductor solution applies exactly to the semiconductor case.

2.4 Fluidization

Most of this section is based on material in two references: Kunii and Levenspiel (28), and Grace (29).

Fluidization is the operation by which solid particles are transformed into a fluidlike state through suspension in a flowing gas or a liquid. This happens when the drag force by the gas moving upward equals or overcomes the weight of the particles. The first application ever was Winkler's coal gasifier, whose desired application was the reaction of coal with addition of steam into CO and H₂. Since then, many applications have been developed using the properties of fluidization : drying of solids, coating of objects and growth of particles are the most famous of them, which make it widely used in the food and chemical industry, as well as in the thermal power plants for instance, where burners use the properties of fluidization to burn coal. The usefulness of a fluidized bed resides in the motion it produces, that generally allows greater transfer coefficients (heat, mass or momentum), and insures homogeneity. Consequently, most papers on fluidization are devoted to a better characterization of the properties of the fluidized bed, which depends on many parameters: gas distributors installed on the grid, spacing between the grid holes through which the gas flows, gas or liquid pressure drop, gas velocity and thermo-physical properties, particles sphericity diameter or particle density.

A typical paper on fluidization will consist of the derivation of an empirical or semi-empirical formula, or will consider one or several of the parameters quoted above as a function of another one. Each fluidized bed is therefore unique, and thus some discrepancies might appear with the misuse of one of the numerous empirical correlations available in the literature. So the researchers specify every time for which ranges of parameter values the considered correlation is valid. However, such a task cannot be performed on all the existing parameters, and this is another reason that sometimes explain the discrepancies. Obviously, the greater the number of correlations used in the design or the study of a fluidized bed, the higher the risk to obtain meaningless results. Thus, it sometimes occurs that calculated results as far as 50% and even one order of magnitude of the observed ones are considered as good approximations. As a consequence, one should remain cautious and aware of the possibility of disappointing predictions.

The fluidization state is greatly dependent on several parameters, which are embedded in the quadratic equation giving the minimum fluidization velocity(30):

$$\frac{1.75}{\epsilon_{mf}^3 \phi_s} \left(\frac{d_p u_{mf} \rho_g}{\mu} \right)^2 + \frac{150(1 - \epsilon_{mf})}{\epsilon_{mf}^3 \phi_s^2} \left(\frac{d_p u_{mf} \rho_g}{\mu} \right) = \frac{d_p^3 \rho_g (\rho_s - \rho_g) g}{\mu^2}, \quad (2.19)$$

where ϕ_s is the sphericity coefficient defined as the ratio of the external surface of a sphere having the same volume as the particle considered to the external surface of this particle. Figure 2.1 shows well the influence of the pellet diameter and the pellet density on the minimum fluidization velocity.

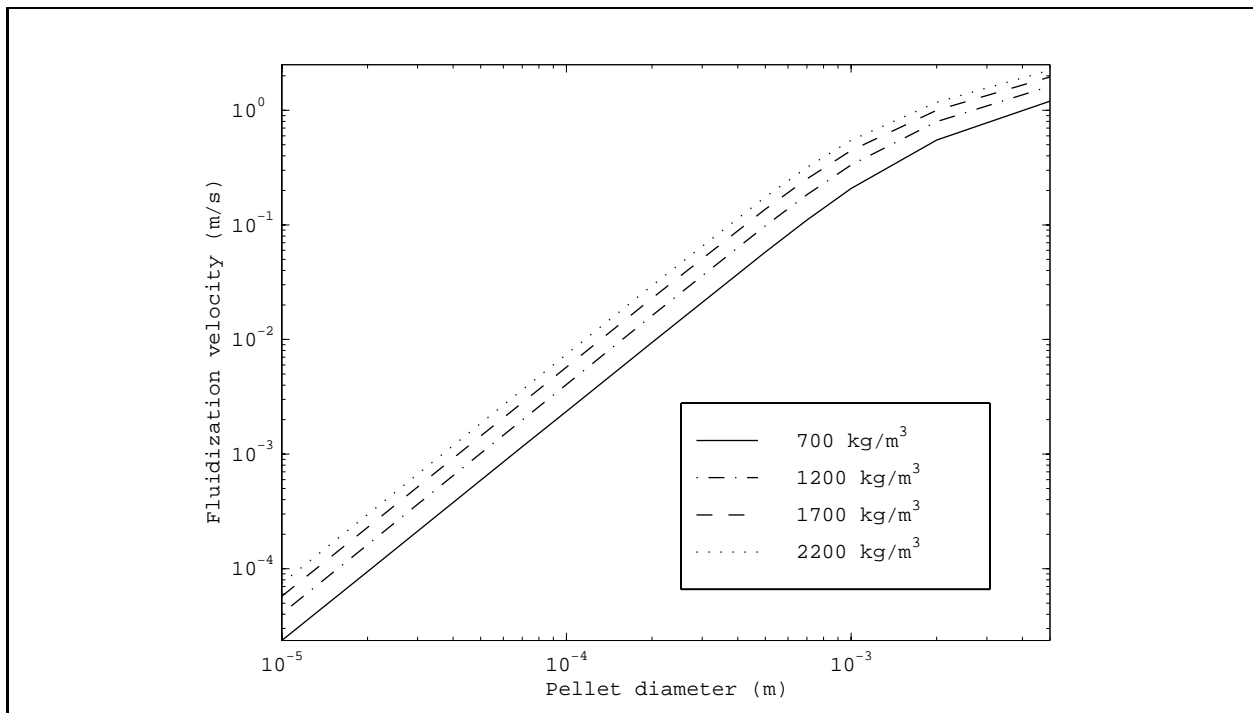


Figure 2.1: Effect of the pellet diameter and the pellet density on the minimum fluidization velocity

2.4.1 The Geldart Classification

By carefully observing the fluidization of all sorts of particles, Geldart (34) developed a classification into four different kinds of particles:

- Group A: aeratable, or materials having a small mean particle size, and/or low density ($< 1.4\text{g/cm}^3$). These solids fluidize easily, with smooth fluidization at low gas velocities and bubbling fluidization at higher velocities. The bubbles that are formed here actually are regions of void. The minimum bubbling velocity, u_{mb} (35), is given by:

$$u_{mb} = 33d_p \left(\frac{\rho_g}{\mu} \right)^{0.1}. \quad (2.20)$$

(only applicable for Geldart A particles)

When these solids are fluidized, the bed expands considerably until bubbles appear. The bubbling mode can be characterized as follows:

- Gas flows simultaneously through the bubbles and the emulsion phase, i.e. the region without bubbles.
- As they move upward, bubbles may split and coalesce. However, the maximum bubble size never exceeds 10 cm, even in large beds.
- Internal motion doesn't improve the fluidization appreciably.
- Gross circulation of solids occurs even with a few bubbles. It becomes more important as the bed gets larger.
- Bubbles turn into axial slugs when they grow to the vessel diameter.

The $65\mu\text{m}$ catalyst particles manufactured by Engelhard Corporation can be classified as Group A particles.

- Group B : sand-like, or most particles of size $40\mu\text{m} < d_p < 500\mu\text{m}$ and density $2.4 < \rho_s < 4\text{g/cm}^3$. These solids fluidize well with vigorous bubble action that grows large. The majority of the gas-solid reactions, metallurgical and others, are run in this regime because the mean size and size distribution of feed particles are usually determined by the upstream processing of the raw materials. Bubbles form as soon as the gas velocities exceed u_{mf} . Like group D particles, $u_{mb} \cong u_{mf}$. At higher gas velocities, the bed behaves as follows:

- Small bubbles form at the distributor and grow and coalesce as they rise through the bed.
 - Bubble size increases roughly linearly with distance above the distributor and excess gas velocity, $u_0 - u_{mf}$.
 - Bubble size is roughly independent of mean particle size.
 - Vigorous bubbling encourages the gross circulation of solids.
- Group C : cohesive, or very fine powders. Normal fluidization is extremely difficult for these solids.
 - Group D : spoutable and/or dense particles. Deep beds of these solids are difficult to fluidize. They behave erratically, giving large exploding bubbles, severe channelling, or spouting behavior if the gas distributor is very uneven. Moreover, bubbles appear as soon as the gas exceeds u_{mf} ; hence $u_{mb} = u_{mf}$. Drying peas, roasting coffee beans, gasifying coal, and some roasting metal ores are such solids, and they are usually processed in shallow beds or in the spouting mode. Group D have the following properties:
 - Bubbles coalesce rapidly and grow to large size.
 - Bubbles rise more slowly than the rest of the gas percolating through the emulsion phase.
 - The dense phase has a low voidage.
 - When the bubble size approaches the bed diameter, flat slugs are observed.
 - These solids spout easily.

The 3.3mm alumina catalyst pellets manufactured by Engelhard Corporation can be classified as Group D particles.

Sometimes, some authors feel the need to propose some classifications derived from the ones above, like the A' Geldart particles or AB Geldart particles which is an uncertain transition region between the Geldart A and Geldart C groups.

A particle diameter of $10\mu\text{m}$ will belong to the Geldart C group, then with an increasing diameter, to the A group, to the B group for a even bigger diameter and then finally to the D group for the particles of about 1-mm size.

For a pellet density of $700\text{kg}/\text{m}^3$, the transition region between C and A particles is at $25\mu\text{m}$, at $200\mu\text{m}$ for the A and B ones, and at $1200\mu\text{m}$ for the B and D ones. For pellet density of

2000kg/m³, the transition region between C and A particles is at 20μm, at 110μm for the A and B ones, and at 700μm for the B and D ones.

2.4.2 The Various Fluidization Types

There exist different kinds of fluidization, depending upon the inlet gas velocity (also called superficial velocity), the particle classification and the nature of the fluid fluidizing the bed (gas or liquid).

- **Smooth fluidization** : an increase in flow rate above minimum fluidization usually results in a smooth and progressive expansion of the bed. Gross flow instabilities remain small, and heterogeneity is not observed under normal conditions. For gas-solid systems, such beds can be observed only under special conditions of fine light particles with dense gas at high pressure. This kind of fluidization is mainly observed for liquid-solid systems.
- **Bubbling fluidization** : this behavior is frequently observed for gas-solid systems. An increase in gas flow rate beyond u_{mf} leads to large instabilities with bubbling and channeling. At higher flow rates, agitation becomes more violent and the movement of solids becomes more vigorous. In addition, the bed doesn't expand much beyond its minimum fluidization volume. Bubbling fluidized beds are sometimes called aggregative fluidized beds or heterogeneous fluidized beds. There exist several empirical or semi-empirical equations for the bubble size and the bubble rise velocity as a function of the height from the perforated plate, but they apply most of the time for precise ranges. For AB, B and D particle groups, the bubble diameter can easily reach tens of centimeters. However, for fine particles (belonging to the Group A), bubble diameters grow to a few centimeters in size, as a result of the equilibrium between coalescence and splitting.

On the basis of simple two-phase theory (see 2.4.3), Davidson and Harrison (31) proposed the following rise velocities,

for single bubbles:

$$u_{br} = 0.711(gd_b)^{0.5}, \quad (2.21)$$

and for bubbles in bubbling beds:

$$u_b = u_0 - u_{mf} + u_{br}. \quad (2.22)$$

Mori and Wen (32), proposed that the bubble size d_b at any height z in the bed be given as:

$$\frac{d_{bm} - d_b}{d_{bm} - d_{b0}} = e^{\frac{-0.3z}{d_t}}, \quad (2.23)$$

where d_{b0} is the initial bubble size formed near the bottom of the bed. For low gas flow rates, if the number of orifices per unit area is N_{or} and all the gas in excess of u_{mf} forms bubbles of equal size, the volumetric gas flow rate of gas from each of the orifices, v_{or} , is found from the expression:

$$u_0 - u_{mf} = v_{or}N_{or}. \quad (2.24)$$

For a low enough flow rate so that the initial bubbles from adjacent orifices are not big enough to touch each other, or $d_{b0} < l_{or}$, the size of the bubble that just forms is given by the single orifice expression (33):

$$v_b = 1.138 \frac{v_{or}^{1.2}}{g^{0.8}}. \quad (2.25)$$

This equation can be rewritten as

$$d_{b0} = 1.3 \frac{v_{or}^{0.4}}{g^{0.2}}. \quad (2.26)$$

The combination of equations 2.24 and 2.26 yields the initial bubble size:

$$d_{b0} = \frac{1.3}{g^{0.2}} \left[\frac{u_0 - u_{mf}}{N_{or}} \right]. \quad (2.27)$$

If l_{or} is the space between adjacent holes, then

$$N_{or} = \frac{1}{l_{or}^2}, \text{ for a square array of holes.} \quad (2.28)$$

$$N_{or} = \frac{2}{\sqrt{3}l_{or}^2}, \text{ for an equilateral triangular array of holes} \quad (2.29)$$

For high gas flow rate, when the initial bubbles are so big that they touch and overlap when formed, the initial bubble size must be taken such that it just accomodates the imposed gas flow and views the neighboring bubbles as just touching. For an equilateral triangular array of touching bubbles, this condition is given by:

$$d_{b0}^2 = \frac{2}{\sqrt{3}N'_{or}}, \quad (2.30)$$

where N'_{or} represents the fictitious orifice spacing that corresponds to these touching bubbles. Replacing N_{or} in eq. 2.27 by N'_{or} yields the initial bubble size at these higher flow rates :

$$d_{b0} = \frac{2.78}{g}(u_0 - u_{mf}). \quad (2.31)$$

- **Sluggish fluidization:** in gas-solid systems, gas bubbles coalesce and grow as they rise, and in a deep enough bed of small diameter, they may eventually become large enough to spread across the vessel. Voids fill most of the column cross-section. The top surface rises and collapses periodically with a reasonably regular frequency. Large and regular pressure fluctuations are observed. In a case of fine particles, they flow smoothly down by the wall around the rising void of gas. This is called slugging, with axial slugs. For coarse particles (our case for the 3.3mm pellets), the portion of the bed above the bubble is pushed forward, as by a piston. Particles rain down from the slug, which finally disintegrates. At about this time, another slug forms and this unstable oscillatory motion is repeated. This is called a **flat slug**. Slugging is especially serious in long narrow fluidized beds. u_{ms} , the minimum slugging velocity, can be estimated using an equation due to Stewart and Davidson(36).

$$u_{ms} = u_{mf} + 0.07\sqrt{gD}. \quad (2.32)$$

- When fine particles are fluidized at a sufficiently high gas flow rate, the terminal velocity is exceeded, the upper surface of the bed disappears, entrainment becomes appreciable, and, instead of bubbles, one observes a turbulent motion of solid clusters and void of gas of various sizes and shapes. This gives the **turbulent fluidized bed**. With a further increase in gas velocity, solids are carried out of the bed with the gas. In this state, we have a disperse-, dilute-, or lean-phase fluidized bed with pneumatic transport of solids.

Using the Geldart classification, and the correlations, the behavior of typical small ($65\mu\text{m}$), or large pellets (3.3mm) can be predicted:

For the $65\mu\text{m}$ pellets, taking a 700 kg/m^3 density, we have:

Minimum fluidization velocity : 0.0123 m/s

Minimum bubbling velocity : 0.00628 m/s

For the 3.3 mm diameter pellets, taking the same mixture for the gas, and the same density for the pellets, we have an identical minimum fluidization and bubbling gas velocities : 0.922 m/s.

2.4.3 More on Fluidization

The two-phase theory tries to simplify the fluidization state by splitting it into two phases. Thus there is an emulsion state or dense phase where, according to the researchers, at a superficial gas velocity u_0 greater than the minimum fluidization velocity, the voidage ϵ_e and superficial gas velocity u_e remain at, respectively, ϵ_{mf} and u_{mf} . The other phase is called the bubble phase.

For Abrahamson and Geldart (37), these findings are too simplistic: u_e and ϵ_e do change with u_0 . These changes were correlated, for A and AB particle groups, through:

$$\left(\frac{\epsilon_e}{\epsilon_{mf}}\right)^3 \left(\frac{1 - \epsilon_{mf}}{1 - \epsilon_e}\right) = \left(\frac{u_e}{u_{mf}}\right)^{0.7}. \quad (2.33)$$

2.5 Heat Transfer Mechanisms in a Fluidized Bed

The heat transfer within a microwave heated fluidized bed is the result of the contribution of three major phenomena: heat generation within pellets, the gas flow around the pellets bringing heat from the bottom to the top of the bed, i.e. the gas convective component of the convection coefficient, and the solid mixing, i.e. the particle convective component of the convection coefficient. Depending on the various types of fluidization, which are mainly the consequence of the particle diameters and gas velocity, the thermal conductivity through the material from the bottom to the top of the bed may or may not be taken into account, in which case a $\frac{\partial^2 T}{\partial x^2}$ term should or should not show up in the differential equation.

From the experimental point of view, it is difficult to highlight separately the contributions of the particle mixing and the gas flow around the particles, therefore only two practices are found in the literature. Thus, after having performed a set of experiments, some researchers defined overall coefficients that accounted for the mixing and the gas convection around the particles, but discarded the thermal conduction through the materials, as reported by Gelperin and Einstein (38), and by Kunii and Levenspiel (39). They obtain small Nusselt number values for low Reynolds numbers three orders of magnitude below the theoretical value of 2 for a single particle in an infinite stationary fluid (see also below the relationship derived by Kothari (40)). Some other researchers take into account the thermal conductivity between the particles, which is according to Xavier and Davidson (41) the right way to proceed in order to obtain consistent Nusselt correlations that yield values above 2. The contradiction between these findings did not lead to many investigations, and in their book, Kunii and Levenspiel do not discard any of these results.

Thus, for Reynolds number less than 100, a number that is exceeded only for gas velocities much in excess of the fluidization velocity or for beds with big pellets, Kothari (40) found an empirical expression that fits the experiments well:

$$\text{Nu} = 0.03Re_p^{1.3} \quad (2.34)$$

Unfortunately, the applicability of this relationship has not been discussed recently for Reynolds numbers less than 0.1, although Kunii and Smith (42) had data in 1961 for Reynolds numbers as small as 0.001 that were fitting the relationship found 6 years later by Kothari. Indeed, the Kunii and Smith work was not reported by Kunii and Levenspiel in 1991. Because of the lack of data, the need of a Nusselt correlation for small particles less than $230\mu\text{m}$ leads to a recommendation of the Kothari correlation as a default correlation, but modeling Reynolds number less than 0.1 will not be performed in this work.

Kunii and Levenspiel (43) think formula 2.34 is correct, but that it yields meaningless results when not correctly adapted to the cases considered. Thus, assuming a plug flow, i.e. a correct exposition of the pellets to the flowing gas, they propose the Ranz formulae (44) for Reynolds greater than 100 :

Heat transfer coefficient at the surface of an isolated sphere moving at a velocity u_0 through a gas:

$$\text{Nu} = 2 + 0.6Re_p^{0.5}Pr^{0.33}. \quad (2.35)$$

For a gas passing at a superficial velocity u_0 through a fixed bed of large isometric particles of sphericity ϕ_s :

$$\text{Nu} = 2 + 1.8Re_p^{0.5}Pr^{0.33}. \quad (2.36)$$

These two relations make sense because the packed bed arrangement increases the turbulence around the particles, which necessarily increases the Nusselt number. Kunii and Levenspiel explain the wide difference between the Ranz and the Kothari formulae by the presence of clouded bubbles in the fluidized bed diminishing greatly the quality of the contact between the gas and the particles. Indeed, the Ranz formulae imply a plug flow for the gas, i.e. permanently in contact with the particles, which is not true for fine particle fluidized beds.

Gunn (45) derived the following expression to predict gas-particle heat transfer in fixed and fluidized beds for voidages in the range of 0.35 to 1:

$$\begin{aligned} \text{Nu} = & (7 - 10\epsilon + 5\epsilon^2)(1 + 0.7Re_p^{0.2}Pr^{0.33}) \\ & + (1.33 - 2.4\epsilon + 1.2\epsilon^2)Re_p^{0.7}Pr^{0.33}. \end{aligned} \quad (2.37)$$

This correlation yields results that are close to the Ranz formulae, but it has the disadvantage of requiring the overall voidage as a function of the gas velocity, a relationship which is not available in the literature for all the Geldart groups.

Wakao et al. (46) produced a correlation that is in good agreement for the fixed bed data corrected for axial thermal conductivity:

$$\text{Nu} = 2 + 1.1Re_p^{0.6}Pr^{0.33}. \quad (2.38)$$

A drying technology book from Vaněček et al. (47) contains more correlations, but they are more than thirty years old and have been rarely used since. Thus, Walton et al. (48) found, for coal particles of sizes from 0.3 to 0.8mm and for the range of values of Re from 6 to 50, the following relation:

$$\text{Nu} = 0.0028Re^{1.7}\left(\frac{d_p}{D}\right). \quad (2.39)$$

From experiments with various materials of particle sizes from 0.83 to 8.9 mm, Sharlovskaya (49) has derived for values of Re from 30 to 120 the relation:

$$\text{Nu} = 0.0097ReFe^{0.53}\left(\frac{L_{fb}}{d_p}\right)^{-0.45}, \quad (2.40)$$

and for values of Re from 120 to 2500 the relation:

$$\text{Nu} = 0.015Re^{0.805}Fe^{0.53}\left(\frac{L_{fb}}{d_p}\right)^{-0.45}, \quad (2.41)$$

where Fe is the Federov number defined by:

$$Fe = 1.1Ar^{0.333}. \quad (2.42)$$

One might be interested in using two different correlations, one for the fine particles, and another one for the coarse particles, but they should, for a certain particle diameter, yield the same Nusselt number, which is not what it is observed when plotting several correlations.

There exists a more sophisticated model for a bubbling bed of fine particles in which bubbles are surrounded by thin clouds and where almost all the gas passes through the bed as bubbles. This approach is derived by Kunii and Levenspiel (43) from mass transfer considerations. Based on unit volume of bubble phase, the total heat interchange across the bubble-cloud boundary is:

$$\begin{aligned}
H_{bc} &= \left(\begin{array}{c} \text{transfer by bulk} \\ \text{flow of gas} \end{array} \right) + \left(\begin{array}{c} \text{transfer by} \\ \text{convection} \end{array} \right), \\
&= \frac{vC_{pg} + h_{bc}S_{bc}}{V_b}, \\
&= 4.5 \left(\frac{u_{mf}\rho_g C_{pg}}{d_b} \right) + 5.85 \frac{(\lambda_g \rho_g C_{pg})^{0.5} g^{0.25}}{d_b^{1.25}}, \tag{2.43}
\end{aligned}$$

where h_{bc} , the heat transfer coefficient at the bubble-cloud interface is given by:

$$h_{bc} = 0.975 \rho_g C_{pg} \left(\frac{\lambda_g}{\rho_g C_{pg}} \right)^{0.5} \left(\frac{g}{d_b} \right)^{0.25}. \tag{2.44}$$

H_{bc} does not consider the possible pickup of heat by particles in the bubble phase. In fact, the particles dispersed in and passing through the bubble phase play an important role in transferring heat from bubble gas to the bed solids. It can be shown for heat transfer that the overall transfer rate, including the heat picked up by particles dispersed in gas bubbles, is given by:

$$H_{total} = \gamma_b \frac{6\text{Nu}^* \lambda_g}{\phi_s d_p^2} \eta_h + H_{bc}. \tag{2.45}$$

From the definition of the heat transfer coefficient:

$$\frac{6}{\phi_s d_p} (1 - \epsilon_f) h_{bed} = \delta H_{total}. \tag{2.46}$$

Combining eqs. 2.45 and 2.46 yields:

$$\text{Nu} = \frac{\delta}{1 - \epsilon_f} \left[\gamma_b \text{Nu}^* \eta_h + \frac{\phi_s d_p^2}{6\lambda} H_{bc} \right], \tag{2.47}$$

where δ , the bubble fraction in a fluidized bed, is given by:

$$\delta = \left(\frac{1 - \epsilon_f}{1 - \epsilon_{mf}} \right) \left(\frac{u_0 - u_{mf}}{u_{br}} \right). \tag{2.48}$$

The adsorption efficiency for heat transfer, η_h is given by:

$$\eta_h = \frac{1}{1 + \alpha_p \left(\frac{\rho_g C_{pg}}{\rho_s C_{ps}} \right)}. \tag{2.49}$$

For fine particles $\alpha \cong 20 - 1000$, thus η_h is close to 1.

However, the correlation 2.47 has the disadvantage of relying on many assumptions and on too many intermediate relationships that may yield inconsistent convection coefficients: it requires the knowledge of the chemical reactor (spacing between the holes of the grid), the bubble size and the bubble rise velocity, that may not be correctly estimated by the correlations, given the small diameter of the bed we use here (2 cm). Finally, Kunii and Levenspiel do not specify for which range of Reynolds number their reasoning is valid.

In all these relationships, the Reynolds and the Prandtl numbers should be evaluated as following:

$$Re_p = Re_{sph} = \frac{d_{sph}u_o\rho}{\mu}, \quad (2.50)$$

and

$$Pr = \frac{C_{pg}\mu}{k_g}, \quad (2.51)$$

where d_{sph} is the equivalent spherical diameter of a particle, i.e. the diameter of the sphere having the same volume as the particle considered. In our model, we will simply refer to spherical particles, i.e. where $d_{sph} = d_p$.

Chapter 3

Heat Transfer Modeling

For our problem, the lumped capacitance hypothesis for a pellet is valid, given the relatively high conductivity of the ceramic and the relatively low efficiency of the convection. Indeed, a calculation of the Biot number shows us that, for any pellet diameter less than about 24mm (a particle size rarely exceeded), $Bi < 0.1$. However, the temperature distribution in any singular pellet will be determined for a more accurate knowledge of the temperature field in the bed. Given the high velocity of the gas, the heat conduction through the gas will also be ignored, in both the radial and axial directions. We neglect the influence of the wall in the gas flow pattern. For a fluidized bed, the conduction of heat from a pellet to neighboring ones through contact areas is probably negligible: first, the maximum contact area (corresponding to the fixed bed case) is very small given the microscopic irregularities that obviously show up at the surface of the particles for this kind of material even though the inevitable wear may increase the contact area; second the motion of the pellets and the subsequent small contact time reduces greatly the possibility of heat flow. According to Mathur (50), radiative heat transfer accounts for only 15% of the total heat transfer at a bed temperature of 900°C, and is negligible for temperatures below 400°C. Since the temperatures of interest for catalytic reactions is around 300°C to 400°C, the radiative heat transfer will not be taken into account. Moreover, considering our installation perfectly insulated, the heat losses resulting from convection at the surface will be discarded. Finally, the heat absorbed or released by any chemical reaction is considered negligible in comparison with the rate of heat produced by microwave irradiation. These assumptions result in a one dimensional, unsteady temperature distribution in the fluidized bed. The unsteadiness results from the heating of the pellets from 25°C to a steady temperature or from the electric field pulsing. For runaway cases, there will not

be any steady state.

For this approach, the electric field will be assumed to be unaffected by the gas and the pellets. As a reference, we use the properties of the alumina pellets with embedded platinum particles manufactured by Engelhard Corporation (51).

3.1 Heat Generation

Heat generation in a material under influence of an electromagnetic field is the consequence of electromagnetic wave propagation through that medium. The amplitude of this phenomenon depends upon intrinsic properties of the material such as the electrical conductivity, σ , the electric permittivity, ϵ , and the magnetic permeability, μ . They are imbedded in the heat generation formula (52):

$$\dot{q} = 2\pi f \epsilon''_{mr} \epsilon_0 |E_{rms}|^2, \quad (3.1)$$

where

$$\epsilon''_{mr} = \frac{\epsilon''_m}{\epsilon_0}, \quad (3.2)$$

and ϵ''_m is the imaginary part of ϵ_m given by equation (eq. 2.13).

3.2 The Convection Inside The Bed

Evaluating the convection coefficient within the bed due to the gas convection around the particles and the gas mixing is the most difficult task in our modeling, since the numerous relationships available in the literature are based on either empirical methods using dimensional analysis, or boundary layer analysis using simplistic assumptions that cannot be accepted for our problem. Moreover, although some of these relations seem fairly well adapted to the fluidized bed, they yield a wide range of values and produce apparently either meaningless coefficients or underestimated ones. Therefore much caution should be taken on the conclusions drawn during this study of the temperature difference between the gas and the pellets that we are seeking to highlight. The reader must keep in mind that the accuracy of the results is only as good as that of the correlations.

In the literature review section, we distinguished two kinds of correlations accounting for both the particle mixing and the gas convection: the ones for small Reynolds number, corresponding

to either small particles or weak gas velocities or both, and the ones for Reynolds number greater than 100. For the first kind of correlations, the Kothari correlation (2.34) will be used.

For the second kind of correlations, it is reasonable to take into account the fact that some particles are almost isolated, whereas some others are being exposed to the gas as though they were in a packed bed. Therefore, the following relationship adapted from the findings of Ranz (44) should be considered for Nusselt numbers greater than 100 :

$$\text{Nu} = 2 + 1.2Re_p^{0.5}Pr^{0.33}. \quad (3.3)$$

The Nusselt number correlation takes into account the void fraction that varies for gas velocities greater than u_{mf} . However, one could also modify the factor 1.2 to some greater values, closer to 1.8, since a higher gas velocity would necessarily make the particle situation approach the case of a single particle. For our problem, we will use the first practice.

Finally, because of the lack of data for the cases where the Reynolds number is less than 0.1, we will increase meaningfully the gas velocity beyond the minimum fluidization velocity such that we obtain Reynolds numbers equal to 0.1.

Figure 3.1 on the next page shows some Nusselt correlations versus the Reynolds number found in the literature. For our problem, the transition between the correlation adapted from the Ranz formulae and the Kothari relationship occurs at a Reynolds number of 101.5. If we take 700 kg/m^3 pellets, the corresponding pellet diameter is 3.415 mm and the minimum fluidization velocity is 0.89 m/s. Finally, for the same material density, a 0.1 Reynolds number corresponds to 0.229mm pellets and a minimum fluidization velocity of 0.013 m/s.

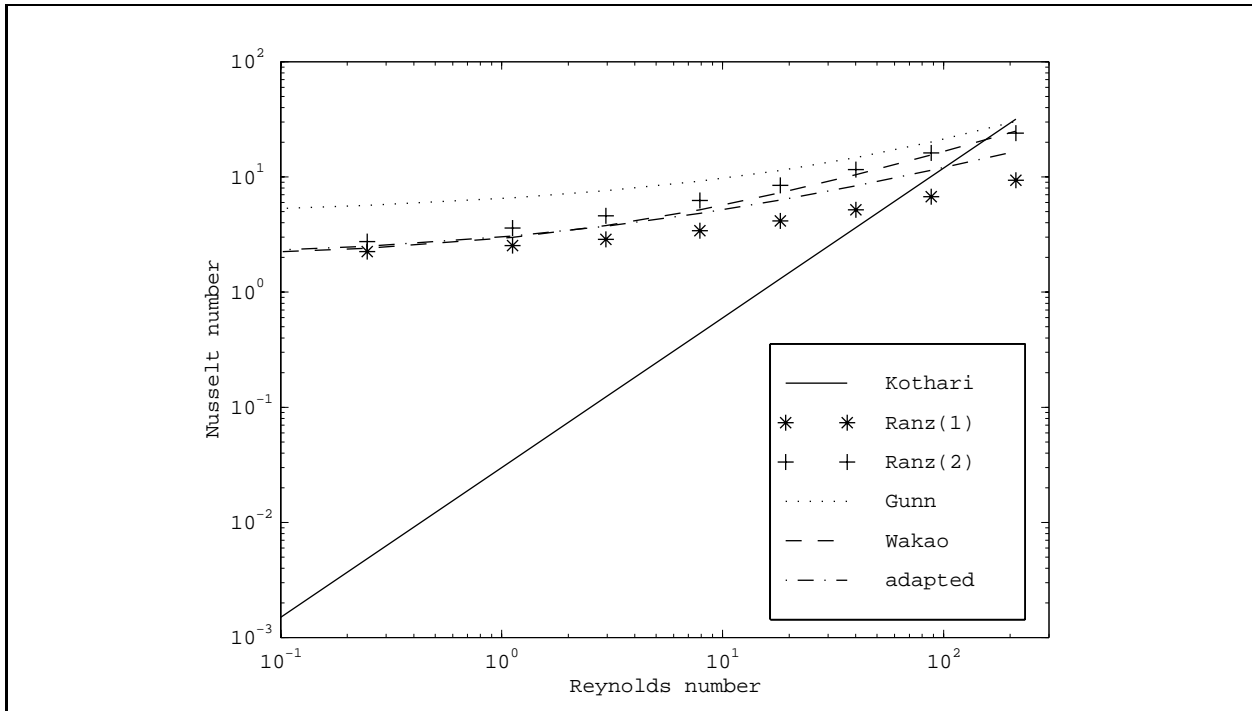


Figure 3.1: Comparison of correlations for the Nusselt number. The correlations used for our problem are the Kothari formula, for Reynolds number between 0.1 and 100 and the formula adapted from Ranz, for Reynolds number bigger 100.

3.3 Energy Equations for the Gaseous and Solid Phases

A control volume analysis is used to develop the energy equations. The bed is discretized into thin layers along the axial direction of the bed. The bed height is referred to the rest position, i.e. when the gas is not flowing. Indeed, we'll show later that the porosity of the fluidized bed is not a factor influencing the temperature distribution in the bed along the dimensionless height, which is defined as:

$$x = \frac{z}{L_{mf}}. \quad (3.4)$$

A simple energy balance gives:

$$\dot{E}_{in} - \dot{E}_{out} + \dot{E}_{gen} = \dot{E}_{st}. \quad (3.5)$$

Two equations are necessary to yield the temperature distributions of the two phases of the fluidized bed, the liquid phase and the solid phase. Therefore, the energy balance will be applied to each of them, for a layer of thickness Δz . Also, the surface area of the pellets within such a layer is given by:

$$\begin{aligned} A_S &= \frac{\frac{\pi D^2}{4} \Delta z (1 - \epsilon) 4\pi \left(\frac{d_p}{2}\right)^2}{\frac{4}{3}\pi \left(\frac{d_p}{2}\right)^3}, \\ &= \frac{3\pi D^2 \Delta z (1 - \epsilon)}{2d_p}. \end{aligned} \quad (3.6)$$

3.3.1 The Gaseous Phase Differential Equation

Incoming Energy

The gas flowing through the control volume considered, with entering temperature $T_g(z)$ and a mass flow rate \dot{m} , is heated by conduction of heat through the continuously renewed boundary layer around the pellets. Thus, the incoming energy is the contribution of both the convection and the “potential” energy, the latter being a function of the intrinsic properties of the incoming gas (temperature, gas capacity) and the mass flow rate. We keep the inlet gas velocity for the gas velocity used in the volume element considered although they differ because of the presence of the pellets, for the two following reasons. First, we cannot directly use the void fraction, which is a volume related variable, to determine the reduction of surface area available for the gas to flow in the interstitial space between the pellets. Indeed, we would need another kind of void fraction related to a surface. Second, the convection coefficient correlations found in the literature are

mostly expressed in terms of the inlet gas velocity, i.e. the only gas velocity in our system that can easily be measured. Therefore, for a layer of thickness Δz :

$$\dot{E}_{in} = hA_s(T_s - T_g) + \dot{m}C_{pg}T_g(z), \quad (3.7)$$

where

$$\dot{m} = \frac{\pi D^2}{4}v_g\rho_g.$$

Outgoing energy

The gas flowing out of the control volume has a new temperature:

$$\dot{E}_{out} = \dot{m}C_{pg}T_g(z + \Delta z). \quad (3.8)$$

Energy Balance

Equating \dot{E}_{in} and \dot{E}_{out} :

$$\frac{6\pi\left(\frac{D}{2}\right)^2\Delta z(1-\epsilon)}{d_p}h(T_s - T_g) - \frac{\pi D^2}{4}v_g\rho_gC_{pg}(T_g(z + \Delta z) - T_g(z)) = 0. \quad (3.9)$$

Dividing by Δz and taking the limit as Δz goes to 0, the differential equation becomes:

$$\frac{6(1-\epsilon)}{d_p v_g \rho_g C_{pg}}(T_s - T_g) - \frac{\partial T_g}{\partial z} = 0. \quad (3.10)$$

After making the change of variable using 3.4:

$$\frac{6hL_{mf}(1-\epsilon)}{d_p v_g \rho_g C_{pg}}(T_s - T_g) - \frac{\partial T_g}{\partial x} = 0. \quad (3.11)$$

The initial condition is $T_g = 25^\circ\text{C}$, at any location in the fluidized bed. The boundary condition, at $x=0$, is also $T_g = 25^\circ\text{C}$.

3.3.2 The Solid Equation

Incoming and Outgoing Energy

From a physical point of view, the incoming and the outgoing energy of the solid phase is represented by the motion of the pellet. Since the effect of the pellet motion is embedded in the convection coefficient by means of a correlation, then the pellet velocity with respect to the axial and location directions will be taken equal to 0.

As stated previously, the flowing gas pulls out some energy generated inside the pellets. This effect can be represented by the following term:

$$\dot{E}_{out} = hA_s(T_g - T_s). \quad (3.12)$$

The Energy Storage

The energy stored by the pellets is given, in a thin layer of thickness Δz , by:

$$\dot{E}_{st} = (1 - \epsilon) \frac{\pi D^2}{4} \Delta z \rho_s C_{ps} \frac{\partial T_s}{\partial t}. \quad (3.13)$$

The Energy Generation

The energy generated by the electromagnetic field is given by:

$$\dot{E}_{gen} = \dot{q}(1 - \epsilon) \frac{\pi D^2}{4} \Delta z. \quad (3.14)$$

Energy Balance

Equating the three terms:

$$\dot{q}(1 - \epsilon) \frac{\pi D^2}{4} \Delta z = hA_s(T_g - T_s) + (1 - \epsilon) \frac{\pi D^2}{4} \Delta z \rho_s C_{ps} \frac{\partial T_s}{\partial t}. \quad (3.15)$$

Thus, the solid differential equation becomes:

$$\frac{6h(T_g - T_s)}{d_p \rho_s C_{ps}} + \frac{\dot{q}}{\rho_s C_{ps}} = \frac{\partial T_s}{\partial t}. \quad (3.16)$$

The initial condition is $T_s = 25^\circ\text{C}$, at any location in the fluidized bed.

3.4 The Temperature Distribution Inside a Pellet

The nonlinear nature of the physical properties of the material with respect to the temperature, i.e. dielectric losses, thermal conductivity of the aluminum oxide, make the use of an exact solution impossible. Therefore, a finite difference model is used to obtain the temperature distribution inside a pellet. The model is largely inspired from the thesis of Lanz (7), with a few modifications.

The one-dimensional conduction equation for a pellet with a volumetric heat generation source is:

$$\rho C_{ps} \frac{\partial T}{\partial t} = \frac{1}{r^2} \frac{\partial}{\partial r} \left(k r^2 \frac{\partial T}{\partial r} \right) + \dot{q}(r, t). \quad (3.17)$$

The integration is performed over an interval dr , between $r_m - \frac{\Delta r}{2}$ and $r_m + \frac{\Delta r}{2}$. Since the specific heat is not as temperature-dependent as the thermal conductivity, it is brought outside the integral. We further obtain:

$$\rho_s C_{ps} \frac{\partial T_s}{\partial t} \int_{r_m - \frac{\Delta r}{2}}^{r_m + \frac{\Delta r}{2}} r^2 dr = \int_{r_m - \frac{\Delta r}{2}}^{r_m + \frac{\Delta r}{2}} \frac{\partial}{\partial r} \left(k r^2 \frac{\partial T_s}{\partial r} \right) dr + \int_{r_m - \frac{\Delta r}{2}}^{r_m + \frac{\Delta r}{2}} r^2 \dot{q}(r, t) dr, \quad (3.18)$$

yielding the finite-difference form:

$$\begin{aligned} \rho_s C_m \left(\frac{T_m^{p+1} - T_m^p}{\Delta t} \right) \left(\frac{r_{m+}^3 - r_{m-}^3}{3} \right) = \\ k_{m+} r_{m+}^2 \left(\frac{T_{m+1}^{p+1} - T_m^{p+1}}{\Delta r} \right) - k_{m-} r_{m-}^2 \left(\frac{T_m^{p+1} - T_{m-1}^{p+1}}{\Delta r} \right) + \dot{q}_m \left(\frac{r_{m+}^3 - r_{m-}^3}{3} \right), \end{aligned} \quad (3.19)$$

where T_m^p and T_m^{p+1} indicate temperatures for an arbitrary node m , at times t^p and t^{p+1} , and

$$C_m = C_{ps}|_{T_m^{p+1}}, \quad (3.20)$$

$$k_m^+ = \frac{k|_{T_{m+1}^{p+1}} + k|_{T_m^{p+1}}}{2}, \quad (3.21)$$

$$k_m^- = \frac{k|_{T_{m-1}^{p+1}} + k|_{T_m^{p+1}}}{2}, \quad (3.22)$$

$$r_m^+ = r_m + \frac{\Delta r}{2}, \quad (3.23)$$

and

$$r_m^- = r_m - \frac{\Delta r}{2}. \quad (3.24)$$

Rearranging the finite-difference form of the differential equation:

$$\begin{aligned} T_m^p \frac{\rho_s C_m}{\Delta t} \frac{r_{m+}^3 - r_{m-}^3}{3} + \dot{q}_m \frac{r_{m+}^3 - r_{m-}^3}{3} = \\ T_{m-1}^{p+1} \left[- \frac{k_{m-} r_{m-}^2}{\Delta r} \right] + \\ T_m^{p+1} \left[\frac{\rho_s C_m}{\Delta t} \frac{r_{m+}^3 - r_{m-}^3}{3} + \frac{k_{m-} r_{m-}^2 + k_{m+} r_{m+}^2}{\Delta r} \right] + \\ T_{m+1}^{p+1} \left[- \frac{k_{m+} r_{m+}^2}{\Delta r} \right]. \end{aligned} \quad (3.25)$$

Two boundary conditions are necessary to get the complete temperature distribution within a pellet. At $r = 0$, we have:

$$\frac{\partial T_s}{\partial r} = 0. \quad (3.26)$$

At $r = \frac{d_p}{2}$, we have, for a convection coefficient uniform over the surface of a pellet:

$$-k \frac{\partial T_s}{\partial r} = -h(T_s - T_g). \quad (3.27)$$

However, this equation cannot be used since it is valid only for a point. Because we are dealing with control volumes, an energy balance is performed over the whole surface of a pellet, using equation 3.5. Therefore, we get:

$$\dot{E}_{in} = -k A_s \frac{\partial T_s}{\partial r}, \quad (3.28)$$

$$\dot{E}_{out} = h A_s (T_s - T_g), \quad (3.29)$$

$$\dot{E}_{gen} = \dot{q} V, \quad (3.30)$$

and

$$\dot{E}_{st} = \rho_s C_{ps} V \frac{\partial T_s}{\partial t}, \quad (3.31)$$

where

$$V = \frac{4\pi(r_m^3 - r_{m-}^3)}{3}. \quad (3.32)$$

This gives:

$$-k A_s \frac{\partial T_s}{\partial r} - h A_s (T_s - T_g) + \dot{q} V = \rho_s C_{ps} V \frac{\partial T_s}{\partial t}. \quad (3.33)$$

yielding the finite-difference form:

$$\begin{aligned} T_m^p \frac{\rho_s C_m}{\Delta t} \frac{r_m^3 - r_{m-}^3}{3} + \dot{q}_m \frac{r_m^3 - r_{m-}^3}{3} + h r_m^2 T_g = \\ T_{m-1}^{p+1} \left[\frac{-k_{m-} r_{m-}^2}{\Delta r} \right] + \\ T_m^{p+1} \left[\frac{\rho_s C_m}{\Delta t} \frac{r_m^3 - r_{m-}^3}{3} + \frac{-k_{m-} r_{m-}^2}{\Delta r} + h r_m^2 \right]. \end{aligned} \quad (3.34)$$

Actually, another boundary condition will be used to be more consistent: the pellet temperature at the surface will be given the value obtained by the solid temperature during the calculation of the temperature profile. That will make little difference with the equation developed above.

3.5 Description of the FORTRAN Program

3.5.1 The Coupled Differential Equations

The differential equations are solved using an improved version of the Runge-Kutta algorithm, the one credited to Gill (54), which applies to a first-order differential equation of the form:

$$\frac{\partial y}{\partial x} = f(x, y). \quad (3.35)$$

According to this method,

$$y_{i+1} = y_i + \frac{h}{6} \left[k_1 + 2 \left(1 - \frac{1}{\sqrt{2}} \right) k_2 + 2 \left(1 + \frac{1}{\sqrt{2}} \right) k_3 + k_4 \right], \quad (3.36)$$

where

$$k_1 = f(x_i, y_i), \quad (3.36a)$$

$$k_2 = f\left(x_i + \frac{1}{2}h, y_i + \frac{1}{2}hk_1\right), \quad (3.36b)$$

$$k_3 = f\left(x_i + \frac{1}{2}h, y_i + \left(-\frac{1}{2} + \frac{1}{\sqrt{2}}\right)h + k_1 + \left(1 - \frac{1}{\sqrt{2}}\right)hk_2\right), \quad (3.36c)$$

and

$$k_4 = f\left(x_i + h, y_i - \frac{1}{\sqrt{2}}hk_2 + \left(1 + \frac{1}{\sqrt{2}}\right)hk_3\right). \quad (3.36d)$$

The FORTRAN program is set up to compute first the temperature of the pellet located at $x=0$, at $t=0+\Delta t$. After that, the gas temperature is calculated at $x=0+\Delta x$, at $t=0+\Delta t$. Then, the pellet temperature located at $x=0+\Delta x$ and at $t=0+\Delta t$ is computed, and so forth.

3.5.2 The Pellet Temperature Distribution

The system of linear equations we obtain for the determination of the temperature distribution inside the pellets yields a tridiagonal matrix of the form:

$$\begin{bmatrix} b_1 & c_1 & 0 & \cdots & & & \\ a_2 & b_2 & c_2 & \cdots & & & \\ & & & \cdots & & & \\ & & & \cdots & a_{N-1} & b_{N-1} & c_{N-1} \\ & & & \cdots & 0 & a_N & b_N \end{bmatrix} \cdot \begin{bmatrix} u_1 \\ u_2 \\ \cdots \\ u_{N-1} \\ u_N \end{bmatrix} = \begin{bmatrix} r_1 \\ r_2 \\ \cdots \\ r_{N-1} \\ r_N \end{bmatrix}.$$

Such a system is easily solved by algorithms that can be found in the literature (55). Between the two references quoted above, i.e. the “tridag” subroutine and the “gaussj” algorithm, the first will be preferred since it is the most economic in terms of computation time and is specially designed for tridiagonal systems such as ours.

Chapter 4

Study of the Parameters

This section is devoted to the study of the parameters using the pellets manufactured by Engelhard Corporation. We'll first pay attention to the different effects caused by the use of the two existing types of alumina, namely the α -alumina and the γ -alumina, and the influence of the mass fraction of the platinum particles embedded in the alumina ceramic on the overall heat generation. The platinum mass fraction will be taken at 5%, and we will often use the 3.3mm pellets.

From the previous chapter, we know that the convection coefficient is going to be strongly affected by the gas velocity. Through all this discussion, we use the consistent approach of setting the gas velocity equal to the minimum fluidization velocity u_{mf} . Indeed, it does not make sense comparing a system with 3.3mm pellets and another one with $65\mu\text{m}$ pellets using the same gas velocities, since it will be impossible practically to perform such a fluidization.

Our second concern will be to establish the influence of the pellet diameter on the temperature profile of the fluidized bed. Figure 4.1 shows how the convection coefficient is diameter dependent. Diameters less than $200\mu\text{m}$ do not show up on this plot because their Reynolds numbers, corresponding to a velocity equal to the minimum fluidization velocities, is less than 0.1. Figure 4.2 shows the ratio of the superficial velocity to the minimum fluidization velocity so that the Reynolds number reaches the critical value of 0.1 that corresponds to the lower limit of applicability of the Kothari correlation.

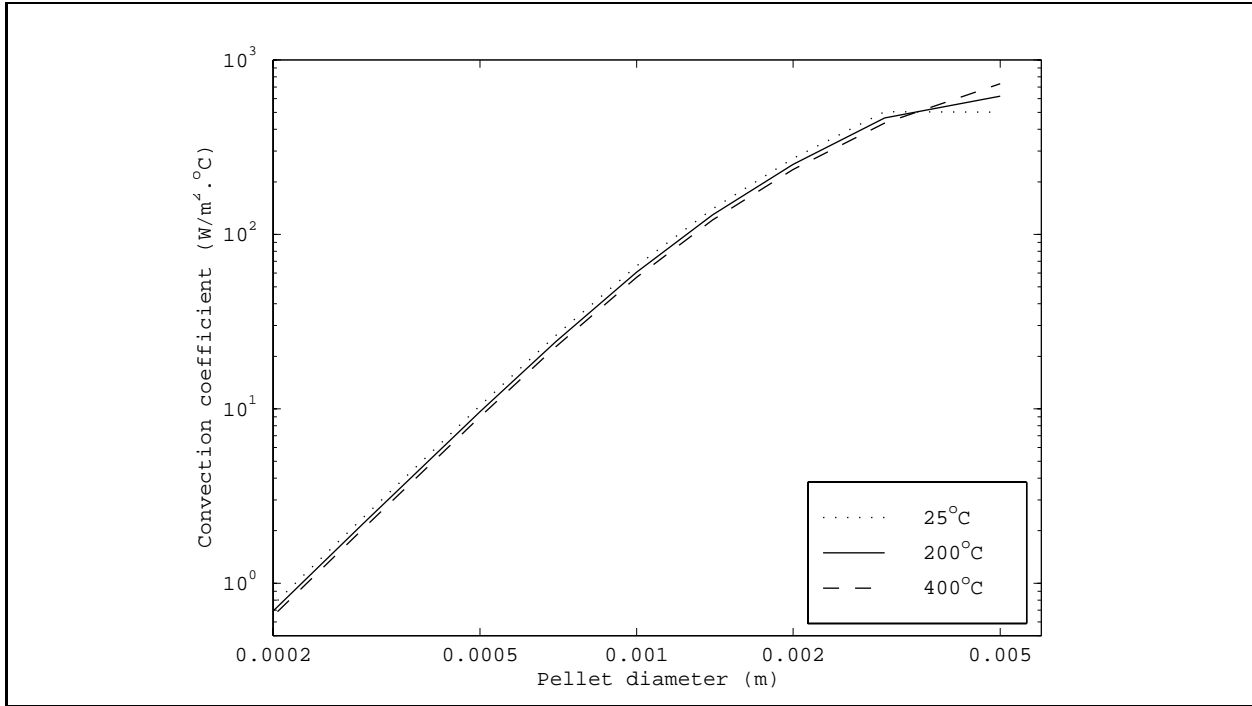


Figure 4.1: Effect of the particle diameter on the convection coefficient, calculated for each particle diameter at the minimum fluidization velocity, as a function of the particle diameter, and at three temperatures.

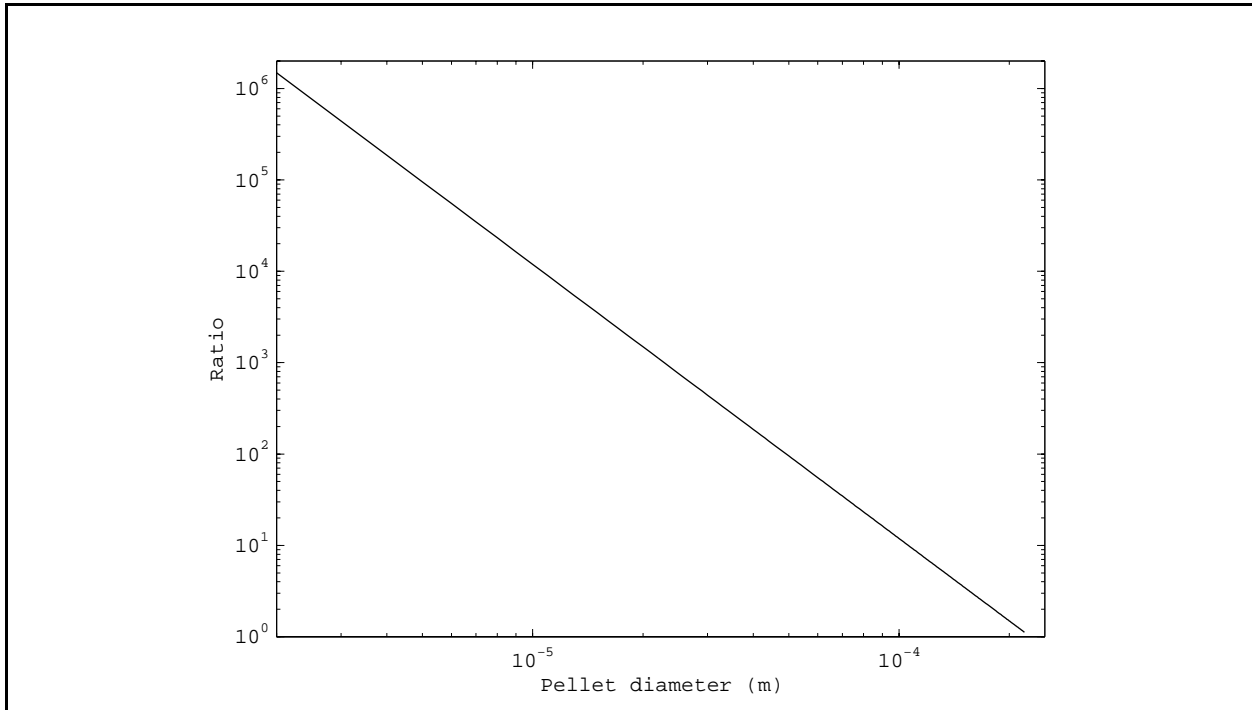


Figure 4.2: Ratio, for each particle diameter, of the gas velocity necessary to reach a Reynolds number of 0.1 to the minimum fluidization velocity calculated at this pellet diameter.

Once the influence of the pellet diameter on the temperature difference between the gas and the pellets has been characterized, we will focus on the important contribution of the gas velocity on the heat transfer within the fluidized bed, and then, how denser pellets affect the minimum fluidization velocity and the subsequent heat transfer.

Further, we will study the effect of the height of the bed and the effect of the pulsing of electric field.

Pulsations can be defined as a succession of time intervals where the electric field is “on” or “off”. A period is defined as the time between two consecutive “on” states. In this thesis, pulsations are referred to by “duty cycle”, i.e. the electric field is said to be pulsed for a duty cycle less than one, otherwise it is described as steady. Of course, a duty cycle value of 1 means the electric field is steady.

The definition of the duty cycle is:

$$duty\ cycle = \frac{t_p}{t_p + t_r}, \quad (4.1)$$

where t_p corresponds to the “on” position duration and t_r corresponds to the “off” position duration.

A uniform electric field means that this electric field is constant with respect to the z location.

For any given case, we assume that all the particles in the bed have the same diameter and are perfectly spherical. The electric field magnitude is chosen to yield meaningful temperatures. For the cases where we set the pellet temperature, we use a temperature equal to 300°C, which is approximately the isomerization temperature of butane. **Except when specified**, the following characteristics are used for both **plots** and **tables** :

- The mass fraction of platinum used is 5%.
- The density of the material is taken at 700 kg/m³, specification provided the manufacturer .
- The gas is a mixture of 75% helium and 25% butane. It has a superficial velocity of 0.89 m/s when using the 3.3mm-pellets.
- The height of the bed is 1 inch, with a void fraction of 0.4 at the minimum fluidization velocity. Indeed, the void fraction for such conditions is the same as for packed bed conditions, although it should be slightly greater for a 65μm-particle bed, in which case the gas has to overcome cohesive forces in addition to the other forces.
- The temperatures appearing on the plots are taken at x=1, i.e. at the exit.

The reader should be careful to distinguish the cases where the electric field is uniform, thus yielding an approximately linear temperature profile, and the cases where the electric field is modified to obtain specific temperature profiles (for instance constant pellet temperature profiles).

4.1 Influence of the Nature of Aluminum Oxide.

The arrangement of the molecule affects many physical properties. For instance carbon has different crystalline forms. For example, diamond is transparent to light whereas the graphite is not. Concerning aluminum oxide, there exist also different structures. The ones considered in this thesis will be α -alumina and γ -alumina. They are affected differently by an electromagnetic field in the sense that their dielectric constant and dielectric loss values are different. There are also other properties that vary depending on the structure of alumina, but the differences are not as relevant. The property that contributes the most to the heat generation is the dielectric loss, and because the dielectric loss of α -alumina increases with respect to the temperature, whereas the dielectric loss of γ -alumina diminishes with respect to the temperature, we will see different responses for an increase in temperature.

Fig. 4.3 illustrates **thermal runaway** for α -alumina pellets, where the difference between steady-state pellet and gas temperatures is plotted versus the electric field strength: beyond a temperature difference between the gas and the pellets of about 200°C, which corresponds to a pellet temperature of about 600°C, the rate of heat generated by the electromagnetic field inside the α -alumina pellets overcomes the rate of heat removal by convection. As a consequence, γ -alumina is recommended for use in a fluidized bed, and the parameter study will be performed only with this type of aluminum oxide. Table 4.1 is added to give a range of the temperatures obtained for platinum-free ceramic.

Also, the presence of 33 nm-particles of platinum doesn't influence similarly the heat generation for the two different kinds of alumina. Thus, the heat generation is almost unchanged for γ -alumina, whereas the change is impressive for α -alumina. This is a consequence of the contribution of the platinum particles in the overall dielectric loss, which is of the same order of magnitude of the dielectric loss of the ceramic support when using α -alumina, but which is of a smaller order of magnitude when using γ -alumina. Figures 4.4 shows well the effect of an increase in platinum mass fraction.

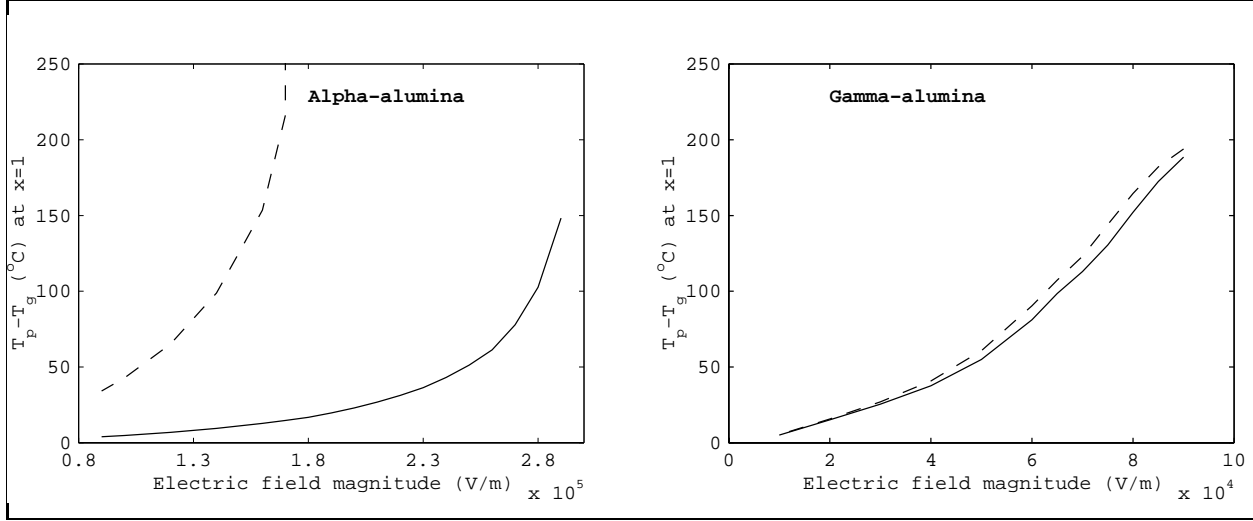


Figure 4.3: Effect of a steady electromagnetic field on steady-state ΔT for γ -alumina. The dashed line represents the pellets with a 5% mass fraction in Pt, whereas the solid line represents the pellets without any Pt.

Table 4.1: Representative values for the heat generation within 3.3mm pellets: effect of the steady and uniform electromagnetic field on ΔT , T_{pel} and T_{gas} for α - and γ -alumina without metallic catalyst particles.

α -alumina				γ -alumina			
E (V/m)	T_{pel} ($^{\circ}$ C)	T_{gas} ($^{\circ}$ C)	ΔT ($^{\circ}$ C)	E (V/m)	T_{pel} ($^{\circ}$ C)	T_{gas} ($^{\circ}$ C)	ΔT ($^{\circ}$ C)
$1.6 \cdot 10^5$	102	89	13	$2 \cdot 10^4$	132	117	15
$2.2 \cdot 10^5$	186	155	31	$4 \cdot 10^4$	300	262	38
$2.8 \cdot 10^5$	391	189	102	$6 \cdot 10^4$	517	436	81

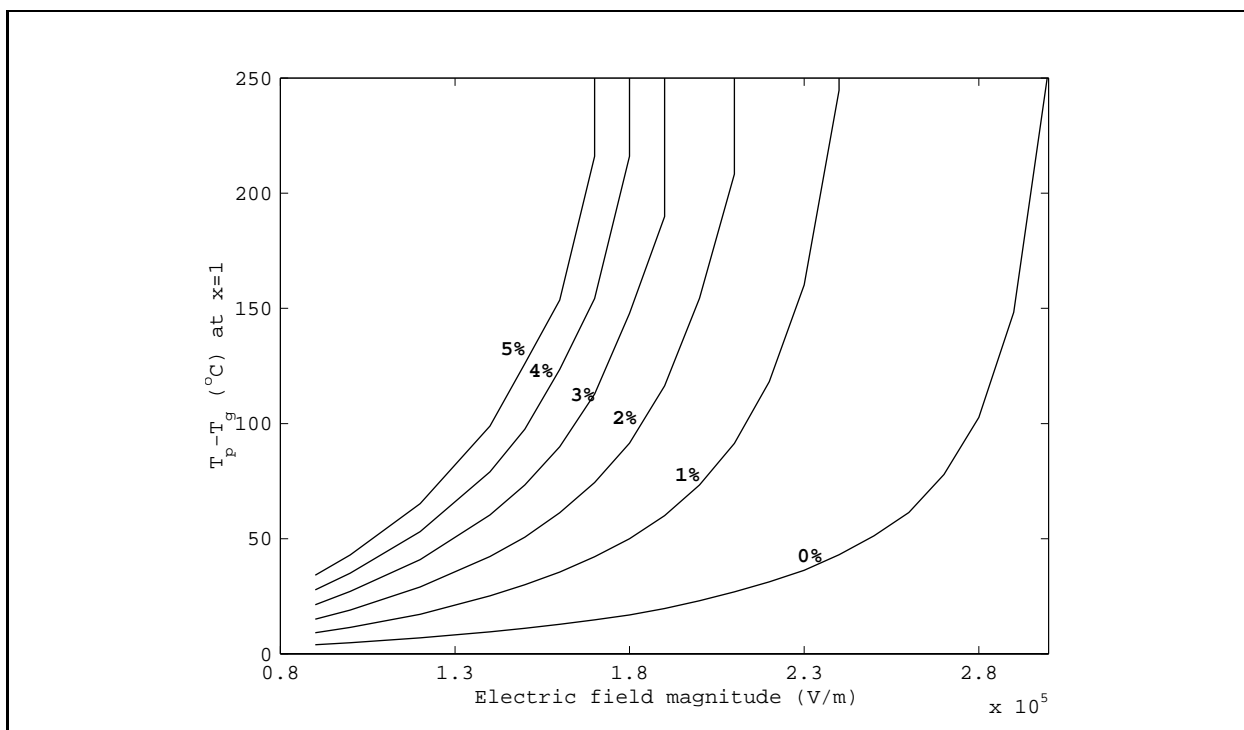


Figure 4.4: Effect of the presence of metallic particles of Pt on ΔT for α -alumina ceramic support and for various platinum mass fractions.

4.2 Influence of the Pellet Diameter.

The study of the pellet diameter is performed here by modifying the gas velocity and the electrical field strength, such that meaningful temperatures, around 300°C, and fluidization conditions are reached. The calculations done for three pellet diameters: 0.3, 1.0 and 3.3 mm yield figure 4.5: the gas velocity and the electrical field strength differ greatly for each case. The necessary modification of the electrical field strength is the consequence of the Reynolds-dependence of the convection coefficient. Indeed, there is a risk of overheating from keeping high electrical field values for the small particle systems because of the weak removal of heat, although the overall heat generation in the bed would remain approximately constant whatever the particle diameter (using the same electric field magnitude).

To obtain a good approximation of the steady-state temperature difference between the gas and the pellets, the heat accumulation term in the energy equation of the gaseous phase is discarded:

$$\Delta T = T_{pellets} - T_{gas} = \frac{\dot{q}d_p}{6h}. \quad (4.2)$$

This relationship shows well that the temperature difference can remain constant as the pellet diameter decreases if the convection coefficient gets diminished too. Since for most diameters of interest, $Re < 100$ or $d_p < 3.4\text{mm}$, we may use $Nu = 0.03Re_p^{1.3}$ to relate the convection coefficient directly to d_p as:

$$\begin{aligned} h &= \frac{Nu\lambda_g}{d_p}, \\ &= \frac{0.03Re_p^{1.3}\lambda_g}{d_p}, \\ &= \frac{0.03\rho_g^{1.3}v_g^{1.3}d_p^{0.3}\lambda_g}{\mu^{1.3}}. \end{aligned} \quad (4.3)$$

Since we take $v_g = u_{mf}$ and knowing from (56) that for small particles:

$$u_{mf} = \frac{d_p^2(\rho_s - \rho_g)g}{150\mu} \frac{\epsilon_{mf}^3\phi_s^2}{1 - \epsilon_{mf}}, \quad (4.4)$$

then the convection coefficient expression becomes:

$$\begin{aligned} h &= \frac{\rho_g^{1.3}(\rho_s - \rho_g)^{1.3}g^{1.3}\epsilon_{mf}^{3.9}\phi_s^{2.6}\lambda_g}{22480\mu^{2.6}(1 - \epsilon_{mf})^{1.3}}d_p^{2.9}, \\ &= ad_p^{2.9}. \end{aligned} \quad (4.5)$$

Therefore ΔT can be written as:

$$\Delta T = b|E_{rms}|^2 d_p^{-1.9}, \quad (4.6)$$

where

$$b = \frac{\pi f \epsilon_0 \epsilon_r''}{3a}. \quad (4.7)$$

Unfortunately, even if it is possible to show such a pattern for big pellets, the more complicated Nusselt correlation and gas fluidization expression make the advantage of using that type of formula very relative. Figure 4.6 shows how well the fluidization velocity is approximated for pellet diameters less than about 0.8 mm. This correlation might be extended to systems where the Reynolds number is less than 0.1 with much caution.

As a conclusion and under the assumption that the Kothari formula 2.34 fits the convection coefficient well, we showed that the temperature difference between the gas and the pellets is not strongly diameter-dependent for small pellet diameters given that we modified the electrical field strength such that the pellet temperature reaches a value of 300°C at the top of the bed. However, the temperature dependence becomes higher as the pellet diameter increases.

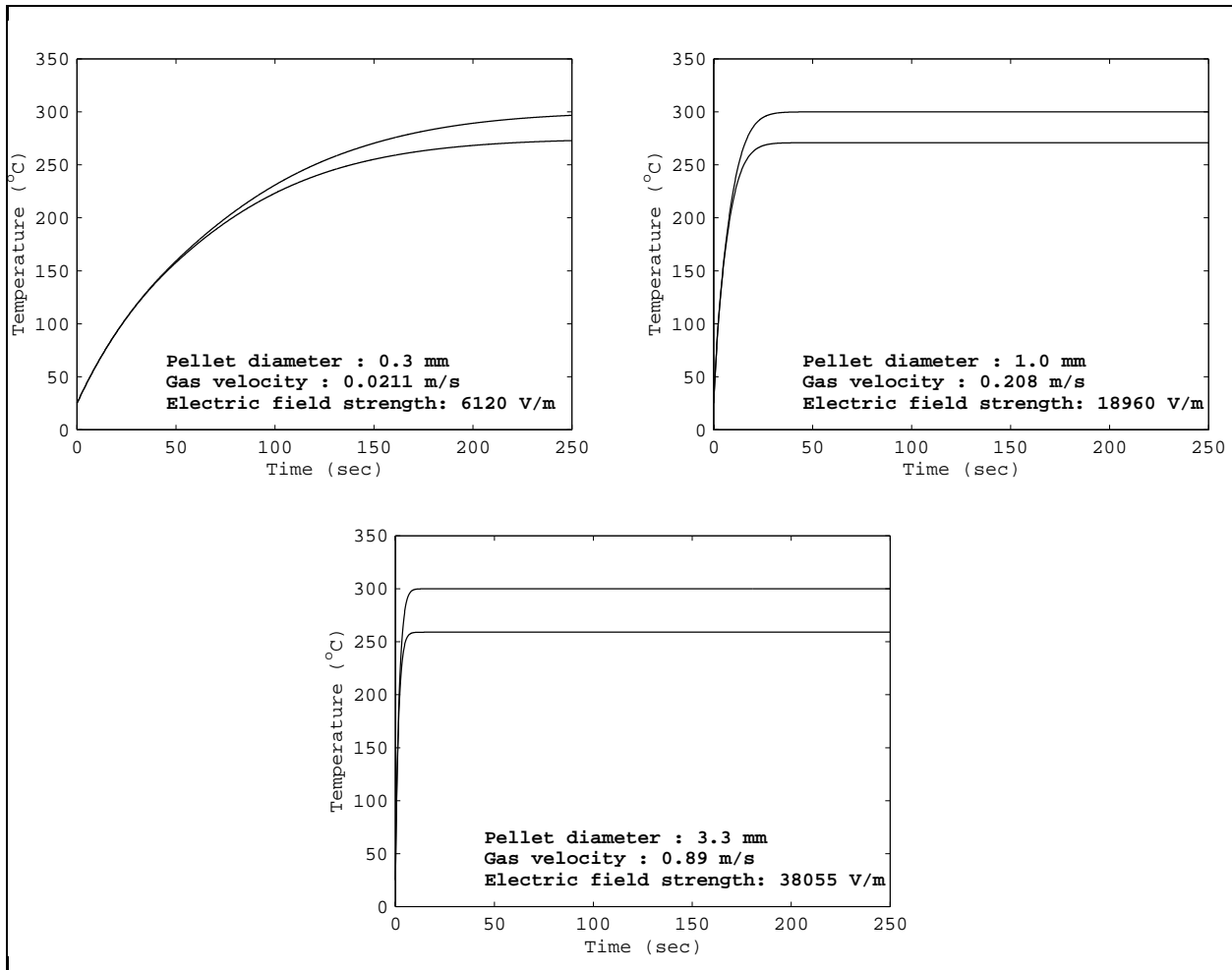


Figure 4.5: Effect of the pellet diameter on the gas and on the pellet temperatures. For each plot, the upper curve is the pellet temperature and the lower curve is the gas temperature.

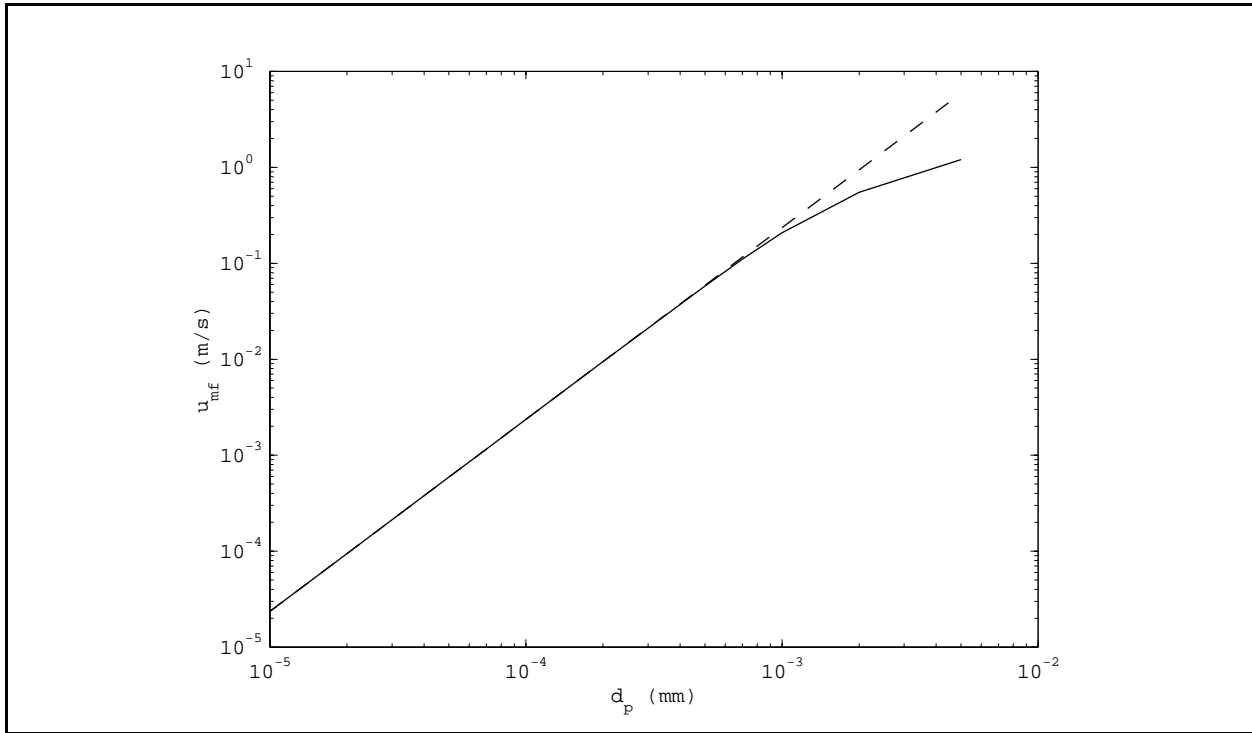


Figure 4.6: The dashed line represents the fluidization velocity calculated by the approximation and the solid line the fluidization velocity calculated by the quadratic equation.

Table 4.2: Effect of the pellet diameter at the minimum fluidization velocity on ΔT , for 700 kg/m^3 pellets. The electric field strength is set such that $T_{\text{pel}} = 300^\circ\text{C}$ at the exit of the one inch bed.

Pellet diameter (mm)	Electric field strength (V/m)	u_{mf} (m/s)	ΔT ($^\circ\text{C}$)
0.23	4705	0.0125	24.9
0.3	6117	0.0212	25.5
0.5	10082	0.058	26.7
0.8	15647	0.141	28.2
1.0	18965	0.208	29.1
1.3	23247	0.315	30.6
1.8	28711	0.487	33.2
2.4	33332	0.667	36.5
3.0	36685	0.819	39.5
3.7	39683	0.97	42.9
4.4	42175	1.1	48.5
5.0	43134	1.2	60.4

4.3 Influence of the Gas Velocity.

Following the same pattern used for the study of the diameter-dependence of the temperature difference between the gas and the pellets, we can highlight the gas-velocity-dependence of the temperature difference. Thus, for $Re < 100$, using equation 4.3, and substituting this relationship into 4.2, the temperature difference can be expressed as:

$$\begin{aligned}\Delta T &= \frac{\pi f \epsilon_0 \epsilon_r'' d_p^{0.7} \mu^{1.3}}{0.09 \rho_g^{1.3} \lambda_g} |E_{rms}|^2 v_g^{-1.3}, \\ &= b |E_{rms}|^2 v_g^{-1.3}.\end{aligned}\tag{4.8}$$

Like the one derived for the diameter dependence, this relationship is valid only for small particles (less than 0.8mm in diameter), and a similar analysis is not interesting for big particles.

As an example, we take $d_p = 500\mu\text{m}$. For this specific diameter, the gas velocity varies between u_{mf} and $20u_{mf}$. The electrical field strength is still modified such that the pellet temperature at the top reaches a value of 300°C . Then we redo the calculations for 3.3mm pellets (figures 4.3 and 4.4). The most striking difference between the two cases resides in how the temperature difference between the gas and the pellets evolves with increasing gas velocities: the 0.5mm pellet case sees the temperature difference decreasing with respect to the gas velocity, while the contrary occurs for the 3.3mm pellets. This can be explained by the switching of the Nusselt number correlations for Reynolds greater than 100.

On the time evolution plots, we see that an increasing gas velocity reduces the time necessary to reach the steady state, by means of a more powerful convection that more rapidly equalizes the pellet temperature. Even if we do not highlight it here, the gas velocity increase leads to the diminution of T_{gas} and T_{pellets} in the presence of a constant electrical field. This is the consequence of a greater rate of removal of heat, due to an increase of the convection coefficient, but also to the greater amount of heat the gas is capable to absorb.

On the other hand, looking at the gaseous phase differential equation, one might think that the void fraction, which will increase as the inlet gas velocity increases above u_{mf} , is a contributing factor of the fluidized-bed-modelling. In fact, we'll have, for any void fraction, by applying the mass conservation of the pellets:

$$\begin{aligned}\Omega L_{mf}(1 - \epsilon_{mf}) &= \Omega L(1 - \epsilon) \\ \text{or } L_{mf}(1 - \epsilon_{mf}) &= L(1 - \epsilon)\end{aligned}$$

That means that $L(1 - \epsilon)$ is constant whatever the conditions in the fluidized bed. As a conclusion and still under the assumption that the Kothari formula and the Ranz correlation fit the convection coefficient well, we showed that the temperature difference between the gas and the pellets has a different dependence on gas velocity for small pellets and large pellets given that we modified the electrical field strength to force a pellet temperature of 300°C at the top of the bed.

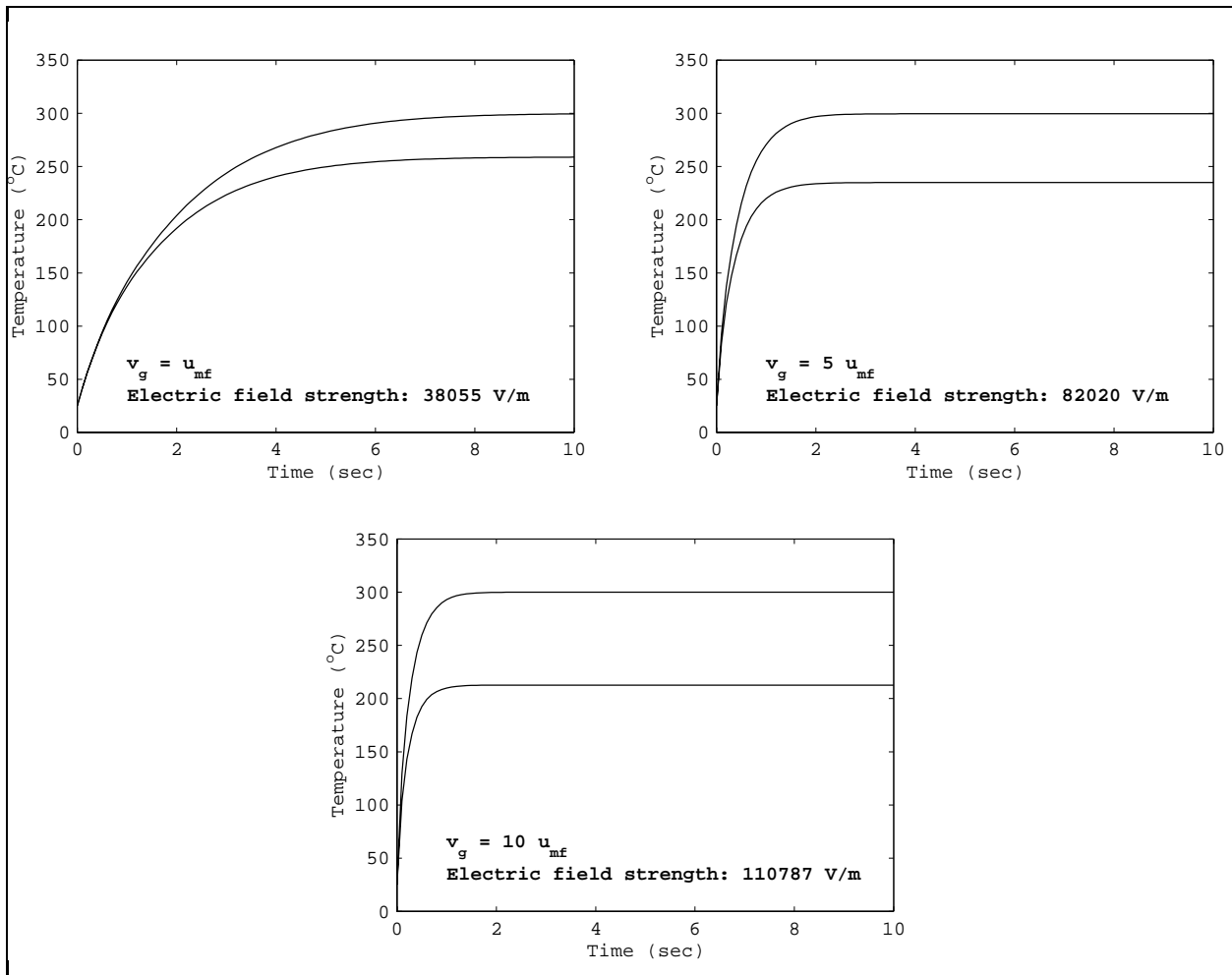


Figure 4.7: Effect of the gas velocity on the gas and on the pellet temperatures for 3.3mm pellets. For each plot, the upper curve is the pellet temperature and the lower curve is the gas temperature.

Table 4.3: Effect of the gas velocity on ΔT for 0.5mm pellets . The electric field strength is set such that $T_{pel}= 300^{\circ}\text{C}$ at the exit of the one inch bed.

Gas velocity ($\frac{v_g}{u_{mf}}$)	Electric field strength (V/m)	ΔT ($^{\circ}\text{C}$)
1	10082	26.7
2	14482	22.4
3	17910	20.2
5	23432	17.8
7	27991	16.5
10	33820	15.1
13	38891	14.2
16	43455	13.5
20	48978	12.9

Table 4.4: Effect of the gas velocity on ΔT for 3.3mm pellets. The electric field strength is set such that $T_{pel}= 300^{\circ}\text{C}$ at the exit of the one inch bed.

Gas velocity ($\frac{v_g}{u_{mf}}$)	Electric field strength (V/m)	ΔT ($^{\circ}\text{C}$)
1	38055	41.0
2	54182	41.3
3	65262	50.7
4	74332	58.3
5	82110	64.7
6	88963	70.3
8	100762	79.6
10	110787	87.3

4.4 Influence of the Pellet Density

The low density of the pellets manufactured by Engelhard Corporation (700 kg/m³) is due to the internal porosity of the pellets. Indeed, high porosities increase the surface of contact between the gaseous molecules and the material, and therefore allow better reaction rates. Thus, the surface area of 3.3mm-pellets accessible to the gas is 80 m²/g, whereas the surface-area of 65μm-particles is 125 m²/g. A smaller porosity will increase the apparent density of the pellets

The first effect of a higher density can be a modification of the pellet classification: with a density of 2000 kg/m³, up from a 700 kg/m³ one, a 800μm pellet will move from the Group B to the Group D Geldart classification (57). The minimum fluidization velocity will also be modified. Following the same pattern used for the study of the diameter dependence and the gas velocity dependence of the temperature difference between the gas and the pellets, we can highlight the pellet density dependence of the temperature difference. Thus, for Re less than 100, we may use equation 4.5, and substituting into 4.2, to express the temperature difference as:

$$\begin{aligned}\Delta T &= \frac{7493\pi f\epsilon_0\epsilon_r''d_p^{-1.9}\mu^{2.6}(1-\epsilon_{mf})^{1.3}}{\rho_g^{1.3}g^{1.3}\epsilon_{mf}^{3.9}\phi_s^{2.6}\lambda_g}|E_{rms}|^2(\rho_s-\rho_g)^{-1.3}, \\ &= b|E_{rms}|^2(\rho_s-\rho_g)^{-1.3}.\end{aligned}\tag{4.9}$$

Like the other relationships derived previously, this is valid only for small particles (less than 0.8mm in diameter) and low density pellets such that the Reynolds number is less than 100. A similar analysis is not interesting for big particles. This may be seen, for example, by taking $d_p = 500\mu\text{m}$. For this specific diameter, the pellet density varies between 700 and 3200 kg/m³, values that depend on the porosity of the ceramic pellets. The electrical field strength is still modified such that the pellet temperature at the top reaches a value of 300°C. Then, redoing the calculations for 3.3mm pellets yields the results in tables 4.5 and 4.6. The two tables do not show any similar pattern probably because of the switching of the Nusselt number correlation occurring at a Reynolds number of 100.

On the time evolution of figure 4.8, we see than an increasing pellet density increases the time necessary to reach the steady state: the heavier pellets act as “heat sinks” and are somewhat less sensitive to the **volumetric** heat generation source.

Finally, in the case where the electric field, gas velocity and pellet diameter are fixed to yield meaningful temperatures and fluidization state, the pellet density increase leads to the increase of T_{gas} and T_{pellets} ; this another side of the “heat sink” effect (table 4.7) .

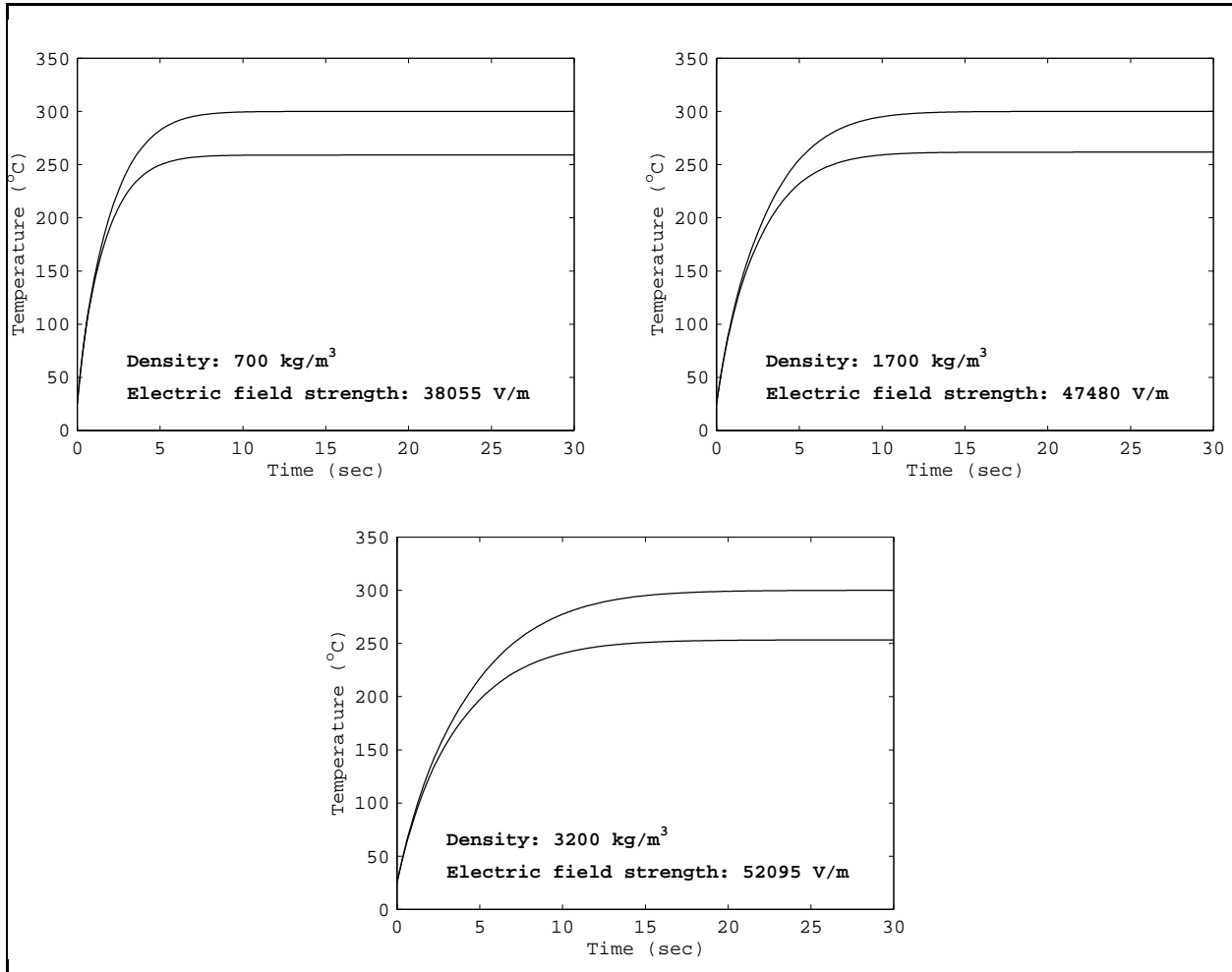


Figure 4.8: Effect of the pellet density on the gas and on the pellet temperatures for 3.3mm pellets. For each plot, the upper curve is the pellet temperature, the lower curve is the gas temperature, and the gas velocity is equal to the minimum fluidization velocity corresponding to the pellet diameter and pellet density.

Table 4.5: Effect of the pellet density at the minimum fluidization velocity, and for 0.5mm pellets, on ΔT . The electric field strength is set such that $T_{\text{pel}} = 300^\circ\text{C}$ at the exit of the one inch bed.

Pellet density (kg/m^3)	Electric field strength (V/m)	u_{mf} (m/s)	ΔT ($^\circ\text{C}$)
700	10082	0.058	26.7
1200	12945	0.098	23.6
1700	15076	0.137	21.9
2200	26773	0.176	20.8
2700	18175	0.213	20.0
3200	19362	0.25	19.4

Table 4.6: Effect of the pellet density at the minimum fluidization velocity, and for 3.3mm pellets, on ΔT . The electric field strength is set such that $T_{\text{pel}} = 300^\circ\text{C}$ at the exit of the one inch bed.

Pellet density (kg/m^3)	Electric field strength (V/m)	u_{mf} (m/s)	ΔT ($^\circ\text{C}$)
700	38055	0.89	41.0
1200	43880	1.22	38.2
1700	47480	1.49	38.3
2200	49560	1.72	41.5
2700	51030	1.93	44.3
3200	52095	2.12	46.6

Table 4.7: Effect of the pellet density, using the minimum fluidization velocity for the 3.3mm, 3200 kg/m^3 pellets (2.12 m/s), on ΔT . The electric field strength is set at 52095 V/m.

Pellet density (kg/m^3)	ΔT ($^\circ\text{C}$)
700	38.2
1200	39.7
1700	41.5
2200	43.2
2700	44.9
3200	46.6

4.5 Influence of the Pulsation of the Electrical Field

In this section, we try to show how pulsing the electric field affects the temperature rise in the bed.

4.5.1 Influence on the Heat Generation

The first consequence of the pulsing of the electromagnetic field is a decrease of the average heat generation intensity within the bed. Table 4.9, when compared with Table 4.8, shows well the gap between the steady electric field situation and the pulsed electric field one. This also leads to a decrease in temperature of both the gas and the pellets. However, for a duty cycle value of 0.5 and identical values for the other parameters, the temperature difference is not divided by two as one might expect, but rather by a coefficient which varies, depending on the cases, between 1.5 and 1.9 (table 4.10 and figure 4.9). Indeed, if we consider that during a short time interval, the power deposited by an electromagnetic field with a duty cycle value of 0.5 is half that of the power deposited by a steady electromagnetic field, i.e. if:

$$P_{0.5} = \frac{1}{2}P_1, \quad (4.10)$$

where

$$P_{0.5} = \int_t^{t+\Delta t} \dot{q}(t)dt, \quad (4.11)$$

and

$$P_1 = \dot{q}\Delta t. \quad (4.12)$$

then, the temperature difference generated between a flowing gas and pellets should logically be halved, according to the simplified energy equation of the gaseous phase, which has the property to be linear:

$$\Delta T = \frac{\dot{q}d_p}{6h} \quad (4.13)$$

This phenomenon is probably the consequence of the nonlinear temperature dependence of the dielectric loss, which is the main factor responsible of the heat generation within the ceramic. The fact that the thermal properties do vary with respect to the temperature is also a factor that contributes to this result.

Table 4.8: Effect of the steady electric field strength on the steady-state gas temperature and pellet temperature at $x=1$, for γ -alumina.

Electric field strength (V/m)	Pellet temperature ($^{\circ}\text{C}$)	Gas temperature($^{\circ}\text{C}$)	Temperature difference ($^{\circ}\text{C}$)
10000	59	53	6
20000	135	119	16
30000	223	194	29
40000	320	276	44
50000	439	370	69
60000	587	484	101
65000	667	549	118
70000	757	617	140
75000	851	690	161
80000	946	766	180
85000	1036	842	194
90000	1120	916	204

Table 4.9: Effect of the pulsed electric field strength on the steady-state gas temperature and pellet temperature, for a duty cycle of 0.5.

Electric field strength (V/m)	Pellet temperature ($^{\circ}\text{C}$)	Gas temperature($^{\circ}\text{C}$)	Temperature difference ($^{\circ}\text{C}$)
10000	41	38	3
20000	84	74	10
30000	139	121	18
40000	198	171	27
50000	261	224	37
60000	332	282	50
65000	371	313	58
70000	414	346	68
75000	460	382	78
80000	510	420	90
85000	563	460	103
90000	616	502	114

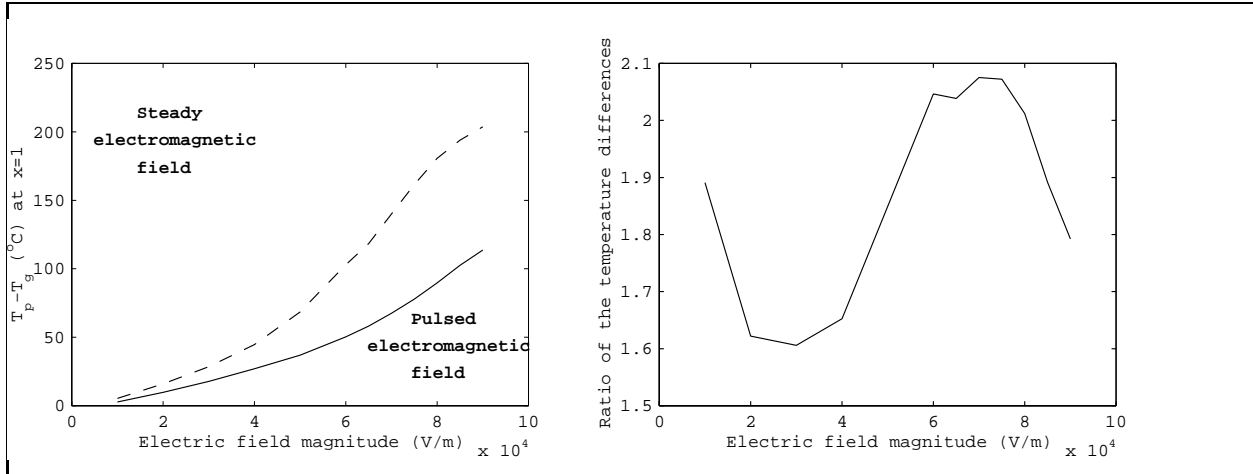


Figure 4.9: Effect of pulsing on the steady-state temperature differences between the gas and the pellets at $x=1$. For the pulsed case, the duty cycle has a value of 0.5. The right hand side figure is the ratio of the temperature difference between the gas and the pellets for a steady electromagnetic field to the temperature difference between the gas and the pellets for a pulsed electromagnetic field.

Table 4.10: Ratio of the temperature difference between the gas and the pellets for a steady electromagnetic field to the temperature difference between the gas and the pellets for a pulsed electromagnetic field

Electric Field Strength (V/m)	Temperature Increase Ratio
10000	1.89
20000	1.62
30000	1.61
40000	1.65
50000	1.85
60000	2.05
65000	2.04
70000	2.08
75000	2.07
80000	2.01
85000	1.89
90000	1.79

4.5.2 Influence of the Period Length

In fig. 4.5.2, we compare time-dependent temperatures for various period lengths. We see that an increasing period makes the oscillations larger, but the average gas and the average pellet temperatures remain identical in all cases. An “average” temperature is defined here as the mean between the top and the bottom values of an oscillation. Moreover, a small period, while the duty cycle remains equal to 0.5, produces a similar transient temperature distribution curve, but with smaller gas and pellet temperatures. Thus, by using the table 4.8 and 4.9 and interpolating, we see that we can obtain the same results with a steady electric field strength of about $3.806 \cdot 10^4$ V/m (see Fig. 4.11).

Therefore, the main effect of diminishing the length of a period is to smooth the transient temperature distribution, and the usefulness of modifying the period length resides in obtaining quasi steady-state.

From another point of view, the micropulsation of the electromagnetic field does not have the effect of increasing the temperature difference between the two phases, contrary to what Wan assumed (14), because of the thermal inertia of the pellets and the weak heat transfer rate between the pellets and the gas.

At the microscopic scale, inside the ceramic pellet, Thomas (10) showed that for the microwave frequency considered, only a few tenths of degree of temperature difference between the metallic particles and the ceramic matrix can be obtained. These plots, however, do not highlight the micropulse effects at the electronic scale that have been suggested to explain the enhancement of chemical reaction rates and yields.

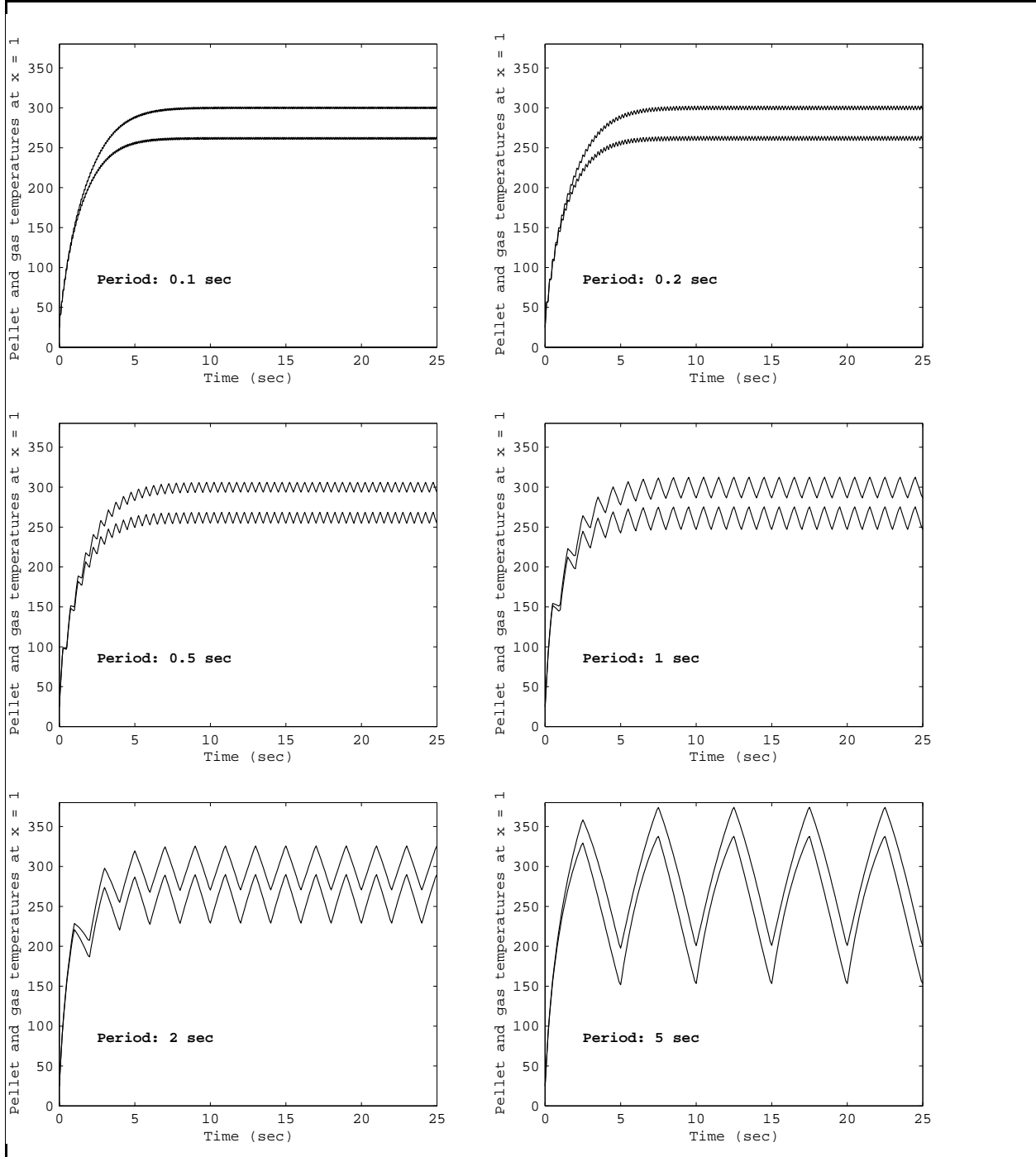


Figure 4.10: Effect of the period of the pulsations on the gas and on the pellet temperatures. For each plot, the upper curve is the pellet temperature, and the lower curve is the gas temperature. The duty cycle is 0.5, while the electric field has a value of 54550 V/m.

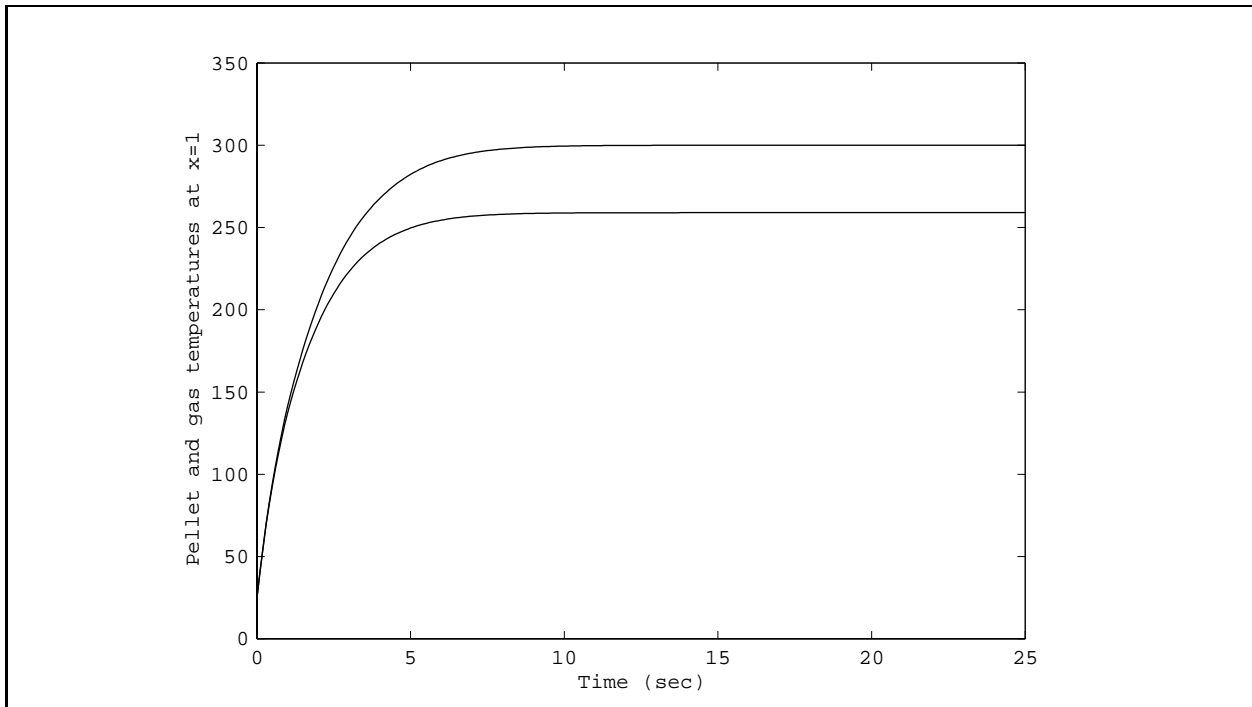


Figure 4.11: This plot shows how a steady electric field can achieve a ΔT equal to the pulsed electric field case. $E_{\text{rms}} = 3.806 \cdot 10^4 \text{ V/m}$. The upper curve of this plot is the pellet temperature and the lower one is the gas temperature. This comparison is made with the upper left hand side plot of figure 4.5.2.

4.5.3 Influence of the Duty Cycle

In figure 4.12, we show the effect of the duty cycle on bed temperatures. As expected, the smaller the duty cycle, the smaller the bed temperature rises. However, it is interesting to know whether the pulsation time has any influence on the ΔT , i.e. if we can reproduce or not, and for any case, the same temperature distribution just by using a smaller non-pulsed electric field.

In fact, we already have a satisfactory result for a duty cycle of 0.5. Thus, whatever the duty cycle value (in our examples 0.2, 0.5 and 0.8), we can obtain identical temperature distribution using a duty cycle value of unity with smaller value of the electric field. This can be checked by comparing Fig. 4.12 with Table 4.8.

Once again, although it seems the pulsation of the electric field is useless, we may need to pulse it for technical reasons. It is interesting that we can obtain identical results when using a pulsed electric field just by increasing its strength. For instance, one might be interested to introduce pulsations to control the bed temperature.

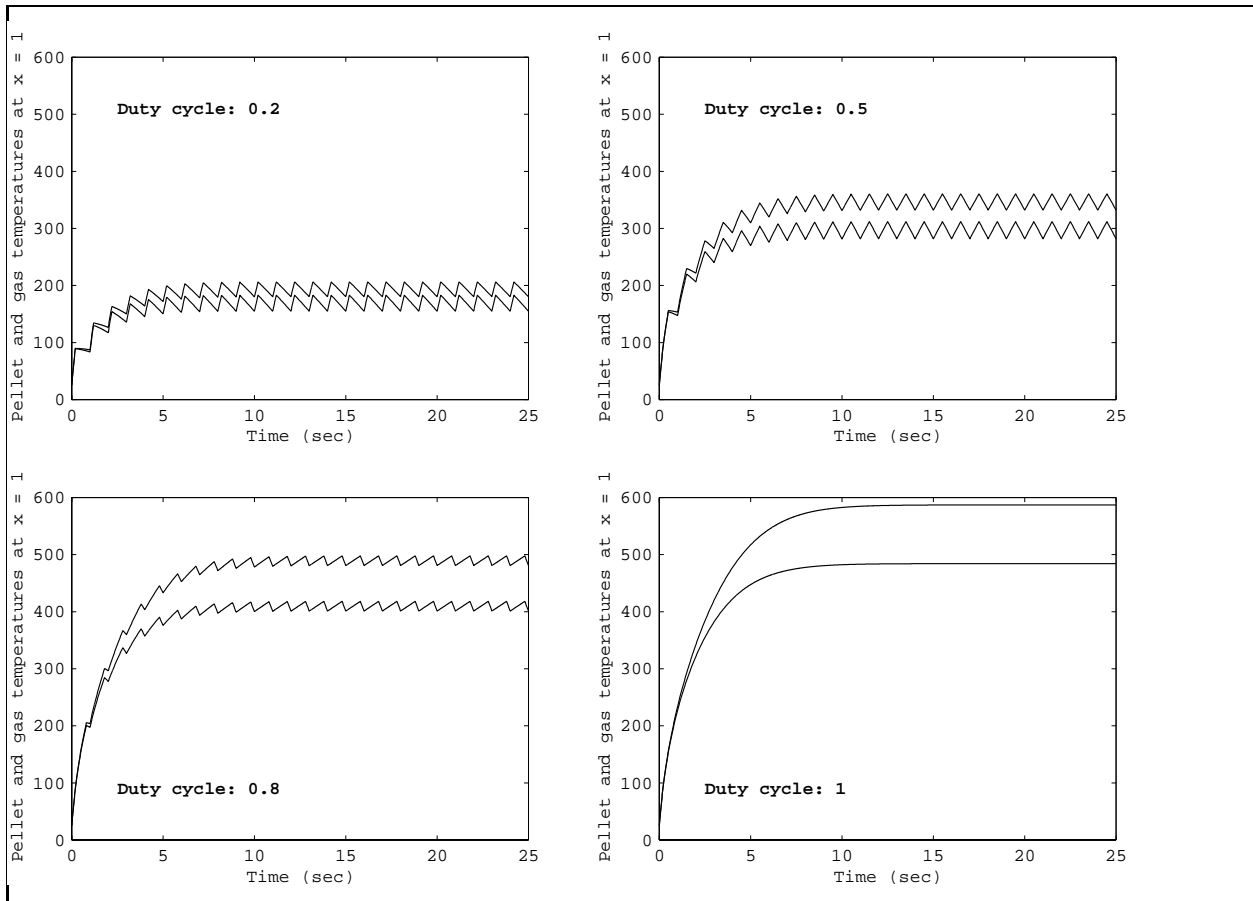


Figure 4.12: Effect of the duty cycle value on the gas temperature and on the pellet temperature. The period of the pulsation is one second and $E_{\text{rms}} = 6 \cdot 10^4$ V/m.

Influence of the Electric Field Strength With Respect to z

Knowing the reaction rates are temperature-dependent and assuming the chemical transformation takes place at the immediate vicinity of the pellets and also inside them (indeed, the pellets are porous), i.e. $T_{\text{gas}} = T_{\text{pellets}}$, we are interested in maintaining the same pellet temperature throughout the bed. This is impossible with a constant electric field with respect to the axial direction. On the contrary, a diminishing electric field with respect to z following a mathematical relationship allows a constant pellet temperature, but ΔT tends to narrow as the gas flows to the top (figure 4.13).

For this case, a third order polynomial for the electric field yields an almost constant pellet temperature in the bed. The limitation of this method resides in the fact that the determination of the coefficients of the polynomial can only be done by visualisation of the plots (gas and pellet temperatures). Another possibility is to modify the heat generation using loops in the program to obtain a constant pellet temperature, but it might be technically impossible to set different electric field strengths for any axial location (see Fig. 4.14).

The code also allows us to give any shape to the pellet temperature versus position curve, unless it violates the condition that $T_{\text{pel}} > T_{\text{gas}}$. For some cases and only during the transient period, the gas temperature can exceed the pellet temperature, i.e. the gas heats the pellets. Figure 4.5.3 shows some arbitrary pellet temperature profiles: the temperature profile of the pellets, on the upper left hand side, has a parabolic shape, but where the gas and the pellet temperature become equal on the decreasing side. The pellet temperature profile, on the upper right hand side, is a straight line going from 300°C to 600°C. By contrast, the plot of the lower right hand side shows a linearly decreasing pellet temperature, but the gas and the pellet temperature become equal at the middle of the bed. Finally, the last pellet temperature profile has a stair-like shape. The electric field that give these pellet temperature profiles are given by figure 4.16. These electric fields are roughly proportional to the temperature differences of the various plots of figure 4.5.3.

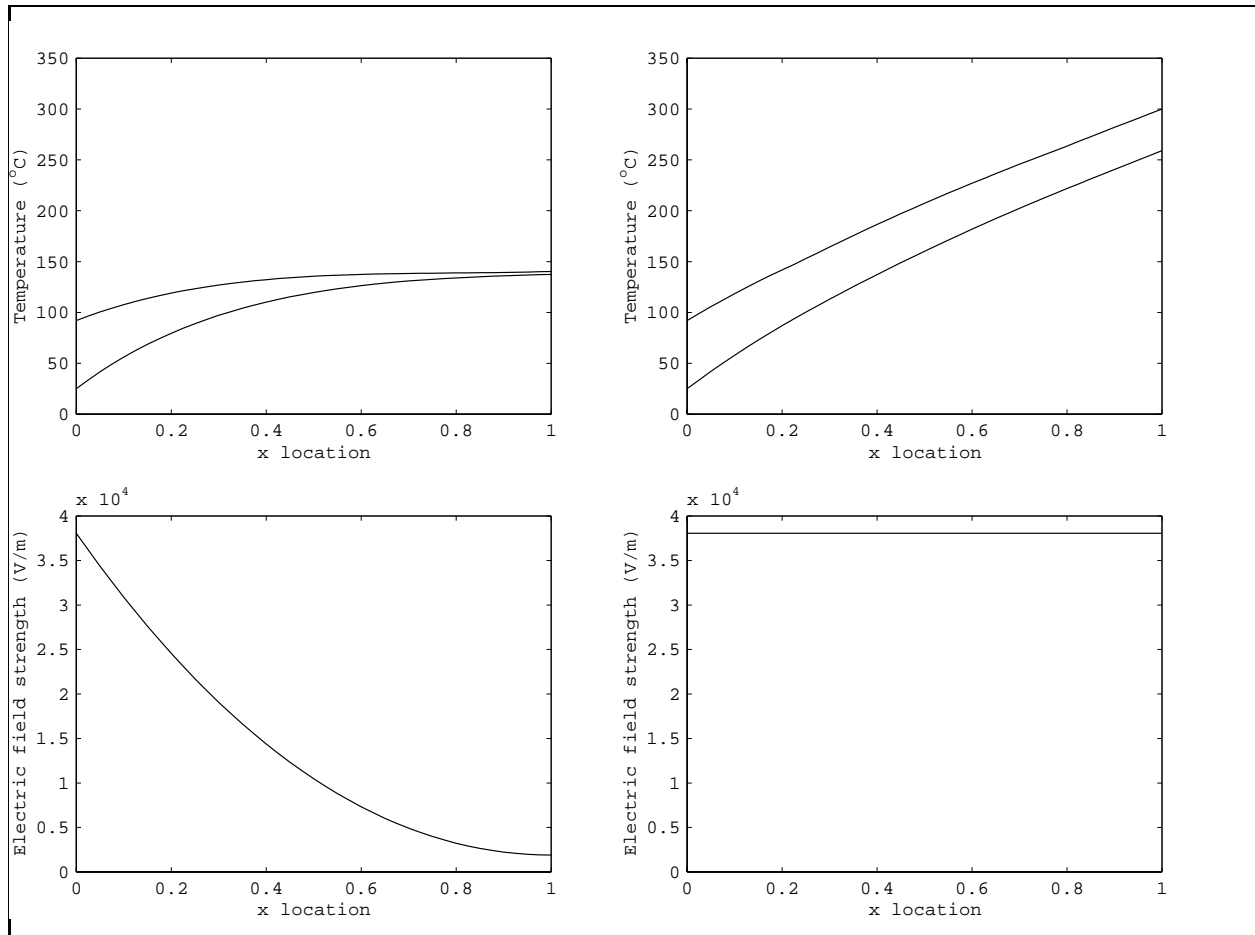


Figure 4.13: The left side of this figure shows a electric field varying by means of a third order polynomial, $E(z) = 3.75 \cdot 10^4(-0.1x^3 + 1.15x^2 - 2x + 1)$ V/m, with the temperature profile of the gas and the pellet above. On the right side, the electric field is uniform, yielding almost constantly rising gas and pellet temperature. $E_{rms} = 3.75 \cdot 10^4$ V/m.

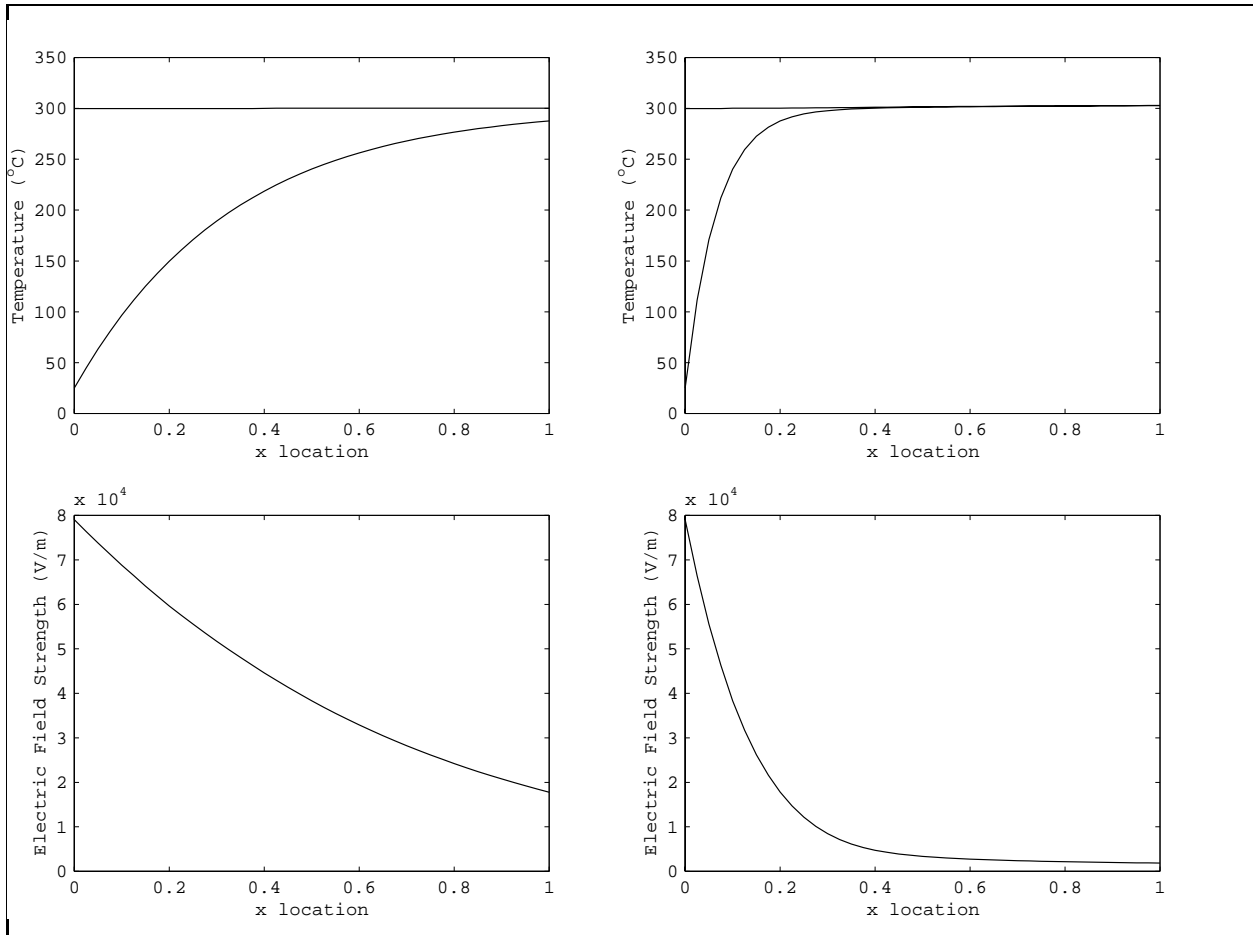


Figure 4.14: Gas and pellet temperature profiles, with their respective electric field underneath, for a one-inch bed (right hand side) and for a five-inch bed (left hand side). For the temperature profiles, the pellet temperature is the upper curve and the gas temperature is the lower curve. For the two cases, $d_p = 3.3\text{mm}$ and $v_g = u_{mf}$.

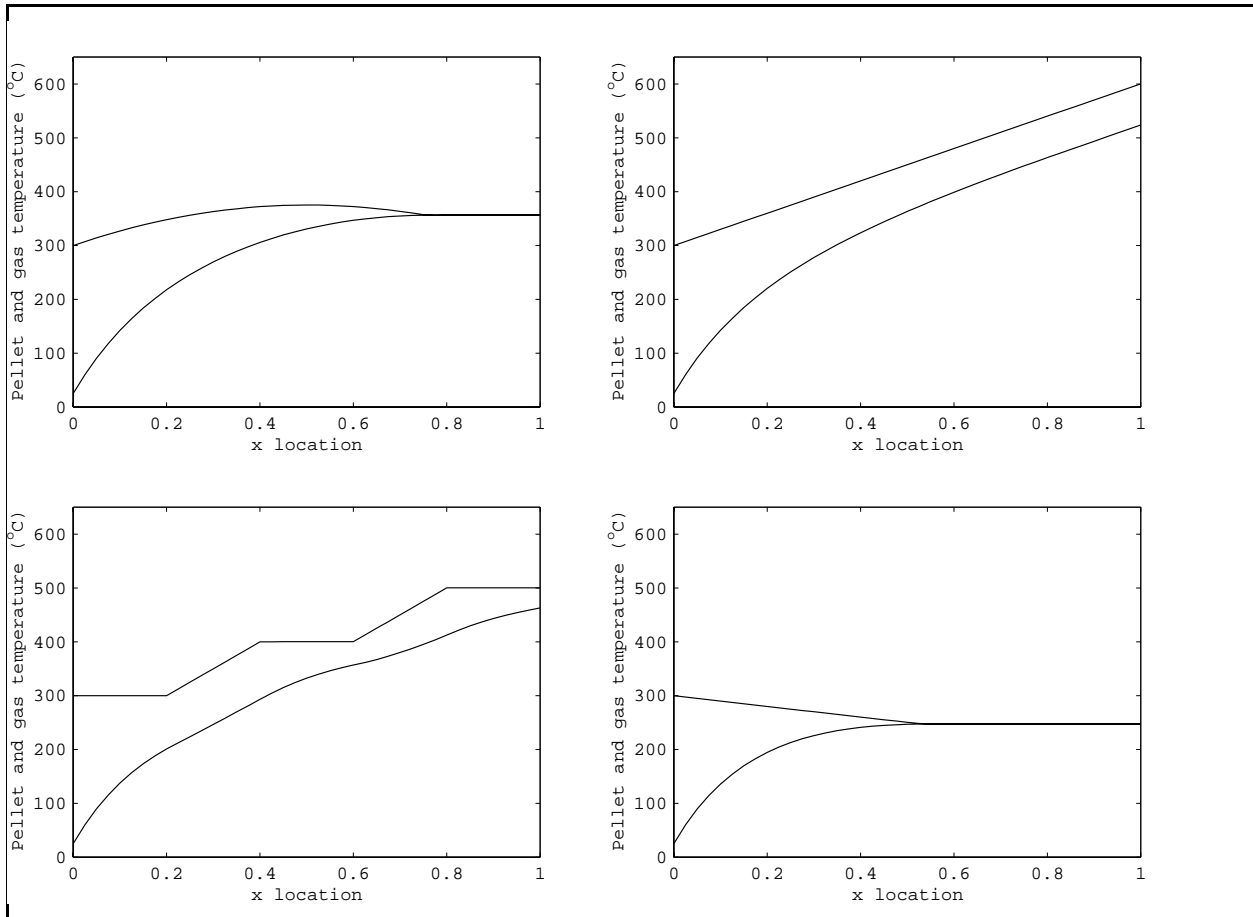


Figure 4.15: Gas and pellet temperatures for a few shapes. For each plot, the pellet temperature is the upper curve and the gas temperature is the lower curve.

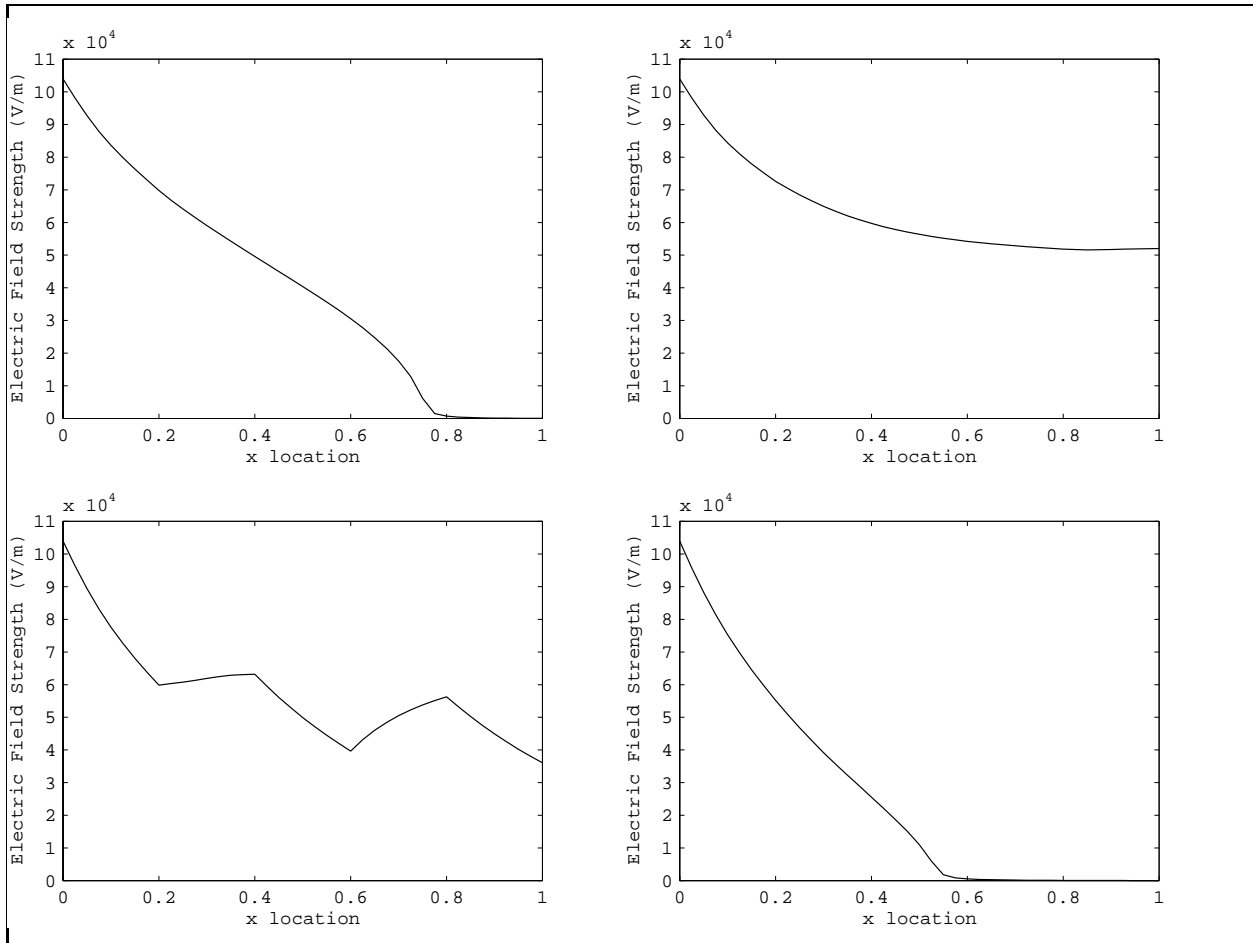


Figure 4.16: These electric field give the temperature profiles of figure 4.5.3.

4.6 Comparison of the Temperature Rise for Different Heights of Pellets in the Fluidized Bed.

As expected, the greater the height of pellets, the higher the exiting gas temperature, as shown in Fig. 4.17. A comparison between different cases shows the non-linearity of the temperature rise evolution with respect to the axial position in the fluidized bed, i.e. a downward concavity is evident. This can be explained by the decrease in the dielectric loss of γ -alumina as the temperature rises. Indeed, the α -alumina (not shown here), whose dielectric loss increases with temperature, shows a concavity directed upwardly. For the same reason, ΔT decreases as the temperature increases. An increasing height of pellets also increases the time required to reach steady-state (see Fig. 4.18). Above all, there is a longer period of time where $T_{\text{gas}} = T_{\text{pel}}$.

In terms of the temperature of 300°C that we want to obtain, a higher height of pellets means a smaller temperature gradient along the x-direction, i.e. the electric field strength needs to be reduced. Previously, we showed that a smaller electric field strength yields a smaller temperature difference between the gas and pellets, therefore, the increase of the height of the bed leads inevitably to a smaller ΔT .

For a large-scale application, a constant electrical field with respect to the axial location means a weak electric field and a much smaller temperature difference between the materials and the gas; if we are interested in getting a constant pellet temperature through the bed, the electrical field must strongly decrease at the bottom of the bed, and then vanish in order to maintain the pellet temperature constant. However, the heat losses, no longer negligible for large scale installations, would require a constant but probably weak electrical field such that the heat generated compensates the losses. One could also consider adding a cooling system within the bed such that the need for the heat generation promotes the temperature difference between the gas and the pellets. Anyway, a cooling system is necessary to absorb the heat released by the exothermic chemical reactions. *A contrario*, an endothermic chemical reaction is more adapted to show the microwave heating efficiency. Obviously, the cooling fluid could not be water, or any strong microwave absorber.

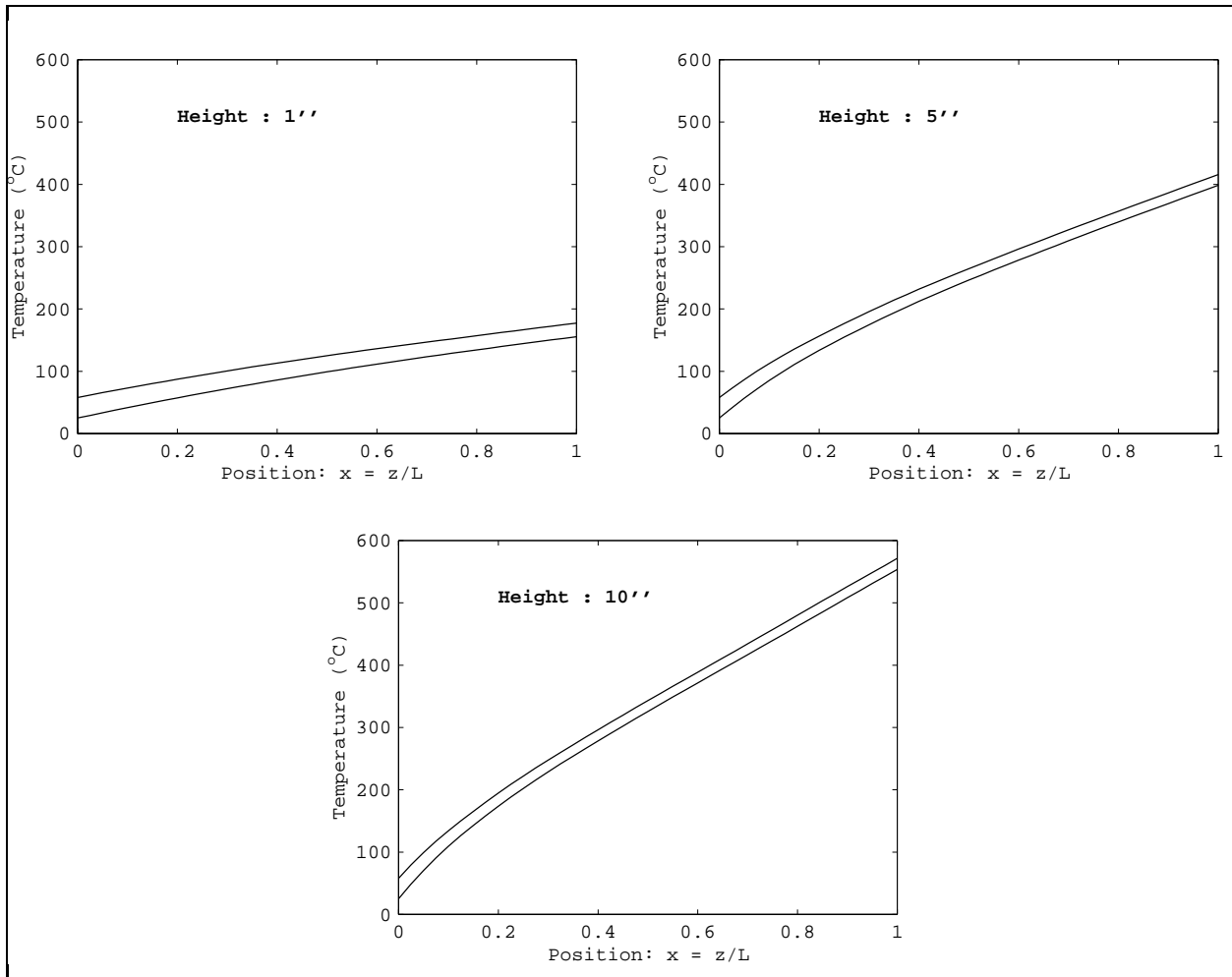


Figure 4.17: Effect of the bed height on the temperature profiles. For each plot, the pellet temperature is the upper curve and the gas temperature is the lower curve. $E_{\text{rms}} = 2.5 \cdot 10^4 \text{ V/m}$.

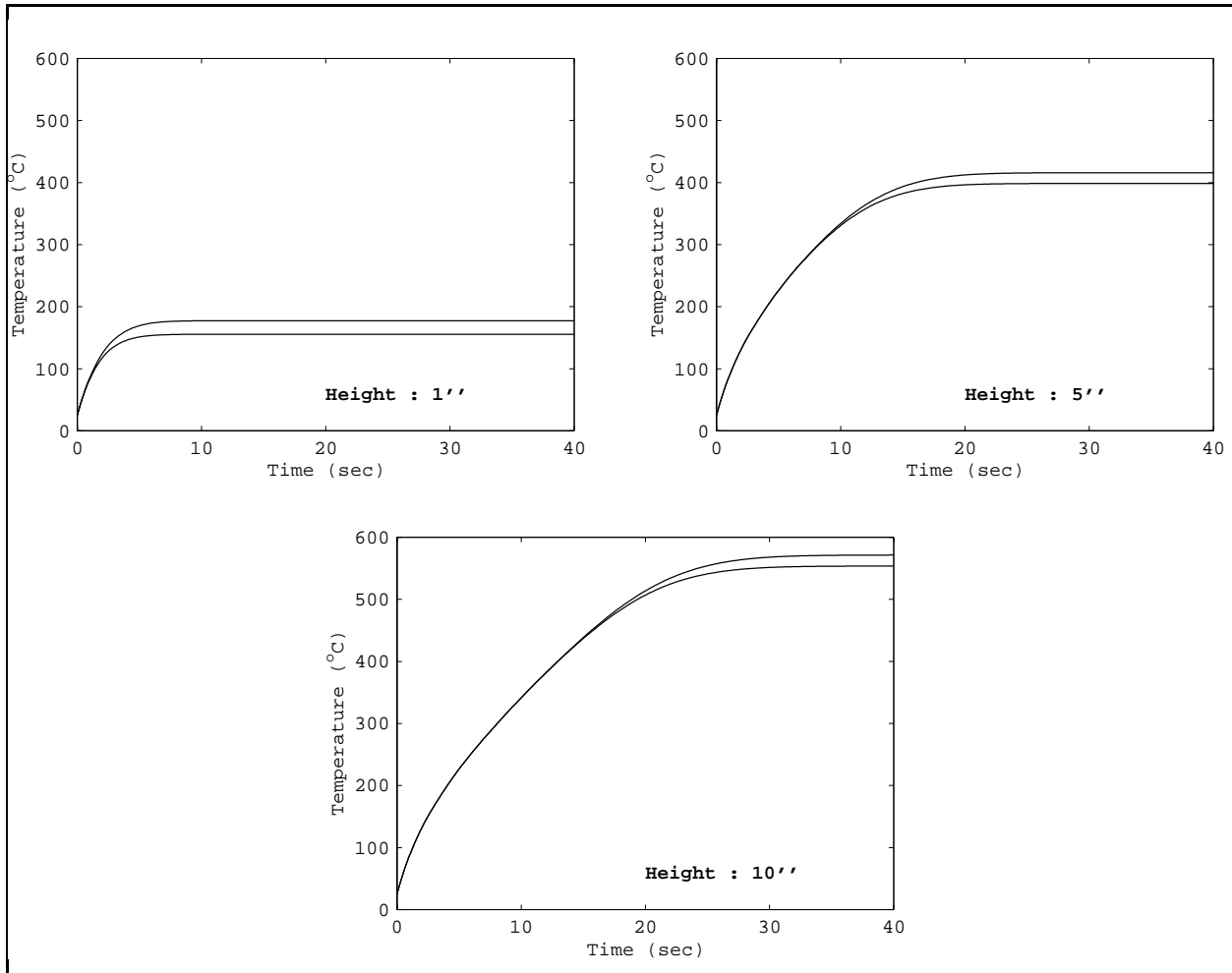


Figure 4.18: Effect of the bed height on the steady-state temperature rise of the pellets and of the gas, as a function of time. $E_{\text{rms}} = 2.5 \cdot 10^4 \text{ V/m}$.

Table 4.11: Effect of the bed height on ΔT for 0.5mm pellets. The electric field strength is set such that the pellets located at the exit have a temperature of $T_{\text{pel}} = 300^\circ\text{C}$.

Beg height (inch)	Electric field strength (V/m)	ΔT ($^\circ\text{C}$)
1	9749	25.0
2	7056	13.1
3	5852	9.0
4	5139	7.0
5	4657	5.7
6	4306	4.9
8	3823	3.9
10	3504	3.2

Table 4.12: Effect of the bed height on ΔT for 3.3mm pellets. The electric field strength is set such that the pellets located at the exit have a temperature of $T_{\text{pel}} = 300^\circ\text{C}$.

Bed height (inch)	Electric field strength (V/m)	ΔT ($^\circ\text{C}$)
1	37336	39.4
2	27141	20.9
3	22459	14.4
4	19651	11.0
5	17736	9.0
6	16329	7.6
8	14372	5.9
10	13055	4.9

Chapter 5

Design of an Optimized Fluidized Bed

The aim of this paper is to study the amplitude of the temperature difference expected by the microwave heating of a chemical fluidized bed reactor to heat the pellets.

From what has been done until now, we can point out two major ideas: it is possible to maintain a relatively high temperature difference when the electrical field strength is constant with respect to the axial direction, but the pellet temperature does not remain constant along this direction, which is not desirable for a chemical reaction; it is possible to compute a electric field capable of producing a constant pellet temperature through the bed, but the temperature difference shrinks as the gas flows to the top.

Consequently, two sections are devoted to the recapitulation of these two aspects, by tabulating calculations made for several varying parameters: the bed height, the gas velocity and the pellet diameter. The third one tries a compromise by fixing a range of pellet temperature evolving from 300°C for the ones located at the bottom of the bed to 350°C for the ones located at the top. Given the caution mentioned previously, these tables do not claim to give an exact solution. Rather, their purpose is to show the trends to expect. The parameters presented in these three tables also try to take into account the remarks concerning the experimental difficulties forecast in the literature review section: the modification of the local electrical field because of the motion of the pellets (20) and the risk of carry-over for too high gas velocities.

5.1 Constant Electric Field with Respect to the Axial Direction

After the description of the Geldart groups in a previous section, it seems that the Geldart A and B particles have the most interesting characteristics in terms of the quality of the fluidization, but Geldart B particles allow greater ΔT than Geldart A particles. Table 5.1 presents a few computations for different cases, to get a better idea of where the optimum should lie. If we consider the primary goal of a chemical bed reactor, i.e. obtaining chemical products with the best conversion and reaction rates which requires a low gas velocity able to allow the gaseous molecules to be in contact long enough times with the catalyst, the group D particles should be discarded. However, using small particles in a microwave heated fluidized bed experiment, Roussy et al. (20) observe that the motion makes the modeling difficult and interferes with the electric field distribution; however, this problem will probably also occur for big moving pellets.

According to the Kunii and Levenspiel chart(57), with a difference in density between the gas and the particle of 0.7g/cm^3 , we are in the group B classification as long as the particle diameter doesn't exceed 1mm.

We must also fit the pellet diameter with the gas velocity: if the gas velocity is too much above the minimum fluidization velocity, we risk carryover, or a somewhat erratic particle movement, which isn't desired. The gas velocity corresponding to the carryover limit, however, moves with the Geldart group: it is closer to the fluidization velocity for Geldart D particles than it is with the Geldart B particles, in terms of the ratio of the gas velocity to the minimum fluidization velocity for the system considered. This is another reason to discard the Geldart D particles. Therefore, we must choose a pellet diameter as high as possible, but still in the Group B classification.

Finally, we must keep in mind that the higher the electric field strength, the greater the ΔT . So we have to associate the gas velocity with the electric field strength and the height of the bed. If the bed height is too great, we obtain high exiting temperatures, and we have to diminish the electric field strength, i.e. we indirectly diminish ΔT .

The conclusion is that there exist many combinations and the best choice depends on what we want to emphasize. If a great ΔT is wanted, a small height and therefore a quite large electric field will be required, and/or a small gas velocity. However, in a large-scale chemical reactor, the calculation of the height of pellets is a problem that will not rely on temperature considerations, but rather on the ability of the system to perform given reaction rates.

Table 5.1: Effect of the particle diameter, the bed height, the gas velocity and the electric field strength on ΔT , for a constant electric field with respect to the axial direction, such that $T_{\text{pel}} = 300^\circ\text{C}$ at the exit of the bed. The 0.5mm pellets belong to the group B of the Geldart classification whereas the 1.4 and 2.3mm pellets belong to the group D.

d_p (mm)	L (inch)	$\frac{v_g}{u_{mf}}$	E_{rms} (V/m)	ΔT_{exit} ($^\circ\text{C}$)
0.5	1	1	9749	25.0
1.4	1	1	23829	29.5
2.3	1	1	31932	34.3
0.5	1	4	19772	17.0
1.4	1	4	48366	20.1
2.3	1	4	64958	28.4
0.5	1	7	26302	14.5
1.4	1	7	64342	17.2
2.3	1	7	84909	38.4
0.5	4	1	5139	7.0
1.4	4	1	12531	8.2
2.3	4	1	16786	9.6
0.5	4	4	10557	4.9
1.4	4	4	25647	5.7
2.3	4	4	33833	7.6
0.5	4	7	14160	4.2
1.4	4	7	34310	4.9
2.3	4	7	44247	10.2
0.5	7	1	4037	4.3
1.4	7	1	9791	5.0
2.3	7	1	13061	5.8
0.5	7	4	8437	3.1
1.4	7	4	20326	3.6
2.3	7	4	26347	4.6
0.5	7	7	11421	2.8
1.4	7	7	27391	3.1
2.3	7	7	34213	6.1

5.2 Constant Pellet Temperature Through the Bed

Still concerned by the quality of the fluidization, we keep using the Geldart B particles, preferred to the Geldart A particles because of the higher ΔT they allow. To achieve a constant pellet temperature throughout the bed, a loop has been added to the program. Starting from an arbitrary electric field value, the local electric field value is adjusted by calculating the gap between the desired temperature and the actual temperature. Then, the local electric field strength is diminished or increased proportionally and finally converges to the necessary value to achieve the desired temperatures.

Table 5.2 gathers some calculations for the mean temperature differences between the gas and the pellets and for the mean electric field in the bed, although the later, used for comparison only, makes no sense. These computations are made for judiciously chosen parameters likely to be encountered in reality, with the exception that for big pellets (2.3mm), a value of 7 for the ratio of the gas velocity to the minimum fluidization velocity may be too high. Thus, the ratio of the gas velocity to the minimum fluidization velocity is included between 1 and 7 while the pellet diameter ranges between 0.5 and 2.3mm. Although the study of the parameters was previously done by using a uniform electric field, most conclusions of the previous sections also apply to a varying electric field. However, in light of table 5.2, a few comments can be added. Looking at the results, we see that a larger height of pellets makes the bed having a larger region with a very small ΔT . A larger pellet diameter allows a larger ΔT average. A greater gas velocity leads to a greater removal of heat, so the electric field gets automatically increased by the code. Consequently, contrary to the case where the electric field was constant, ΔT is very gas-velocity dependent.

In table 5.2 and 5.3, the temperature difference is expressed in terms of the mean temperature, calculated by summing the ΔT of all the nodes, and then dividing this sum by the number of nodes.

Table 5.2: Effect of the particle diameter, the bed height, the gas velocity and the electric field strength on ΔT , for a varying electric field such that $T_{\text{pel}} = 300^\circ\text{C}$ at any location. The 0.5mm pellets belong to the group B of the Geldart classification whereas the 1.4 and 2.3mm pellets belong to the group D.

d_p (mm)	L (inch)	$\frac{v_g}{u_{mf}}$	E_{rms} (V/m)	ΔT_{mean} ($^\circ\text{C}$)
0.5	1	1	8401	34.0
1.4	1	1	21404	40.3
2.3	1	1	30340	47.3
0.5	1	4	14422	22.5
1.4	1	4	36921	26.7
2.3	1	4	58523	44.2
0.5	1	7	17808	19.1
1.4	1	7	47746	22.9
2.3	1	7	85122	59.9
0.5	4	1	2870	9.0
1.4	4	1	6889	10.6
2.3	4	1	9646	12.4
0.5	4	4	4821	6.0
1.4	4	4	11593	7.1
2.3	4	4	17928	11.5
0.5	4	7	5929	5.2
1.4	4	7	14241	6.1
2.3	4	7	26302	15.5
0.5	7	1	1943	5.4
1.4	7	1	4507	6.3
2.3	7	1	6220	7.3
0.5	7	4	3267	3.7
1.4	7	4	7577	4.3
2.3	7	4	11401	6.8
0.5	7	7	4016	3.2
1.4	7	7	9314	3.7
2.3	7	7	16444	9.1

5.3 A Compromise Between Two Requirements

It is likely that the reaction rates remain approximately equal or of the same order of magnitude in a certain interval of temperature. However, this interval can only be determined by a very good knowledge of the kinetics (initiation and propagation phases, ...) and the chemical phenomena of the catalysis (adsorption, desorption, ...). This observation suggests that a compromise can be found between a pellet temperature increasing constantly through the bed and allowing a quite large ΔT , and a constant pellet temperature permitting constant reaction rates but a small ΔT . Therefore, the purpose of table 5.3, designed similarly to table 5.2, is to gather calculations such as the pellet temperature is forced to increase linearly from 300°C to 350°C. The table is also made with parameters likely to be encountered in reality, with the exception that for big pellets (2.3mm), a value of 7 for the ratio of the gas velocity to the minimum fluidization velocity may be too high.

As expected, the model yields higher average temperature differences and higher average electric field values than table 5.2, and we see well an increase of the temperature difference that ranges from 10 to 20%.

Table 5.3: Effect of the particle diameter, the bed height, the gas velocity and the electric field strength on ΔT , for a pellet temperature rising constantly through the bed (300°C to 350°C). The 0.5mm pellets belong to the group B of the Geldart classification whereas the 1.4 and 2.3mm pellets belong to the group D.

d_p (mm)	L (inch)	$\frac{v_g}{u_{mf}}$ (V/m)	E_{rms}	ΔT_{mean} ($^{\circ}\text{C}$)
0.5	1	1	10330	39.5
1.4	1	1	26079	46.9
2.3	1	1	35998	54.9
0.5	1	4	19366	26.4
1.4	1	4	48752	31.3
2.3	1	4	71457	50.2
0.5	1	7	24794	22.3
1.4	1	7	62877	26.9
2.3	1	7	98749	67.8
0.5	4	1	4220	10.5
1.4	4	1	10585	12.4
2.3	4	1	14605	14.5
0.5	4	4	8027	7.1
1.4	4	4	20081	8.3
2.3	4	4	28843	13.2
0.5	4	7	10431	6.1
1.4	4	7	26044	7.2
2.3	4	7	39930	17.8
0.5	7	1	3003	6.3
1.4	7	1	7478	7.3
2.3	7	1	10269	8.6
0.5	7	4	5793	4.3
1.4	7	4	14371	5.0
2.3	7	4	20328	7.8
0.5	7	7	7577	3.7
1.4	7	7	18740	4.4
2.3	7	7	27907	10.4

Chapter 6

Conclusions and Recommendations

6.1 Conclusions

Using 3.3 mm-pellets at the minimum fluidization velocity, we demonstrated the possibility of significant temperature differences between the gas and the pellets. The study of the major parameters shows that α -alumina isn't suitable for experiments because of the thermal runaway. Platinum catalyst particles have very little effect on the heat generation strength for γ -alumina pellets. Large pellet diameters, with diameters bigger than 1mm, allow greater ΔT , but make fluidization more difficult, while small particles, with diameters smaller than 0.3mm, don't achieve significant enough ΔT . In terms of the Geldart classification, the Geldart B particles fit the best for our concerns. The Geldart A particles don't achieve sufficiently high temperature differences. When the electric field is uniform, greater gas velocities do not affect ΔT , but will decrease the overall temperature of the gas and the pellets, as well as the reaction rate, assuming that for most hydrocarbon reactions, reaction rates get larger as the temperature is higher. Modified pellet densities move the boundaries between the Geldart groups: a higher density makes fluidization more difficult, whereas lighter pellets tend to widen the suitable zone.

With uniform electric field, greater heights of pellets favour a smaller ΔT , due to the diminishing dielectric loss of γ -alumina with respect to T . When T_{pel} is fixed, the section where T_{gas} approaches T_{pel} becomes longer, and therefore makes ΔT smaller. A greater height of pellets requires more time to reach steady state, i.e. there is a longer period of time where temperature differences are small.

Moreover, a few interesting correlations directly link the important parameters and the

temperature difference between the gas and pellets, but only for particles smaller than about 0.8mm in diameter.

During experiments, a few difficulties will likely be encountered: large gas flow rates will be required to fluidize the bed; the erratic movement of the pellets in the fluidized bed will probably be a very deleterious effect for velocities higher than the minimum fluidization velocity and height of pellets greater than approximately 2cm. The high flow rates will produce low reaction rates. The measurement of the pellet temperature will be a challenging task. Neglecting the heat losses due to radiation and the release or the absorption of heat due to the chemical reactions may lead to errors, especially for low gas velocities, given that the removal of heat by convection is reduced. For a uniform electric field with respect to the axial direction, the temperature gradient along the axial direction of the bed will be dramatic. Knowing the reaction rates are very temperature-dependent, chemical kinetics will be different at the bottom than or at the top of the bed. This will make such a fluidized bed a complicated chemical reactor. It will be technically difficult to generate an electric field varying axially to produce uniform pellet temperature. The assumption that the temperature difference between the flowing gas and the pellets has an effect on the chemical reactions within a fluidized bed should be carefully studied knowing that the outside surface of spherical pellets, where ΔT has been computed, is small compared to the internal surface obtained by the presence of porosities, where ΔT is very likely to be equal to 0.

However, the measurement of the exiting gas temperature should be a good indicator of the model accuracy. For small heights of 3.3mm-pellets, the erratic movement due to the fluidization state shouldn't be too disturbing.

For a uniform electric field with respect to the axial direction, the model showed that we had a margin for the pellets diameter, i.e. a smaller ΔT than the one we get for 3.3 mm pellets, would still be suitable for hydrocarbon reactions. This is true for the $500\mu\text{m}$ pellets that belong to the Group B and should still yield a appreciable ΔT . Unfortunately, such beds are not interesting because the pellet temperature along the axial direction varies too much, which is not desirable for chemical reaction.

By modifying axially the shape of the electric field, we can obtain any meaningful pellet temperature profile. For axially uniform pellet temperatures, ΔT shrinks to almost 0°C . Therefore, a compromise has been found, following the requirements evoked earlier. The most interesting particles are the ones that are fluidized easily, and that allow a minimum temperature difference

between the gas and the pellets. Depending on what is considered important (quality of fluidization or ΔT), the pellet diameter can be changed from $500\mu\text{m}$ to 4mm , the inlet gas velocity from u_{mf} to $10u_{\text{mf}}$. Finally, a large bed height leads inevitably to a very small ΔT .

6.2 Limitations and recommendations

Much work remains to be done on microwave heating in chemical fluidized beds: this model could be improved by using an electric field model accounting for the geometry of the waveguide and the motion of the pellets; then the validation of the assumptions, especially for the convection coefficient correlations made all along this work, is indispensable. Finally, microwave heating can be a powerful tool to deepen the knowledge on heat transfer in fluidized bed, by offering an alternative to the experimental methods usually used to correlate the main parameters of the fluidized bed and the heat transfer.

Bibliography

- [1] J.K.S. Wan and M.C. Depew *International Conference on Microwave Chemistry* Institute of Chemical Process Fundamentals, Academy of Sciences of the Czech Republic, Prague, ISBN 80-86186-01-6 J. Čermák, M. Hájek, J. Hetflejš and J. Včelák eds., PL7.
- [2] D.A.C. Stueriga and P. Gaillard *Journal of Microwave Power and Electromagnetic Energy*, **31**:2, 87–113 (1996).
- [3] G. Nimtz, P. Marquart and H. Gleiter *Journal of Crystal Growth*, **86**, 66 (1988).
- [4] G. Roussy and J.A. Pearce (1995) *Foundations and Industrial Applications of Microwaves and Radio Frequency Fields*. John Wiley & Sons Ltd, West-Sussex, England, p 318–323.
- [5] Y. Polsky and Y. Bayazitoglu *Journal of Heat Transfer*, **117**, 751 (1995).
- [6] M.M.R. Williams and S.K. Loyalka (1991) *Aerosol Science Theory and Practice*. Pergamon, Oxford, United Kingdom.
- [7] J.E. Lanz (1998) *A Numerical Model of Thermal Effects in a Microwave Irradiated Catalyst Bed* M.S. Thesis, Virginia Polytechnic Institute and State University, Blacksburg (1998).
- [8] D.M.P. Mingos *International Conference on Microwave Chemistry* Institute of Chemical Process Fundamentals, Academy of Sciences of the Czech Republic, Prague, ISBN 80-86186-01-6 J. Čermák, M. Hájek, J. Hetflejš and J. Včelák eds., PL1.
- [9] D.O. Hayward, D.M.P. Mingos and X. Zhang *Unpublished results* (1998).
- [10] J.R. Thomas Jr. *Catalysis Letters*, **49**, 137–141 (1997).
- [11] J. Jacob and L.H.L. Chia *Journal of Materials Science*, **30**:21, 5321–5327 (1995).
- [12] R.N. Gedye, F.E. Smith and K.C. Westaway *Canadian Journal of Chemistry*, **66**, 17 (1988).

- [13] D.R. Baghurst, D.M.P. Mingos and M.J. Watson *Journal of Organometallic Chemistry*, **368**, C43 (1989).
- [14] J.K.S. Wan *Research on Chemical Intermediates*, **19**:2, 147–158 (1993).
- [15] M.S. Ioffe, S.D. Pollington and J.K.S. Wan *Journal of Catalysis*, **151**, 349–355 (1995).
- [16] G. Roussy, S. Hilaire, J.-M. Thiébaud, G. Maire, F. Garin, S. Ringler *Applied Catalysis A: General*, **156**, 167–180 (1997).
- [17] K.R. Baker, E. Marand and J.D. Graybeal *PMSE*, **66**, 422 (1990).
- [18] E. Marand, K.R. Baker and J.D. Graybeal *Macromolecules*, **25**, 2243 (1992).
- [19] F. Chemat, E. Esveld, M. Poux and J.-L. Di Martino *Journal of Microwave Power and Electromagnetic Energy*, **33**:2, 88–94 (1998).
- [20] G. Roussy, S. Jassm, and J.-M. Thiébaud *Journal of Microwave Power and Electromagnetic energy*, **30**:3, 178–187 (1995).
- [21] O. Molerus *Powder Technology*, **70**, 4 (1992).
- [22] O. Molerus *Powder Technology*, **70**, 7–13 (1992).
- [23] C. Gibson, I. Matthews and A. Samuel *Journal of Microwave Power and Electromagnetic Energy*, **23**, 17 (1988).
- [24] J.C. Hedrick, D.A. Lewis, G.D. Lyle, S.D. Wu, T.C. Ward and J.E. McGrath *PMSE*, **60**, 438 (1989).
- [25] W.H. Hayt Jr. (1989) *Engineering Electromagnetics*, 5th ed. McGraw-Hill Book Company, New-York .
- [26] G. Roussy and J.A. Pearce (1995) *Foundations and Industrial Applications of Microwaves and Radio Frequency Fields*. John Wiley & Sons Ltd, West-Sussex, England, p 258–328.
- [27] D.M.P. Mingos and D.R. Baghurst *Chemical Society Reviews*, **20**, 1 (1991).
- [28] D. Kunii and O. Levenspiel (1991) *Fluidization Engineering*, 2nd ed. Butterworth-Heinemann, Boston, p 77–79.

- [29] J.R. Grace and H. Bi (1997) *Circulating Fluidized Beds*, J. R. Grace, A. A. Avidan and T. M. Knowlton (eds.), p 8.
- [30] D. Kunii and O. Levenspiel (1991) *Fluidization Engineering*, 2nd ed. Butterworth-Heinemann, Boston, p 69.
- [31] J.F. Davidson and D. Harrison (1963) *Fluidized Particles* Cambridge University Press, New-York.
- [32] S. Mori and C.Y. Wen *A.I.Ch.E Journal*, **21**, 109 (1975).
- [33] J.F. Davidson and B.O.G. Schüler *Trans. Inst. Chem. Eng*, **38**, 335 (1960).
- [34] D. Geldart *Powder Technology*, **7**, 285 (1973), **19**, 133 (1978).
- [35] D. Geldart and A.R. Abrahamsen *Powder Technology*, **19**, 133–136 (1978).
- [36] P.S.B. Stewart and J.F. Davidson *Powder Technology*, **1**, 61–80 (1967).
- [37] A.R. Abrahamson and D. Geldart *Powder Technology*, **26**, 35–47 (1980).
- [38] N.I. Gelperin and V.G. Einstein (1971) *Fluidization* J.F. Davidson and D. Harrison eds., Academic Press, London, p 471.
- [39] D. Kunii and O. Levenspiel (1969) *Fluidization Engineering*, 2nd ed. Wiley, New-York, chapter 7.
- [40] A.K. Kothari *M.S. Thesis, Illinois Institute of Technology*, Chicago (1967).
- [41] A.M. Xavier and J.F. Davidson *Fluidization*, 2nd ed. J.F. Davidson R. Clift and D. Harrison eds., Academic Press, London, p 456–457.
- [42] D. Kunii and J.M. Smith *A.I.Ch.E Journal*, **7**, 29 (1961).
- [43] D. Kunii and O. Levenspiel (1991) *Fluidization Engineering*, 2nd ed. Butterworth-Heinemann, Boston, p 271–274.
- [44] W.E. Ranz *Chemical Engineering Progress*, **48**, 297 (1952).
- [45] D.J. Gunn *International Journal of Heat and Mass Transfer*, **21**, 467 (1978).
- [46] N. Wakao, S. Kaguei and T. Funazkri *Chemical Engineering Science*, **34**, 325–336 (1979).

- [47] V. Vaněček, M. Markvart and R. Drbohlav *Fluidized Bed Drying*, I.L. Hepner ed., Chemical and Process Engineering Series, London, p 44–45.
- [48] J.S. Walton, R.L. Olson and O. Levenspiel *Ind. Eng. Chem.*, **44**, (1952).
- [49] N.I. Siriomiaticnikov and V.F. Volkov (1959) *Protzessi v Kipyashchem Sloye* Metalurgizdat, Sverdlovsk.
- [50] A. Mathur *International Journal of Heat and Mass Transfer*, **33**:9, 1929–1936 (1990).
- [51] Engelhard Corporation, Chemical Catalysts Group, 554 Engelhard Drive - Seneca, South Carolina, 29768 - USA.
- [52] G. Roussy and J.A. Pearce (1995) *Foundations and Industrial Applications of Microwaves and Radio Frequency Fields*. John Wiley & Sons Ltd, West-Sussex, England, p 153.
- [53] O. Molerus and J. Schweinzer (1989) *Fluidization VI* J. R. Grace, L.W. Schmidt and M.A. Bergougnou (eds.), Engineering Foundation, New-York, p 685.
- [54] S. Gill *Proc. Cambridge Phil. Soc.*, **47**, 96–208 (1951).
- [55] W.H. Press, S.A. Teukolsky, W.T. Vetterling and B.P. Flannery (1992) *Numerical Recipes in Fortran 77, Second Edition: The Art of Scientific Computing* Cambridge University Press, Cambridge, UK, p 30,43.
- [56] D. Kunii and O. Levenspiel (1991) *Fluidization Engineering*, 2nd ed. Butterworth-Heinemann, Boston, p 69.
- [57] D. Kunii and O. Levenspiel (1991) *Fluidization Engineering*, 2nd ed. Butterworth-Heinemann, Boston, p 78.
- [58] C.R. Wilke *Journal of Chemical Physics*, **18**, 517–519 (1950).
- [59] F.P. Incropera and D.P. DeWitt (1990) *Fundamentals of Heat and Mass Transfer, Third Edition* John Wiley & Sons Inc., New-york, p A5–A7.
- [60] W.M. Kays and M.E. Crawford (1993) *Convective Heat and Mass Transfer, Third Edition* McGraw-Hill, Series in Mechanical Engineering, p548.

- [61] G. Van Wylen, R. Sonntag and C. Borgnakke (1994) *Fundamentals of Classical Thermodynamics, Fourth Edition* John Wiley & Sons Inc., New-york, p 745.
- [62] F.P. Incropera and D.P. DeWitt (1990) *Fundamentals of Heat and Mass Transfer, Third Edition* John Wiley & Sons Inc., New-york, p A17.
- [63] R.M. Roos and J.R. Thomas Jr. *Materials Research Society - Symposium Proceedings* Microwave Processing of Materials V ISBN 1-55899-333-9 M.F. Iskander, J.O Kiggans Jr. and J.-C. Bolomey eds., v430, p 345–350.
- [64] J.R. Thomas Jr. Importance of Dielectric Properties in Modeling of Microwave Sintering of Ceramics *Microwaves: Theory and Application in Materials processing III, CT59* American Ceramic Society, Ohio.
- [65] Mitchell Jackson (1997) *Personal communication*

Appendix A

Thermophysical Properties

A.1 Gas Mixture Formulae

Wilke (58) derived a semi-empirical formula that can be used to determine the gas conductivity and the gas viscosity of a mixture of gases:

$$\mu = \sum_{i=1}^n \frac{x_i \mu_i}{\sum_{j=1}^n x_j \Phi_{ij}}, \quad (\text{A.1})$$

in which

$$\Phi_{ij} = \frac{1}{\sqrt{8}} \left(1 + \frac{M_i}{M_j}\right)^{-\frac{1}{2}} \left[1 + \left(\frac{\mu_i}{\mu_j}\right)^{\frac{1}{2}} \left(\frac{M_j}{M_i}\right)^{\frac{1}{4}}\right]^2, \quad (\text{A.2})$$

where n is the number of chemical species in the mixture; x_i and x_j are the mole fractions of species i and j ; μ_i and μ_j are the viscosities of species i and j at the system temperature and pressure; and M_i and M_j are the corresponding molecular weights. Φ_{ij} is dimensionless and is equal to 1 when $i=j$.

For all the other thermophysical properties a simple weighted average is used.

A.2 Thermal Conductivities

A.2.1 Alumina

Table A.1: Thermal Conductivity of Aluminum Oxide (59)

Temperature (°C)	Thermal Conductivity (W/m.°C)
27	36
127	27
227	16
727	7.6
1227	5.4

A.2.2 Butane

Table A.2: Thermal Conductivity of Butane

Temperature (°C)	Thermal Conductivity (W/m.°C)
7	$1.38 \cdot 10^{-2}$
27	$1.61 \cdot 10^{-2}$
47	$1.84 \cdot 10^{-2}$
67	$2.08 \cdot 10^{-2}$
87	$2.33 \cdot 10^{-2}$
97	$2.45 \cdot 10^{-2}$
107	$2.57 \cdot 10^{-2}$
117	$2.71 \cdot 10^{-2}$
127	$2.84 \cdot 10^{-2}$
137	$2.97 \cdot 10^{-2}$
147	$3.10 \cdot 10^{-2}$
157	$3.24 \cdot 10^{-2}$
167	$3.38 \cdot 10^{-2}$
177	$3.52 \cdot 10^{-2}$
187	$3.66 \cdot 10^{-2}$
207	$3.95 \cdot 10^{-2}$
227	$4.24 \cdot 10^{-2}$
247	$4.55 \cdot 10^{-2}$
267	$4.86 \cdot 10^{-2}$
287	$5.17 \cdot 10^{-2}$
307	$5.49 \cdot 10^{-2}$
327	$5.80 \cdot 10^{-2}$

A.2.3 Helium

Table A.3: Thermal Conductivity of Helium (60)

Temperature (°C)	Thermal Conductivity (W/m.°C)
27	$1.56 \cdot 10^{-1}$
47	$1.64 \cdot 10^{-1}$
67	$1.71 \cdot 10^{-1}$
87	$1.78 \cdot 10^{-1}$
127	$1.90 \cdot 10^{-1}$
177	$2.08 \cdot 10^{-1}$
227	$2.22 \cdot 10^{-1}$
277	$2.38 \cdot 10^{-1}$
327	$2.53 \cdot 10^{-1}$
377	$2.68 \cdot 10^{-1}$
427	$2.81 \cdot 10^{-1}$
477	$2.86 \cdot 10^{-1}$
527	$3.09 \cdot 10^{-1}$
577	$3.23 \cdot 10^{-1}$
627	$3.36 \cdot 10^{-1}$
677	$3.49 \cdot 10^{-1}$
727	$3.62 \cdot 10^{-1}$
827	$3.86 \cdot 10^{-1}$
927	$4.10 \cdot 10^{-1}$

A.2.4 Platinum

Table A.4: Thermal Conductivity of Platinum (59)

Temperature (°C)	Thermal Conductivity (W/m.°C)
-73	72.6
127	71.8
327	73.2
527	75.6
727	78.7
927	82.6
1227	89.5

A.3 Heat Capacities

A.3.1 Alumina

Table A.5: Heat Capacity of Aluminum Oxide (59)

Temperature ($^{\circ}\text{C}$)	Heat capacity ($\text{J}/\text{kg}\cdot^{\circ}\text{C}$)
20	768.4
50	822.5
100	899.8
150	963.1
200	1015
300	1090
400	1139
500	1172
600	1196
700	1215
800	1233
900	1250
1000	1266
1100	1281

A.3.2 Butane

The butane heat capacity ($\text{J}/\text{kg}\cdot^{\circ}\text{C}$) is generated by a third-order polynomial (61):

$$C_{pC_4H_{10}}(T) = 68.03 + 638.6\theta - 31.54\theta^2 + 0.602\theta^3, \quad (\text{A.3})$$

where

$$\theta = \frac{T + 273.15}{100},$$

and T is expressed in $^{\circ}\text{C}$.

A.3.3 Helium

The helium heat capacity is constant with respect to temperature: $C_{p\text{He}} = 5193\text{J/kg}\cdot^\circ\text{C}$ (62).

A.3.4 Platinum

Table A.6: Heat Capacity of Platinum (59)

Temperature ($^\circ\text{C}$)	Heat capacity ($\text{J/kg}\cdot^\circ\text{C}$)
-73	125
127	136
327	141
527	146
727	152
927	157
1227	165

A.4 Dynamic Viscosities

A.4.1 Butane

Table A.7: Dynamic Viscosity of Butane

Temperature ($^{\circ}\text{C}$)	Dynamic Viscosity (Pa.s)
0	$6.84 \cdot 10^{-6}$
100	$9.26 \cdot 10^{-6}$
200	$1.17 \cdot 10^{-5}$
300	$1.40 \cdot 10^{-5}$
400	$1.64 \cdot 10^{-5}$
500	$1.87 \cdot 10^{-5}$
600	$2.11 \cdot 10^{-5}$

A.4.2 Helium

Table A.8: Dynamic Viscosity of Helium (60)

Temperature ($^{\circ}\text{C}$)	Dynamic Viscosity (Pa.s)
27	$1.99 \cdot 10^{-5}$
77	$2.22 \cdot 10^{-5}$
127	$2.43 \cdot 10^{-5}$
177	$2.64 \cdot 10^{-5}$
227	$2.84 \cdot 10^{-5}$
327	$3.22 \cdot 10^{-5}$
427	$3.59 \cdot 10^{-5}$
527	$3.94 \cdot 10^{-5}$
627	$4.28 \cdot 10^{-5}$
727	$4.62 \cdot 10^{-5}$
827	$4.94 \cdot 10^{-5}$
927	$5.25 \cdot 10^{-5}$
1027	$5.56 \cdot 10^{-5}$

A.5 Electric and dielectric properties

A.5.1 Electrical Conductivity of Bulk Platinum

The following formula calculates the temperature-varying electrical conductivity of platinum (7):

$$\sigma_b(T) = \frac{1}{\rho_0\alpha(T - T_0) + \rho_0}, \quad (\text{A.4})$$

where

ρ_0 : resistivity at 20°C (m/S),

α : resistivity coefficient ($^{\circ}\text{C}^{-1}$),

and

T_0 : base temperature (20°C).

The following formula calculates the size-varying electrical conductivity for metallic particles (3):

$$\sigma_{eff}(T) = \left(\frac{d_{par}}{5 \cdot 10^{-6}}\right)^3 \sigma_b(T) \quad (\text{A.5})$$

A.5.2 Dielectric Loss

α -alumina

Table A.9: Dielectric loss of α -alumina (63)

Temperature ($^{\circ}$ C)	Dielectric loss
25	0.00363
99	0.00395
184	0.00508
281	0.0068
356	0.00886
430	0.0112
562	0.0163
705	0.0224
800	0.0282
903	0.0358
973	0.0429
1025	0.0503
1050	0.0561
1089	0.0833
1132	0.114

γ -alumina

Table A.10: Dielectric loss of γ -alumina (63)

Temperature ($^{\circ}$ C)	Dielectric loss
29	0.3921
35	0.3893
149	0.231
262	0.1693
371	0.1528
478	0.1521
582	0.1514
684	0.1505
784	0.1493
881	0.1481
976	0.1421
1068	0.1311

A.5.3 Dielectric Constant

α -alumina

The dielectric constant (ϵ') is generated by a fourth-order polynomial (64):

$$\epsilon'(T) = 7.331 - 9.12 \cdot 10^{-4}T + 6.428 \cdot 10^{-6}T^2 - 6.531 \cdot 10^{-9}T^3 + 2.578 \cdot 10^{-12}T^4, \quad (\text{A.6})$$

where T is expressed in $^{\circ}\text{C}$.

γ -alumina

Table A.11: Dielectric constant of γ -alumina (65)

Temperature ($^{\circ}\text{C}$)	Dielectric constant
29	4.487
35	4.5
149	5.04
162	4.448
371	4.652
478	4.917
582	4.647
684	4.441
784	4.313
881	4.196
976	4.046
1068	3.717

Appendix B

Fortran code

This appendix is designed to make the computer program easily used by the non familiar user. It is composed of a section explaining the principle of each function or subroutine and describing the variables used throughout the model, a section in which the subroutines and the functions necessary to the modeling are listed, and a third one with three main programs that correspond to three versions.

The first version determines the temperature distribution for the parameters listed in the “parameters” file. The second version determines the electrical field distribution for the parameters listed in the “parameters” file and for the desired temperature distribution. The third version is more complete since it can determine the electrical field corresponding to the “paramaters” file and the desired temperature, run this electrical field with the same parameters, and then determine the temperature distribution within a single pellet at any given location and at any time, which should be specified by the user from the computer keyboard. Three subroutines will be added to this version.

B.1 Subroutine and Variable Description

bsigpt(tt) Calculates the bulk conductance of the platinum (S/m)

capa(tt) Calculates the heat capacity of the gas mixture (kJ/kg.°C)

capaal(tt) Calculates the heat capacity of the aluminum oxide(kJ/kg.°C)

capabut(tt) Calculates the heat capacity of the butane (kJ/kg.°C)

capapt(tt) Calculates the heat capacity of the platinum(kJ/kg.°C)

capaso(tt) Calculates the heat capacity of the aluminum oxide(kJ/kg.°C)

coeffg(tt) Calculates a coefficient in the gaseous phase equation

coeffs1(tt,te) Calculates a coefficient in the solid phase equation

coeffs2(tt,coord) Calculates a coefficient in the solid phase equation

conduc(tt) Gives the thermal conductivity of the gas mixture (W/m.°C)

conducual(tt) Gives the thermal conductivity of the aluminum oxide (W/m.°C)

conducbut(tt) Gives the thermal conductivity of the butane (W/m.°C)

conduche(tt) Gives the thermal conductivity of the helium (W/m.°C)

conducpt(tt) Gives the thermal conductivity of the platinum particles (W/m.°C)

coordi(pty,dy) Gives dy, the non-dimensionalized space between two consecutive points along the axial direction

delta(tt,te) Calculates an estimation of the steady-state temperature difference between the gas and the pellets (°C)

epdpa(tt) Calculates the dielectric loss of alpha-alumina

epdpg(tt) Calculates the dielectric loss of gamma-alumina

epdppt(tt) Calculates the dielectric loss of platinum

eppa(tt) Calculates the dielectric constant of alpha-alumina

eppg(tt) Dielectric constant of gamma-alumina

fgas(tpel,tgas) Function used in the Runge-Kutta algorithm of the gaseous phase equation

fluidizationvelocity(umf) Gives the minimum fluidization velocity (m/s)

fsolid(ipulse,time,tgas,tpel,coord) Function used in the Runge-Kutta algorithm of the solid phase equation

h(tt) Calculates the convection coefficient (W/m².°C)

kuttagas(tt) Calculates the gas temperature of the (n+1) node

kuttasolid(ipulse,time,dt,tgas,tpel,coord) Calculates the solid temperature of the current node

pmix(p1,p2) Calculates some properties of the mixture helium-butane (viscosity and conductivity)

pr(tt) Calculates the Prandtl number

qsigpt(tt) Calculates the size-dependent electrical conductivity of platinum

ro(tt) Calculates the gas density (kg/m^3)

v(tt) Calculates the velocity of the gas (m/s)

visco(tt) Calculates the viscosity of the gas mixture ($\text{Pa}\cdot\text{s}$)

viscobut(tt) Calculates the viscosity of the butane ($\text{Pa}\cdot\text{s}$)

viscohe(tt) Calculates the viscosity of the helium ($\text{Pa}\cdot\text{s}$)

Block1/ dt,numbersteps,inner

dt : time step duration (sec).
numbersteps : number of time steps used.
inner : number of inner iteration.

Block2/ frac

frac : helium gas fraction.

Block3/ diamereac,diamepar,emf,epsilon,fl,velocity,rhoal,troom

diamereac : reactor diameter (m).
diamepar : pellet diameter (m).
emf : porosity at the minimum fluidization velocity.
epsilon : porosity at any velocity.
fl : bed height (inch).
velocity : inlet gas velocity (m/s).
rhoal : aluminum oxide density (kg/m³).
troom : room temperature (oC).

Block4/ freq,epsi0,pi,magn,ivar

freq : electromagnetic field frequency (Hz).
epsi0 : permittivity of free space (8.854.10⁻¹² F/m).
pi : 3.1415
magn : electric field magnitude (V/m).
ivar : specifies if the heat generation is modified by means of the function.

Block5/ dpt,rhopt,fpt

dpt : platinum catalyst particle diameter (m).
rhopt : platinum density (kg/m³).

fpt : mass fraction of platinum in the pellets.

Block6/ tshell,sapel,volpel

tshell : thickness of the Pt/Al₂O₃ region (m).

sapel : surface area of a single catalyst pellet (m²).

volpel : volume of a single catalyst pellet (m³).

Block8/ ial,imix,ipt

ial : specifies which alumina support is used, alpha or gamma.

imix : specifies which mixture formula is used.

ipt : specifies whether the platinum conductivity is evaluated at the bulk value, or compensated for size dependence.

Block9/ tpulse,periode,tpulse1

tpulse : "on" position duration (sec).

periode : duration between two consecutives starting "on" positions (sec).

tpulse1 : duty cycle value.

B.2 Parameter File

ial	2
imix	1
ipt	2
ipulse	2
ivar	2
inner	1
troom	2.5d1
tpulse	5.0d-1
periode	1.0d0
dt	1.0d-1
numbersteps	5.0d2
frac	7.5d-1
freq	2.45d9
emf	4.0d-1
epsilon	4.0d-1
tshell	0.0d0
dpt	3.3d-8
rhopt	2.138d4
fpt	5.0d-2
magn	3.75d4
diamereac	1.0d-2
diamepar	3.3d-3
velocity	8.9d-1
rhoal	7.0d2
fl	2.54d-2

B.3 Subroutines

These subroutines are valid for the three versions. They are arranged in alphabetical order.

```
function bsigpt(tt)
c.....calculates the bulk conductance of platinum

c.....rho0: resistivity at 293K
c.....alpha: resistivity coefficient at 293K
c.....t0: base temperature

implicit double precision (a-h,o-y)
data rho0,alpha,t0/10.6d-08,3.9d-03,2.0d1/

bsigpt=1.0d0/(rho0*alpha*(tt-t0)+rho0)
return
end

c-----
function capa(tt)
c.....calculates the heat capacity of the mixture

implicit double precision(a-h,o-y)
common/Block2/frac

capa=(1.0d+0-frac)*capabut(tt)+frac*5.193d+03
return
end

c-----
function capaal(te)
c.....calculates the heat capacity of the alumina

c.....a, b, x and y: buffer variables used to process the
c.....linear interpolation of the solid heat capacity
c.....tpts and kpts: vectors containing respectively the
c.....temperatures and their related solid heat capacity values

implicit double precision(a-h,o-y)
dimension tpts(14),kpts(14)

data tpts/2.0d+01,5.0d+01,1.0d+02,1.5d+02,2.0d+02,3.0d+02
&,4.0d+02,5.0d+02,6.0d+02,7.0d+02,8.0d+02,9.0d+02,
&1.0d+03,1.1d+03/
data kpts/7.684d+02,8.225d+02,8.998d+02,9.631d+02,1.0146d+03
&,1.0899d+03,1.139d+03,1.1719d+03,1.1957d+03,1.215d+03
&,1.2325d+03,1.2496d+03,1.2661d+03,1.2814d+03/

if (te.ge.tpts(14)) then
a=(kpts(14)-kpts(13))/(tpts(14)-tpts(13))
b=kpts(14)-a*tpts(14)
capaal=a*te+b
```

```

        return
    else
    do 5 i=1,13
        a=tpts(i)
        b=tpts(i+1)
        x=kpts(i)
        y=kpts(i+1)
        if(te.eq.a) then
            capaal=x
            return
        else
            if(te.gt.a.and.te.lt.b)then
                capaal=(te-a)/(b-a)*(y-x)+x
            return
            endif
        endif
    5 continue
    endif
    if (te.lt.tpts(1)) then
        a=(kpts(2)-(kpts(1)))/(tpts(2)-tpts(1))
        b=kpts(2)-a*tpts(2)
        capaal=a*te+b
    return
    endif
end

```

```

-----
function capabut(tt)

c.....calculates the heat capacity of the butane
c.....a, b, c, d: coefficients of the polynomial determining
c.....the butane heat capacity

implicit double precision(a-h,o-y)
data a,b,c,d/3.954d0,37.12d0,-1.833d0,0.03498d0/

theta=(tt+2.73d2)/1.0d2
capabut=a+b*theta+c*theta**2+d*theta**3
capabut=capabut/58.124d-03
return
end

```

```

-----
function capapt(te)
c.....calculates the heat capacity of platinum

c.....a, b, x and y are buffer variables used to process the
c.....linear interpolation of the solid heat capacity
c.....tpts and kpts are vectors containing respectively the
c.....temperatures and their helium conductivity values

implicit double precision (a-h,o-y)
double precision tpts(7),kpts(7)

```

```

data tpts/-7.3d+01,1.27d+01,3.27d+01,5.27d+01,7.27d+02
&,9.27d+02,1.227d+03/
data kpts/1.25d+02,1.36d+02,1.41d+02,1.46d+02,1.52d+02
&,1.57d+02,1.65d+02/

```

```

if (te.ge.tpts(7)) then
  a=(kpts(7)-(kpts(6)))/(tpts(7)-tpts(6))
  b=kpts(7)-a*tpts(7)
  capapt=a*te+b
  return
else
do 5 i=1,6
  a=tpts(i)
  b=tpts(i+1)
  x=kpts(i)
  y=kpts(i+1)
  if(te.eq.a) then
    capapt=x
    return
  else
    if(te.gt.a.and.te.lt.b)then
      capapt=(te-a)/(b-a)*(y-x)+x
      return
    endif
  endif
5 continue
endif
if (te.lt.tpts(1)) then
  a=(kpts(2)-(kpts(1)))/(tpts(2)-tpts(1))
  b=kpts(2)-a*tpts(2)
  capapt=a*te+b
  return
endif
end

```

```

-----
function capaso(te)
c.....calculates the heat capacity of the mixture Pt-Al2O3

implicit double precision (a-h,o-z)
common/Block5/ dpt,rhopt,fpt

capaso=capaal(te)*(1.0d0-fpt)+capapt(te)*fpt
return
end

```

```

-----
function coeffg(tt)
c.....calculates a coefficient in the gaseous phase equation

implicit double precision(a-h,o-y)
common/Block3/ diamereac,diamepar,emf,epsilon,
&fl,velocity,rhoal,troom

```

```

    coeffg=6*h(tt)*(1-epsilon)*fl/(diamepar*velocity*ro(troom)*
&capa(tt))
    return
end

-----
function coeffs1(tt,te)
c.....calculates a coefficient in the solid phase equation

    implicit double precision(a-h,o-y)
    common/Block3/ diamereac,diamepar,emf,epsilon,
&fl,velocity,rhoal,troom

    coeffs1=6.0d+0*h(tt)/(diamepar*rhoal*capaso(te))
    return
end

-----
function coeffs2(te,coord)
c.....calculates a coefficient in the solid phase equation

c.....q: heat generation
c.....var: the coefficient multiplying the heat generation
c.....value to modify the shape of the pellet temperature profile
c.....with respect to the axial direction

    implicit double precision(a-h,o-y)
    double precision magn
    complex zepm

    common/Block3/ diamereac,diamepar,emf,epsilon,
&fl,velocity,rhoal,troom
    common/Block4/ freq,epsi0,pi,magn,ivar

    q=freq*epsi0*abs(aimag(zepm(te)))*(2.0d+0)*pi*
&(magn)**2
    if (ivar.eq.1) then
        var=exp(-coord**1.08)
    else
        var=1
    endif
    coeffs2=q/(rhoal*capaso(te))*var
    return
end

-----
function conduc(tt)
c.....calculates the thermal conductivity of the gas mixture

c.....p1 and p2: respectively the conductivity of helium and butane

    implicit double precision(a-h,o-y)

```

```

p1=conduche(tt)
p2=conducbut(tt)
conduc=pmix(p1,p2)
return
end

```

```

-----
function conducal(tt)
c.....calculates the thermal conductivity of the Pt-Al2O3 mixture

c.....a, b, x and y are buffer variables used to process the
c.....linear interpolation of the solid heat capacity
c.....tpts and kpts are vectors containing respectively the
c.....temperatures and their helium conductivity values

implicit double precision (a-h,o-y)
double precision tpts(5),kpts(5)
data tpts/2.70d+01,1.27d+02,2.27d+02,7.27d+02,1.227d+3/

data kpts/3.6d0,2.7d0,1.6d0,7.6d0,5.4d0/

if (tt.ge.tpts(5)) then
  a=(kpts(5)-(kpts(4)))/(tpts(5)-tpts(4))
  b=kpts(5)-a*tpts(5)
  conducal=a*tt+b
  return
else
do 5 i=1,4
  a=tpts(i)
  b=tpts(i+1)
  x=kpts(i)
  y=kpts(i+1)
  if(tt.eq.a) then
    conducal=x
    return
  else
    if(tt.gt.a.and.tt.lt.b)then
      conducal=(tt-a)/(b-a)*(y-x)+x
      return
    endif
  endif
5 continue
endif
if (tt.lt.tpts(1)) then
  a=(kpts(2)-(kpts(1)))/(tpts(2)-tpts(1))
  b=kpts(2)-a*tpts(2)
  conducal=a*tt+b
  return
endif
end
-----

```

```

function conducbut(tt)
c.....calculates the thermal conductivity of the butane

c.....a, b, x and y are buffer variables used to process the
c.....linear interpolation of the solid heat capacity
c.....tpts and kpts are vectors containing respectively the
c.....temperatures and their related butane conductivity values

    implicit double precision (a-h,o-y)
    double precision tpts(22),kpts(22)
    data tpts/7.00d+00,2.70d+01,4.70d+01,6.70d+01,8.70d+01,9.70d+01
2,1.07d+02,1.17d+02,1.27d+02,1.37d+02,1.47d+02,1.57d+02,1.67d+02
3,1.77d+02,1.87d+02,2.07d+02,2.27d+02,2.47d+02,2.67d+02,2.87d+02
4,3.07d+02,3.27d+02/
    data kpts/1.38d-02,1.61d-02,1.84d-02,2.08d-02,2.33d-02,2.45d-02
2,2.57d-02,2.71d-02,2.84d-02,2.97d-02,3.10d-02,3.24d-02,3.38d-02
3,3.52d-02,3.66d-02,3.95d-02,4.24d-02,4.55d-02,4.86d-02,5.17d-02
4,5.49d-02,5.80d-02/

    if (tt.ge.tpts(22)) then
        a=(kpts(22)-kpts(21))/(tpts(22)-tpts(21))
        b=kpts(22)-a*tpts(22)
        conducbut=a*tt+b
        return
    else
        do 6 i=1,21
            a=tpts(i)
            b=tpts(i+1)
            x=kpts(i)
            y=kpts(i+1)
            if(tt.eq.a) then
                conducbut=x
                return
            else
                if(tt.gt.a.and.tt.lt.b)then
                    conducbut=(tt-a)/(b-a)*(y-x)+x
                    return
                endif
            endif
        6        continue
    endif
    if (tt.lt.tpts(1)) then
        a=(kpts(2)-(kpts(1)))/(tpts(2)-tpts(1))
        b=kpts(2)-a*tpts(2)
        conducbut=a*tt+b
        return
    endif
end

c-----
function conduche(tt)
c.....calculates the thermal conductivity of the helium

```

c.....a, b, x and y are buffer variables used to process the
c.....linear interpolation of the solid heat capacity
c.....tpts and kpts are vectors containing respectively the
c.....temperatures and their helium conductivity values

```

implicit double precision (a-h,o-y)
double precision tpts(23),kpts(23)
data tpts/2.70d+01,4.70d+01,6.70d+01,8.70d+01,1.07d+02
2,1.27d+02,1.47d+02,1.67d+02,1.87d+02,2.07d+02,2.27d+02
3,2.77d+02,3.27d+02,3.77d+02,4.27d+02,4.77d+02,5.27d+02
4,5.77d+02,6.27d+02,6.77d+02,7.27d+02,8.27d+02,9.27d+02/
data kpts/1.56d-01,1.64d-01,1.71d-01,1.78d-01,1.84d-01
2,1.90d-01,1.97d-01,2.04d-01,2.11d-01,2.17d-01,2.22d-01
3,2.38d-01,2.53d-01,2.68d-01,2.81d-01,2.86d-01,3.09d-01
4,3.23d-01,3.36d-01,3.49d-01,3.62d-01,3.86d-01,4.10d-01/

if (tt.ge.tpts(23)) then
  a=(kpts(23)-(kpts(22)))/(tpts(23)-tpts(22))
  b=kpts(23)-a*tpts(23)
  conduche=a*tt+b
  return
else
  do 5 i=1,22
    a=tpts(i)
    b=tpts(i+1)
    x=kpts(i)
    y=kpts(i+1)
    if(tt.eq.a) then
      conduche=x
      return
    else
      if(tt.gt.a.and.tt.lt.b)then
        conduche=(tt-a)/(b-a)*(y-x)+x
        return
      endif
    endif
  5 continue
endif
if (tt.lt.tpts(1)) then
  a=(kpts(2)-(kpts(1)))/(tpts(2)-tpts(1))
  b=kpts(2)-a*tpts(2)
  conduche=a*tt+b
  return
endif
end

```

c-----
function conducpt(te)
c.....calculates the thermal conductivity of the platinum
c.....a, b, x and y are buffer variables used to process the

c.....linear interpolation of the solid heat capacity
c.....tpts and kpts are vectors containing respectively the
c.....temperatures and their helium conductivity values

```

implicit double precision (a-h,o-y)
double precision tpts(7),kpts(7)
data tpts/-7.3d+01,1.27d+01,3.27d+01,5.27d+01,7.27d+02
&,9.27d+02,1.227d+03/
data kpts/7.26d+01,7.18d+01,7.32d+01,7.56d+01,7.87d+01
&,8.26d+01,8.95d+01/

if (te.ge.tpts(7)) then
  a=(kpts(7)-(kpts(6)))/(tpts(7)-tpts(6))
  b=kpts(7)-a*tpts(7)
  conducpt=a*te+b
  return
else
do 5 i=1,6
  a=tpts(i)
  b=tpts(i+1)
  x=kpts(i)
  y=kpts(i+1)
  if(tt.eq.a) then
    conducpt=x
    return
  else
    if(te.gt.a.and.te.lt.b)then
      conducpt=(te-a)/(b-a)*(y-x)+x
      return
    endif
  endif
5 continue
endif
if (te.lt.tpts(1)) then
  a=(kpts(2)-(kpts(1)))/(tpts(2)-tpts(1))
  b=kpts(2)-a*tpts(2)
  conducpt=a*te+b
  return
endif
end

```

c-----

```

function conducso(te)
c.....calculates the thermal conductivity of a Pt-Al203 mixture

implicit double precision(a-h,o-z)
common/Block5/ dpt,rhopt,fpt

conducso=conducual(te)*(1.0d0-fpt)+conducpt(te)*fpt
return
end

```

```

-----
      subroutine coordi(dy)
c.....calculates the dimensionless coordinates of the nodes within
c.....the bed

c.....pty1: number of nodes along the axial direction
c.....y: dimensionless coordinates of the nodes
c.....dy: dimensionless space between two consecutives nodes

      implicit double precision (a-h,o-z)
      integer pty
      double precision y(0:40)

      pty1=4.1d1
      pty=41
      dy=1/(pty1-1)
      y(0)=0.0d+0
      y(pty-1)=1.0d+0
      rewind 14
      do 1 j=1,pty-2
        y(j)=y(j-1)+dy
1 continue
      open(unit=14,file='coordinates')
      write (14,*)y
      rewind 14
      end

-----

      function deltat(te,tt)
c.....calculates an estimation of the steady-state temperature
c.....difference between the gas and the pellets

c.....q: heat generation

      implicit double precision(a-h,o-y)
      double precision magn
      complex zepm
      common/Block3/ diamereac,diamepar,emf,epsilon,
&fl,velocity,rhoal,troom
      common/Block4/ freq,epsi0,pi,magn,ivar

      q=freq*epsi0*abs(aimag(zepm(te)))*(2.0d+0)*pi
&magn**2
      deltat=q*diamepar/(6*h(tt))
      end

-----

      function epdpa(tt)
c.....calculates the dielectric loss of alpha-alumina

c.....a, b, x and y are buffer variables used to process the
c.....linear interpolation of the solid heat capacity
c.....tpts and kpts are vectors containing respectively the

```

c.....temperatures and their related dielectric loss values

```
implicit double precision (a-h,o-y)
double precision tpts(15),kpts(15)
data tpts/2.50d+01,9.90d+01,1.84d+02,2.81d+02,3.56d+02
2,4.30d+02,5.62d+02,7.05d+02,8.00d+02,9.03d+02,9.73d+02
3,1.025d+03,1.05d+03,1.089d+03,1.132d+03/
data kpts/3.63d-03,3.95d-03,5.08d-03,6.80d-03,8.86d-03
2,1.12d-02,1.63d-02,2.24d-02,2.82d-02,3.58d-02,4.29d-02
3,5.03d-02,5.61d-02,8.33d-02,1.14d-01/
```

```
if (tt.ge.tpts(15)) then
  a=(kpts(15)-(kpts(14)))/(tpts(15)-tpts(14))
  b=kpts(15)-a*tpts(15)
  epdpa=a*tt+b
  return
else
do 5 i=1,14
  a=tpts(i)
  b=tpts(i+1)
  x=kpts(i)
  y=kpts(i+1)
  if(tt.eq.a) then
    epdpa=x
    return
  else
    if(tt.gt.a.and.tt.lt.b)then
      epdpa=(tt-a)/(b-a)*(y-x)+x
    return
  endif
endif
5 continue
endif
if (tt.lt.tpts(1)) then
  a=(kpts(2)-(kpts(1)))/(tpts(2)-tpts(1))
  b=kpts(2)-a*tpts(2)
  epdpa=a*tt+b
  return
endif
end
```

c-----
function epdpg(tt)
c.....calculates the dielectric loss of gamma-alumina

c.....a, b, x and y are buffer variables used to process the
c.....linear interpolation of the solid heat capacity
c.....tpts and kpts are vectors containing respectively the
c.....temperatures and their related dielectric loss values

```
implicit double precision (a-h,o-y)
double precision tpts(12),kpts(12)
data tpts/2.90d+1,3.50d+01,1.49d+02,2.62d+02,3.71d+02,4.78d+02
```

```

2,5.82d+02,6.84d+02,7.84d+02,8.81d+02,9.76d+02,1.068d+03/
data kpts/3.9213d-01,3.893d-01,2.310d-01,1.693d-01,1.528d-01
2,1.521d-01,1.514d-01,1.505d-01,1.493d-01,1.481d-01,1.421d-01
3,1.311d-01/

```

```

if (tt.ge.tpts(12)) then
  a=(kpts(12)-(kpts(11)))/(tpts(12)-tpts(11))
  b=kpts(12)-a*tpts(12)
  epdpg=a*tt+b
  return
else
do 5 i=1,11
  a=tpts(i)
  b=tpts(i+1)
  x=kpts(i)
  y=kpts(i+1)
  if(tt.eq.a) then
    epdpg=x
    return
  else
    if(tt.gt.a.and.tt.lt.b)then
      epdpg=(tt-a)/(b-a)*(y-x)+x
    return
  endif
endif
5 continue
endif
if (tt.lt.tpts(1)) then
  a=(kpts(2)-(kpts(1)))/(tpts(2)-tpts(1))
  b=kpts(2)-a*tpts(2)
  epdpg=a*tt+b
  return
endif
end

```

c-----

```

function epdppt(tt)
c.....calculates the dielectric loss of platinum

implicit double precision (a-h,o-y)
double precision magn
common/Block4/ freq,epsi0,pi,magn,ivar
common/Block8/ ial,imix,ipt

if (ipt.eq.1) then
  epdppt=bsigpt(tt)/(2.0d0*pi*freq*epsi0)
elseif(ipt.eq.2) then
  epdppt=qsigpt(tt)/(2.0d0*pi*freq*epsi0)
else
  pause 'Epdppt function failed'
endif
return
end

```

```

-----
function eppa(tt)
c.....calculates the dielectric constant of alpha alumina

implicit double precision (a-h,o-y)
double precision a(5)
data a/7.331d0,-9.120d-04,6.428d-06,-6.531d-09,2.578d-12/

sum=0.0d0
do 5 i=1,4
    sum=tt*(sum+a(6-i))
5    continue
eppa=sum+a(1)
return
end

```

```

-----
function eppg(tt)
c.....calculates the dielectric constant of gamma alumina

c.....a, b, x and y are buffer variables used to process the
c.....linear interpolation of the solid heat capacity
c.....tpts and kpts are vectors containing respectively the
c.....temperatures and their related dielectric constant values

implicit double precision (a-h,o-y)
double precision kpts(12),tpts(12)
data tpts/2.90d+01,3.50d+01,1.49d+02,1.62d+02,3.71d+02,4.78d+02,
&5.82d+02,6.84d+02,7.84d+02,8.81d+02,9.76d+02,1.068d+03/
data kpts/4.487d0,4.4982d0,5.0396d0,4.4478d0,4.6517d0,4.9169d0,
&4.6465d0,4.441d0,4.3126d0,4.196d0,4.0462d0,3.7173d0/

if (tt.ge.tpts(12)) then
    a=(kpts(12)-(kpts(11)))/(tpts(12)-tpts(11))
    b=kpts(12)-a*tpts(12)
    eppg=a*tt+b
    return
else
do 5 i=1,11
    a=tpts(i)
    b=tpts(i+1)
    x=kpts(i)
    y=kpts(i+1)
    if(tt.eq.a) then
        eppg=x
        return
    else
        if(tt.gt.a.and.tt.lt.b)then
            eppg=(tt-a)/(b-a)*(y-x)+x
            return
        endif
endif

```

```

        endif
5      continue
      endif
      if (tt.lt.tpts(1)) then
          a=(kpts(2)-(kpts(1)))/(tpts(2)-tpts(1))
          b=kpts(2)-a*tpts(2)
          eppg=a*tt+b
          return
      endif
      end
end

-----
      function fgas(tgas,tpel)
c.....function used in the Runge-Kutta algorithm of the gaseous
c.....phase equation

      implicit double precision(a-h,o-y)
      common/Block3/ diamereac,diamepar,emf,epsilon,fl
      &,velocity,rhoal,troom

      fgas=coeffg(tgas+troom)*(tpel-tgas)
      return
      end

-----
      subroutine fluidizationvelocity(umf)

      implicit double precision (a-h,o-y)

      common/Block3/ diamereac,diamepar,emf,epsilon,fl
      &,velocity,rhoal,troom

      x2=1.75*(diamepar*ro(troom)/visco(troom))**2/emf**3
      x1=150*(1-emf)*diamepar*ro(troom)/visco(troom)/emf**3
      x0=-diamepar**3*ro(troom)*(rhoal-ro(troom))
      &*9.81/visco(troom)**2

      delta=x1**2-4*x2*x0

      umf=(-x1+delta**0.5d0)/(2*x2)
      return
      end

-----
      function fsolid(ipulse,time,tgas,tpel,coord)
c.....function used in the Runge-Kutta algorithm of the
c.....solid phase equation

c.....ee: used to avoid round-off errors
c.....time1: time related to the period
c.....time2: dimensionless time related

      implicit double precision(a-h,o-y)

```

```

common/Block3/ diamereac,diamepar,emf,epsilon,fl
&,velocity,rhoal,troom
common/Block9/ tpulse,periode,tpulse1

ee=2.0d-5
time1=time/periode+ee
time2=time1-int(time1)
if ((time2.le.tpulse1).or.(ipulse.ne.1)) then
  fsolid=coeffs1(tgas+troom,tpel+troom)*(tgas-tpel)
& +coeffs2(tpel+troom,coord)
  return
else
  fsolid=coeffs1(tgas+troom,tpel+troom)*(tgas-tpel)
  return
endif
end

```

c-----

```

function h(tt)
c.....calculates the convection coefficient

implicit double precision(a-h,o-y)
double precision nu
common/Block3/ diamereac,diamepar,emf,epsilon,
&fl,velocity,rhoal,troom

re=ro(tt)*v(tt)*diamepar/visco(tt)

if (re.lt.1.0155d2) then
  nu=0.03*re**1.3
else
  nu=2+1.2*re**0.5*pr(tt)**(1.0d0/3.0d0)
endif

h=conduc(tt)/diamepar*nu
end

```

c-----

```

function kuttagas(dy,tgas,tpel)
c.....calculates the gas temperature of the following node

implicit double precision(a-h,o-y)
double precision kuttagas
double precision k1,k2,k3,k4

k1=fgas(tgas,tpel)
k2=fgas(tgas+0.5*dy*k1,tpel)
k3=fgas(tgas+(-0.5+1/2**(0.5))*dy*k1+(1-1/2**(0.5))
&*dy*k2,tpel)
k4=fgas(tgas-1/2**(0.5)*dy*k2+(1+1/2**(0.5))*dy*k3
&,tpel)
kuttagas=dy/6.0*(k1+2*(1-1/2**(0.5))*k2+2*
&(1+1/2**(0.5))*k3+k4)

```

```

return
end

-----
function kuttasolid(ipulse,time,dt,tgas,tpel,coord)
c.....calculates the solid temperature of the following node

implicit double precision(a-h,o-y)
double precision kuttasolid
double precision k1,k2,k3,k4

k1=fsolid(ipulse,time,tgas,tpel,coord)
k2=fsolid(ipulse,time+0.5*dt,tgas,tpel+0.5*dt*k1,coord)
k3=fsolid(ipulse,time+0.5*dt,tgas,tpel+(-0.5+1/2**(0.5))
&*dt*k1+(1-1/2**(0.5))*dt*k2,coord)
k4=fsolid(ipulse,time+dt,tgas,tpel-1/2**(0.5)*dt*k2+
&(1+1/2**(0.5))*dt*k3,coord)

kuttasolid=dt/6.0*(k1+2*(1-1/2**(0.5))*k2+2*
&(1+1/2**(0.5))*k3+k4)
return
end

-----
function pmix(p1,p2)
c.....calculates the properties of a gas mixture
c.....(thermal conductivity and viscosity)

implicit double precision (a-h,o-y)
common/Block2/ frac
common/Block3/ diamereac,diamepar,emf,epsilon,
&f1,velocity,rhoal,troom
data mw1,mw2/4.0d0,58.12d0/

x1=(frac/mw1)/(frac/mw1+(1.0d0-frac)/mw2)
x2=1.0d0-x1
term1=1.0d0+dsqrt(p1/p2)*(mw2/mw1)**(0.25d0)
term1=term1/dsqrt(8.0d0*(1.0d0+mw1/mw2))
phi12=term1
term1=1.0d0+dsqrt(p2/p1)*(mw1/mw2)**(0.25d0)
term1=term1/dsqrt(8.0d0*(1.0d0+mw2/mw1))
phi21=term1
phi11=1.0d0
phi22=1.0d0
pmix=x1*p1/(x1*phi11+x2*phi12)+x2*p2/(x1*phi21+x2*phi22)
return
end

-----
function pr(tt)
c.....calculates the Prandtl number of the mixture

implicit double precision(a-h,o-y)

```



```

common/Block2/frac

pr=capa(tt)*visco(tt)/conduc(tt)
return
end

-----
function qsigpt(tt)
c.....calculates the size dependent electrical conductivity of Platinum

implicit double precision (a-h,o-y)
common/Block5/ dpt,rhopt,fpt

qsigpt=bsigpt(tt)*((dpt/5.0d-06)**3)
return
end

-----
function ro(tt)
c.....calculates the density of the mixture

implicit double precision(a-h,o-y)
common/Block2/frac

ro=frac*(1.7847d-01)*(1.0d+02)/(1.01325d+02)*2.7315d+02/(tt+
&2.7315d+02)+(1.0d+0-frac)*(1.0d+02)/(1.01325d+02)*2.519d0*
&(2.7315d+02)/(tt+2.7315d+02)
return
end

-----
function v(tt)
c.....calculates the velocity of the gas

implicit double precision(a-h,o-y)
common/Block3/ diamereac,diamepar,emf,epsilon,
&fl,velocity,rhoal,troom

v=velocity*ro(troom)/ro(tt)
return
end

-----
function visco(tt)
c.....calculates the viscosity of the mixture

implicit double precision (a-h,o-y)

p1=viscohe(tt)
p2=viscobut(tt)
visco=pmix(p1,p2)
return
end

```

```

-----
function viscobut(tt)
c.....calculates the viscosity of the butane

c.....a, b, x and y are buffer variables used to process the
c.....linear interpolation of the solid heat capacity
c.....tpts and kpts are vectors containing respectively the
c.....temperatures and their related butane viscosity values

implicit double precision (a-h,o-y)
double precision tpts(7),kpts(7)
data tpts/0.00d+00,1.00d+02,2.00d+02,3.00d+02
2,4.00d+02,5.00d+02,6.00d+02/

data kpts/6.84d-06,9.26d-06,1.17d-05,1.40d-05
2,1.64d-05,1.87d-05,2.11d-05/
if (tt.ge.tpts(7)) then
  a=(kpts(7)-(kpts(6)))/(tpts(7)-tpts(6))
  b=kpts(7)-a*tpts(6)
  viscobut=a*tt+b
  return
else
do 6 i=1,6
  a=tpts(i)
  b=tpts(i+1)
  x=kpts(i)
  y=kpts(i+1)
  if(tt.eq.a) then
    viscobut=x
    return
  else
    if(tt.gt.a.and.tt.lt.b)then
      viscobut=(tt-a)/(b-a)*(y-x)+x
    return
  endif
endif
6 continue
endif
if (tt.lt.tpts(1)) then
  a=(kpts(2)-(kpts(1)))/(tpts(2)-tpts(1))
  b=kpts(2)-a*tpts(2)
  viscobut=a*tt+b
  return
endif
end

```

```

-----
function viscohe(tt)
c.....calculates the viscosity of the helium

c.....a, b, x and y are buffer variables used to process the

```

c.....linear interpolation of the solid heat capacity
c.....tpts and kpts are vectors containing respectively the
c.....temperatures and their related helium viscosity values

```

implicit double precision (a-h,o-y)
double precision tpts(13),kpts(13)
data tpts/2.70d+01,7.70d+01,1.27d+02,1.77d+02,2.27d+02,3.27d+02
2,4.27d+02,5.27d+02,6.27d+02,7.27d+02,8.27d+02,9.27d+02,1.027d+03/
data kpts/1.99d-05,2.22d-05,2.43d-05,2.64d-05,2.84d-05,3.22d-05
3,3.59d-05,3.94d-05,4.28d-05,4.62d-05,4.94d-05,5.25d-05,5.56d-05/

if (tt.ge.tpts(13)) then
  a=(kpts(13)-kpts(12))/(tpts(13)-tpts(12))
  b=kpts(13)-a*tpts(13)
  viscohe=a*tt+b
  return
else
do 5 i=1,12
  a=tpts(i)
  b=tpts(i+1)
  x=kpts(i)
  y=kpts(i+1)
  if(tt.eq.a) then
    viscohe=x
    return
  else
    if(tt.gt.a.and.tt.lt.b)then
      viscohe=(tt-a)/(b-a)*(y-x)+x
      return
    endif
  endif
5 continue
endif
if (tt.lt.tpts(1)) then
  a=(kpts(2)-(kpts(1)))/(tpts(2)-tpts(1))
  b=kpts(2)-a*tpts(2)
  viscohe=a*tt+b
  return
endif
end

```

c-----
function zepm(tt)
c.....calculate the effective dielectric loss of Al2O3 & Pt mixture

```

implicit double precision (a-h,o-y)
double precision magn
complex zep1,zep2,znum,zden,zepm
common/Block3/ diamereac,diamepar,emf,epsilon,
&fl,velocity,rhoal,troom
common/Block4/ freq,epsi0,pi,magn,ivar
common/Block5/ dpt,rhopt,fmt

```

```

common/Block6/ tshell,sapel,volpel
common/Block8/ ial,imix,ipt

ptmass=(fpt/(1.0d0-fpt))*volpel*rhoal
volfrac=ptmass/(rhopt*volpel)
if (ial.eq.1)then
  zep1=dcmplx(eppa(tt),-epdpa(tt))
  elseif(ial.eq.2) then
    zep1=dcmplx(eppg(tt),-epdpg(tt))
  else
    pause 'problem 1'
endif
zep2=dcmplx(1.0d0,-epdppt(tt))

if (imix.eq.1) then
c.....using the Rayleigh Formula
  znum=zep1*(2.0d0*zep1+zep2)+2.0d0*volfrac*zep1*(zep2
&-zep1)
  zden=(2.0d0*zep1+zep2)-volfrac*(zep2-zep1)
  zepm=znum/zden
  return
c.....using the Maxwell-Garnet theory
  else if (imix.eq.2) then
    r=1.0d0-volfrac
    znum=zep1*(zep2*(3.0d0-2.0d0*r)+2.0d0*r*zep1)
    zden=r*zep2+zep1*(3.0d0-r)
    zepm=znum/zden
    return
c.....using the Licktnecker Formula in Roussy (eq8.71)
  else if (imix.eq.3) then
    zepm=zep1**(1.0d0-volfrac)*zep2**volfrac
    return
  else
    pause 'problem 2'
endif
end

```

B.4 Main Programs

B.4.1 Version One

This version gives the gas and the pellet temperature profile; the transients data are saved in the tgas and the tpel files; the data at the end of the iterations are saved into the flow file.

```
program model_one
c.....the program is set up to calculate the gas and pellet temperature

implicit double precision(a-h,o-z)
double precision coord(0:40),tpel(0:40)
double precision tgas(0:40),tetam(0:40)
double precision magn
double precision kuttagas,kuttasolid
double precision tgas1(5),tpel1(5)
integer writ(5)
character*16 parameter

common/Block1/ dt,numbersteps,inner
common/Block2/ frac
common/Block3/ diamereac,diamepar,emf,epsilon,
&fl,velocity,rhoal,troom
common/Block4/ freq,epsi0,pi,magn,ivar
common/Block5/ dpt,rhopt,fpt
common/Block6/ tshell,sapel,volpel
common/Block8/ ial,imix,ipt
common/Block9/ tpulse,periode,tpulse1

data writ/0,10,20,30,40/

c----- ial=1: alpha alumina
c----- imix=1 : Rayleigh formula
c----- imix=2 : Maxwell-Garnet Theory
c----- ipt=1 : Pt conductivity evaluated a the bulk value
c----- ipt=2 : Pt conductivity compensated for size dependance
c----- ipulse=1 : Electric field is pulsed
c----- ivar=1 : Electric field is pulsed axially with the function...

c.....Creates the 41 nodes
pty=41
call coordi(dy)

epsi0=8.8542d-12
pi=3.1415965352d+0

rewind 14
rewind 15
rewind 16
rewind 17
```

```
rewind 18
```

```
c.....Read the parameters from the "parameters" file
```

```
open(unit=18,file='parameters')
  read(18,*)parameter,ial
  read(18,*)parameter,imix
  read(18,*)parameter,ipt
  read(18,*)parameter,ipulse
  read(18,*)parameter,ivar
  read(18,*)parameter,inner
  read(18,*)parameter,troom
  read(18,*)parameter,tpulse
  read(18,*)parameter,periode
  read(18,*)parameter,dt
  read(18,*)parameter,numbersteps
  read(18,*)parameter,frac
  read(18,*)parameter,freq
  read(18,*)parameter,emf
  read(18,*)parameter,epsilon
  read(18,*)parameter,tshell
  read(18,*)parameter,dpt
  read(18,*)parameter,rhopt
  read(18,*)parameter,fpt
  read(18,*)parameter,magn
  read(18,*)parameter,diamereac
  read(18,*)parameter,diamepar
  read(18,*)parameter,velocity
  read(18,*)parameter,rhoal
  read(18,*)parameter,fl
```

```
sapel=4*(diamepar/2.0)**2*pi
volpel=pi*4.0/3.0*(diamepar/2.0)**3
tpulse1=tpulse/periode
```

```
c----- Initialization of the temperatures
```

```
do 1 i=0,pty-1
  tetam(i)=0.0d+0
  tgas(i)=0.0d+0
  tpel(i)=0.0d+0
1 continue
```

```
time=0.0d+0
open(unit=15,file='tgas')
write(15,*) tgas(40)
```

```
c.....records the initial gas temperature at the 40th node in the "tgas" file
```

```
c.....to record all the nodes, delete "(40)"
```

```
open(unit=16,file='tpel')
write(16,*) tpel(40)
```

```
c.....records the initial pellet temperature at the 40th node in the "tpel" file
```

```
c.....to record all the nodes, delete "(40)"
```

```

open(unit=14,file='coordinates')
read(14,*) coord
write(6,*) coord

do 4 k=1,numbersteps
  do 3 j=1,inner
    do 2 i=0,pty-1
      tpel(i)=tetam(i)+kuttasolid(ipulse,time,dt,
&      tgas(i),tpel(i),coord(i))
      if (i.lt.pty-1) then
        tgas(i+1)=tgas(i)+kuttagas(dy,tgas(i),tpel(i))
      endif
2      continue
3      continue
      time=time+dt
      do 5 i=0,pty-1
        tetam(i)=tpel(i)
5      continue

c.....Print the temperatures on the screen and in
c.....the files "tgas" and "tpel"
      do 6 i=1,5
        tpel1(i)=tpel(writ(i))
        tgas1(i)=tgas(writ(i))
6      continue
      write(6,7) tgas1
7      format (5(1x,F5.1),2x,F5.2)
      write(6,7) tpel1,time
      write(6,8)
8      format(/)
      open(unit=15,file='tgas')
      write(15,*) tgas(40)
c.....records the transient gas temperature at the 40th node in the
c....."tgas" file; to record all the nodes, delete "(40)"
      open(unit=16,file='tpel')
      write(16,*) tpel(40)
c.....records the transient pellet temperature at the 40th node in the
c....."tpel" file; to record all the nodes, delete "(40)"

4      continue

      do 9 i=1,pty-1
        open(unit=17,file='flow')
        write(17,*) tpel(i),tgas(i),tpel(i)-tgas(i),magn
9      continue
c.....Save the gas and the pellet temperature in the "flow" file
c.....at the end of the iterations

end

```

B.4.2 Version Two

This version determines the electric field yielding the pellet temperature profile specified by in the code. The electric field is saved into the flow file with the gas and pellet temperature profile at the end of the iteration are saved into the tgas and tpel files.

```
program model_two
c.....the program is set up to calculate the gas and pellet temperature

implicit double precision(a-h,o-z)
double precision coord(0:40),tpel(0:40)
double precision tgas(0:40),tetam(0:40)
double precision field(0:40),diff(0:40),fixtem(0:40)
double precision magn
double precision kuttagas,kuttasolid
double precision tgas1(5),tpel1(5)
integer writ(5)
character*16 parameter

common/Block1/ dt,numbersteps,inner
common/Block2/ frac
common/Block3/ diamereac,diamepar,emf,epsilon,
&fl,velocity,rhoal,troom
common/Block4/ freq,epsi0,pi,magn,ivar
common/Block5/ dpt,rhopt,fpt
common/Block6/ tshell,sapel,volpel
common/Block8/ ial,imix,ipt
common/Block9/ tpulse,periode,tpulse1

data writ/0,10,20,30,40/

c----- ial=1 : alpha alumina
c----- imix=1 : Rayleigh formula
c----- imix=2 : Maxwell-Garnet Theory
c----- ipt=1 : Pt conductivity evaluated a the bulk value
c----- ipt=2 : Pt conductivity compensated for size dependance
c----- ipulse=1 : Electric field is pulsed
c----- ivar=1 : Electric field is pulsed axially with the function...

c.....Creates the nodes
pty=41
call coordi(dy)

epsi0=8.8542d-12
pi=3.1415965352d+0

rewind 14
rewind 15
rewind 16
rewind 17
```



```

c.....Read the parameters from the "parameters" file
  open(unit=18,file='parameters')
    read(18,*)parameter,ial
    read(18,*)parameter,imix
    read(18,*)parameter,ipt
    read(18,*)parameter,ipulse
    read(18,*)parameter,ivar
    read(18,*)parameter,inner
    read(18,*)parameter,troom
    read(18,*)parameter,tpulse
    read(18,*)parameter,periode
    read(18,*)parameter,dt
    read(18,*)parameter,numbersteps
    read(18,*)parameter,frac
    read(18,*)parameter,freq
    read(18,*)parameter,emf
    read(18,*)parameter,epsilon
    read(18,*)parameter,tshell
    read(18,*)parameter,dpt
    read(18,*)parameter,rhopt
    read(18,*)parameter,fpt
    read(18,*)parameter,magn
    read(18,*)parameter,diamereac
    read(18,*)parameter,diamepar
    read(18,*)parameter,velocity
    read(18,*)parameter,rhoal
    read(18,*)parameter,fl

    sapel=4*(diamepar/2.0)**2*pi
    volpel=pi*4.0/3.0*(diamepar/2.0)**3
    tpulse1=tpulse/periode

c----- Calculates the fluidization velocity upon request
c      call fluidizationvelocity(umf)
c      write(6,*)'Fluidization velocity:',umf
c      write(6,*)'What gas velocity'
c      read(5,*)velocity

c----- Initialization of the temperatures
  do 1 i=0,pty-1
    tetam(i)=0.0d+0
    tgas(i)=0.0d+0
    tpel(i)=0.0d+0
1 continue

  time=0.0d+0
  open(unit=15,file='tgas')
  write(15,*) tgas(40)
  open(unit=16,file='tpel')

```

```

write(16,*) tpel(40)

open(unit=14,file='coordinates')
read(14,*)coord

do 10 i=0,pty-1
  fixtem(i)=3.0d2
10 continue

do 11 i=0,pty-1
  field(i)=magn
11 continue

do 4 k=1,numbersteps
  do 3 j=1,inner
    do 2 i=0,pty-1
      magn=field(i)-30
      tpel(i)=tetam(i)+kuttasolid(ipulse,time,dt,
&      tgas(i),tpel(i),coord(i))
      diff(i)=(tpel(i)-(fixtem(i)-troom))/(fixtem(i)
&      -troom)*1.5d0
      magn=magn*(1-diff(i))
      field(i)=magn
      if (i.lt.pty-1) then
        tgas(i+1)=tgas(i)+kuttagas(dy,tgas(i),tpel(i))
      endif
    2 continue
  3 continue
  time=time+dt
  do 5 i=0,pty-1
    tetam(i)=tpel(i)
  5 continue

c.....Print the temperatures on the screen and in
c.....the files "tgas" and "tpel"
  do 6 i=1,5
    tpel1(i)=tpel(writ(i))
    tgas1(i)=tgas(writ(i))
  6 continue
  write(6,7) tgas1
  7 format (5(1x,F5.1),2x,F5.2)
  write(6,7) tpel1,time
  write(6,8)
  8 format(/)
  open(unit=15,file='tgas')
  write(15,*) tgas(40)
  open(unit=16,file='tpel')
  write(16,*) tpel(40)

  4 continue

c.....Save the pellets temperature profile in the "flow" file
c.....as well as the electrical field

```

```
do 9 i=0,pty-1
open(unit=17,file='flow')
write(17,*) field(i),tpel(i),tgas(i),tpel(i)-tgas(i)
9 continue

end
```

B.4.3 Version Three

This version does the same things as the previous versions, and also determines the temperature profile in a pellet for any location and at any time.

```
c-----
      SUBROUTINE tridag(a,b,c,r,u,n)
c..Thomas algorithm for solution of tridiagonal systems
c from Numerical Recipies in Fortran 77 [ref]
      INTEGER n,NMAX
      double precision a(n),b(n),c(n),r(n),u(n)
      PARAMETER (NMAX=500)
      INTEGER j
      REAL bet,gam(NMAX)
      if(b(1).eq.0.)pause 'tridag: rewrite equations'
      bet=b(1)
      u(1)=r(1)/bet
      do 11 j=2,n
         gam(j)=c(j-1)/bet
         bet=b(j)-a(j)*gam(j)
         if(bet.eq.0.)pause 'tridag failed'
         u(j)=(r(j)-a(j)*u(j-1))/bet
11      continue
      do 12 j=n-1,1,-1
         u(j)=u(j)-gam(j+1)*u(j+1)
12      continue
      return
      end

c-----
      subroutine pelletcoordi(nb,r,dr)
c.....calculates the coordinates inside a pellet

c.....pty1: number of nodes along the axial direction
c.....y: dimensionless coordinates of the nodes
c.....dy: dimensionless space between two consecutives nodes

      implicit double precision(a-h,o-y)
      integer pty
      double precision r(0:nb-1),dr

      common/Block3/diamereac,diamepar,emf,epsilon,
&fl,velocity,rhoal,troom

      r(0)=0.0d0
      dr=diamepar/(2.0d0*(nb-1))
      do 1 i=1,nb-1
         r(i)=r(i-1)+dr
1      continue

      open(unit=25,file='pelletcoord')
      write (25,*) r,dr
```

```

rewind 25
end

c-----
      subroutine pelletdistribution(dist,LocaDist,TimeDist,nb)
c.....calculates the temperature distribution inside a pellet at any
c.....location and at any time

      implicit double precision(a-h,o-y)
      complex zepm
      double precision coord(0:40)
      double precision mat(0:20,0:20),AA(0:20,1)
      double precision a(21),b(21),c(21),u(21),R(21)
      double precision q(0:20), qp(0:20),radius(0:20)
      double precision dist(0:20),Tprev(0:20)
      double precision kmm(0:20),kmp(0:20),rmm(0:20),rmp(0:20)
      double precision magn,LocaDist

      common/Block3/ diamereac,diamepar,emf,epsilon,
&fl,velocity,rhoal,troom
      common/Block4/ freq,epsi0,pi,magn,ivar

      nb=21

      call pelletcoordi(nb,radius,dr)
      open(unit=25,file='pelletcoord')
      read(25,*) radius,dr
      rewind 25

      do 1 i=0,nb-1
        Tprev(i)=0.0d0
1      continue

      rewind 26
      open(unit=26,file='pelldistfile')
      read(26,*) prevtime,Tout,tpel
2      open(unit=26,file='pelldistfile')
      read(26,*) acttime,Tout,tpel
c.....initialization
      do 3 i=0,nb-1
        dist(i)=tpel
3      continue

      do 4 k=1,4

c.....initialization
      do 5 i=0,nb-1
        kmp(i)=0.0d0
        kmm(i)=0.0d0
        rmm(i)=0.0d0
        rmp(i)=0.0d0
        AA(i,1)=0.0d0

```

```

        do 6 j=0,nb-1
            mat(i,j)=0.0d0
6         continue
5     continue

    dtime=acttime-prevtime

c.....There are three types of nodes in the modeling of the temperature
c.....inside a pellet: the central node, at r=0, at which a symmetry is
c.....observed, the exterior node, that is in contact with the outer gas
c.....and the interior nodes, the remaining ones between the center and
c.....the boundary.

c.....interior nodes
    do 7 i=1,nb-2
        qp(i)=freq*epsi0*abs(aimag(zepm(dist(i)+troom)))
&(2.0d+0)*pi*(magn)**2
        if (ivar.eq.1) then
            var=exp(-LocaDist**1.08)
        else
            var=1.0d0
        endif
        q(i)=qp(i)*var
        kmm(i)=(conducso(dist(i-1)+troom)+conducso(dist(i)+troom))/2.0d0
        kmp(i)=(conducso(dist(i+1)+troom)+conducso(dist(i)+troom))/2.0d0
        rmm(i)=radius(i)-dr/2.0d0
        rmp(i)=radius(i)+dr/2.0d0
        mat(i,i-1)=-((kmm(i)*rmm(i)**2)/dr
        mat(i,i)=rhoal*capaso(dist(i)+troom)*(rmp(i)**3-rmm(i)**3)/
&(3.0*dtime)+(kmm(i)*rmm(i)**2+kmp(i)*rmp(i)**2)/dr
        mat(i,i+1)=-((kmp(i)*rmp(i)**2)/dr
        AA(i,1)=(rmp(i)**3-rmm(i)**3)*q(i)/3.0d0
&+Tprev(i)*rhoal*capaso(dist(i)+troom)*(rmp(i)**3-rmm(i)**3)
&/((3.0d0*dtime)
7     continue

c.....central node
    rmm(0)=radius(0)-dr/2.0d0
    rmp(0)=radius(0)+dr/2.0d0
    kmp(0)=(conducso(dist(1)+troom)+conducso(dist(0)+troom))/2.0d0
    qp(0)=freq*epsi0*abs(aimag(zepm(dist(0)+troom)))*(2.0d+0)*pi*
&(magn)**2
    if (ivar.eq.1) then
        var=exp(-LocaDist**1.08)
    else
        var=1.0d0
    endif
    q(0)=qp(0)*var
    mat(0,0)=1.0d0
c     mat(0,0)=rhoal*capaso(dist(0)+troom)/dtime+6.0d0*kmp(0)/dr**2
c     mat(0,1)=-6.0d0*kmp(dist(0)+troom)/dr**2
    mat(0,1)=-1.0d0
c     AA(0,1)=q(0)+rhoal*capaso(dist(0)+troom)*Tprev(0)/dtime

```

```

AA(0,1)=0.0d0

c.....exterior node
rmm(nb-1)=radius(nb-1)-dr/2.0d0
rmp(nb-1)=radius(nb-1)+dr/2.0d0
kmm(nb-1)=(conducso(dist(nb-1)+troom)+conducso(dist(nb-2)
&troom))/2.0d0
qp(nb-1)=freq*epsi0*abs(aimag(zepm(dist(nb-1)+troom)))
&*(2.0d+0)*pi*(magn)**2
if (ivar.eq.1) then
  var=exp(-LocaDist**1.08)
else
  var=1.0d0
endif

c.....Uncomment to use the other BC method (Par. 3.4)
c   q(nb-1)=qp(nb-1)*var
c   mat(nb-1,nb-1)=rhoal*capaso(dist(nb-1)+troom)*(radius(nb-1)**3-
c   &rmm(nb-1)**3)/(3.0*dtime)+h(Tout+troom)*radius(nb-1)**2
c   &kmm(nb-1)*rmm(nb-1)**2/dr
c   mat(nb-1,nb-2)=-kmm(nb-1)*rmm(nb-1)**2/dr
c   AA(nb-1,1)=q(nb-1)*(radius(nb-1)**3-rmm(nb-1)**3)/3.0d0+
c   &(Tout*radius(nb-1)**2*h(Tout+troom))+rhoal
c   &*capaso(dist(nb-1)+troom)*(radius(nb-1)**3-rmm(nb-1)**3)
c   &*Tprev(nb-1)/(3.0*dtime)
c.....Comment the two next statements to use the above BC method.
mat(nb-1,nb-1)=1.0d0
AA(nb-1,1)=tpel

c.....adaptation to solving subroutines
do 8 i=1,nb
  R(i)=AA(i-1,1)
8  continue

do 9 i=1,nb
  b(i)=mat(i-1,i-1)
10 continue

a(1)=0.0d0
c(nb)=0.0d0
do 11 i=1,nb-1
  a(i+1)=mat(i,i-1)
  c(i)=mat(i-1,i)
11 continue

call tridag(a,b,c,R,u,nb)

do 12 i=0,nb-1
  dist(i)=u(i+1)
12 continue
4  continue
do 13 i=0,nb-1
  Tprev(i)=dist(i)

```

```

13  continue
    if (acttime.eq.TimeDist) then
    do 14 i=0,nb-1
        open(unit=27,file='pellettemperature')
        write(27,*) radius(i),dist(i)
14  continue

    go to 15
    else
    prevtime=acttime
    go to 2
    endif

15  rewind 27
    rewind 26
    return
    end

```

```

c-----
    subroutine fielddeter(pty,field)
c.....determines the electrical field

    implicit double precision (a-h,o-y)

    double precision fixtem(0:40),diff(0:40),tgas(0:40)
    double precision tpel(0:40),tetam(0:40),test1(0:40)
    double precision field(0:40),coord(0:40)
    double precision kuttagas,kuttasolid,magn
    double precision tpel1(5),tgas1(5)
    integer writ(5),decision,pty
    character*16 parameter
    character*1 kind

    common/Block4/ freq,epsi0,pi,magn,ivar

    data writ/0,10,20,30,40/

    epsi0=8.8542d-12
    pi=3.1415965352d+0
    ee=1.0d-6

    rewind 14
    rewind 15
    rewind 16
    rewind 17
    rewind 18
    rewind 19

c.....Read the parameters from the "parameters" file
    open(unit=18,file='parameters')
        read(18,*)parameter,ial
        read(18,*)parameter,imix
        read(18,*)parameter,ipt

```



```

read(18,*)parameter,ipulse
read(18,*)parameter,ivar
read(18,*)parameter,inner
read(18,*)parameter,troom
read(18,*)parameter,tpulse
read(18,*)parameter,periode
read(18,*)parameter,dt
read(18,*)parameter,numbersteps
read(18,*)parameter,frac
read(18,*)parameter,freq
read(18,*)parameter,emf
read(18,*)parameter,epsilon
read(18,*)parameter,tshell
read(18,*)parameter,dpt
read(18,*)parameter,rhopt
read(18,*)parameter,fpt
read(18,*)parameter,magn
read(18,*)parameter,diamereac
read(18,*)parameter,diamepar
read(18,*)parameter,velocity
read(18,*)parameter,rhoal

sapel=4*(diamepar/2.0)**2*pi
volpel=pi*4.0/3.0*(diamepar/2.0)**3
tpulse1=tpulse/periode

open(unit=14,file='filecoordinates')
read(14,*)coord,dy

do 20 i=0,pty-1
    tetam(i)=0.0d+0
    tgas(i)=0.0d+0
    tpel(i)=0.0d+0
20 continue

1  write(6,*) 'What kind of temperature distribution '
   write(6,*) 'do you want for the pellets'
   write(6,*) '(constant(1), linear(2), polynomial(3))?'
   read (5,*) kind
   if ((kind.eq.'1').or.(kind.eq.'2').or.(kind.eq.'3')) then
       write(6,2)
2   format(/'Steady-state solid temperature at x=0')
       read(5,*) t0
       do 3 i=0,pty-1
           fixtem(i)=t0
3   continue
       if ((kind.eq.'2').or.(kind.eq.'3')) then
           write(6,4)
4   format(/'Steady-state solid temperature at x=1')
           read(5,*) tf
           do 5 i=0,pty-1
               fixtem(i)=t0+(tf-t0)*coord(i)
5   continue

```

```

        if (kind.eq.'3')then
            do 6 i=0,pty-1
                fixtem(i)=0.0d0
                fixtem(i)=t0+2*(tf-t0)*coord(i)+
        &         (t0-tf)*(coord(i))**2
6         continue
            endif
        endif
    else
        go to 1
    endif

    write(6,*) 'Give the "time" step, please'
    write(6,*) '(!: No physical meaning)'
    read (5,*) dt
c.....Temperatures desired

    time=0.0d+0
    do 7 i=0,pty-1
        field(i)=magn
7    continue

    decision=1

8    if (decision.eq.1) then
        time=time+dt
c        magn=field(0)
        do 10 j=1,inner
            do 9 i=0,pty-1
                magn=field(i)-30
                tpel(i)=tetam(i)+kuttasolid(ipulse,time,dt,
        &         tgas(i),tpel(i),coord(i))
                diff(i)=(tpel(i)-(fixtem(i)-troom))/(fixtem(i)
        &         -troom)*1.5d0
                magn=magn*(1-diff(i))
                field(i)=magn
                if (i.lt.pty-1) then
                    tgas(i+1)=tgas(i)+kuttagas(dy,tgas(i),tpel(i))
                endif
9            continue
10        continue
            decision=0
            do 11 i=0,pty-1
                test1(i)=(tpel(i)-tetam(i))/tpel(i)
                if (abs(test1(i)).gt.1.0d-6) then
                    decision=1
                    numbersteps=numbersteps+1
                endif
11        continue
            if (decision.eq.0) then
                write(6,*) 'The electric field has been'
                write(6,*) 'determined'
                open(unit=19,file='electricfield')

```

```

        write(19,*) field
        return
    endif
do 12 i=0,pty-1
    tetam(i)=tpel(i)
12    continue
do 13 i=1,5
    tpel1(i)=tpel(writ(i))
    tgas1(i)=tgas(writ(i))
13    continue
    write(6,14) tgas1
14    format (5(1x,F5.1),2x,F5.2)
    write(6,14) tpel1,time
    write(6,14)
15    format(/)
    if((time-int(time+ee)).lt.(1.0d-4)) then
        write(6,*) time
    endif
endif

go to 8

do 16 i=0,pty-1
    open(unit=17,file='flow3')
    write(17,*) i,tpel(i),tgas(i),tpel(i)-tgas(i)
16    continue
do 17 i=0,pty-1
    tetam(i)=0.0d+0
    tgas(i)=0.0d+0
    tpel(i)=0.0d+0
17    continue
    rewind 7
end

```

```

c-----
    subroutine profiletemp(pty,mode,steady,tgas,tpel,time,
        &TempDist,TimeDist,LocaDist)
c.....determines the temperature distribution as a function of time for
c.....any time and any given location

```

```

    implicit double precision(a-h,o-y)

```

```

    double precision tgas1(5),tpel1(5),field(0:40)
    double precision tgas(0:40),tpel(0:40),tetam(0:40)
    double precision test1(0:40),coord(0:40)
    double precision magn,markgas,markpel,interloc,LocaDist
    double precision markgasbis,markpelbis,kuttagas,kuttasolid
    integer writ(5),pty,decision,step
    character*1 steady,TempDist,mode
    character*16 parameter

```

```

    common/Block1/ dt,numbersteps,inner
    common/Block2/ frac

```

```
common/Block3/ diamereac,diamepar,emf,epsilon,  
&fl,velocity,rhoal,troom  
common/Block4/ freq,epsi0,pi,magn,ivar  
common/Block5/ dpt,cppt,rhopt,fpt  
common/Block6/ tshell,sapel,volpel  
common/Block8/ ial,imix,ipt  
common/Block9/ tpulse,periode,tpulse1
```

```
data writ/0,10,20,30,40/
```

```
epsi0=8.8542d-12  
pi=3.1415965352d+0  
ee=1.0d-6
```

```
rewind 14  
rewind 15  
rewind 16  
rewind 17  
rewind 18  
rewind 19
```

```
c.....Read the parameters from the "parameters" file
```

```
open(unit=18,file='parameters')  
  read(18,*)parameter,ial  
  read(18,*)parameter,imix  
  read(18,*)parameter,ipt  
  read(18,*)parameter,ipulse  
  read(18,*)parameter,ivar  
  read(18,*)parameter,inner  
  read(18,*)parameter,troom  
  read(18,*)parameter,tpulse  
  read(18,*)parameter,periode  
  read(18,*)parameter,dt  
  read(18,*)parameter,numbersteps  
  read(18,*)parameter,frac  
  read(18,*)parameter,freq  
  read(18,*)parameter,emf  
  read(18,*)parameter,epsilon  
  read(18,*)parameter,tshell  
  read(18,*)parameter,dpt  
  read(18,*)parameter,rhopt  
  read(18,*)parameter,fpt  
  read(18,*)parameter,magn  
  read(18,*)parameter,diamereac  
  read(18,*)parameter,diamepar  
  read(18,*)parameter,velocity  
  read(18,*)parameter,rhoal  
  read(18,*)parameter,fl
```

```
sapel=4*(diamepar/2.0)**2*pi  
volpel=pi*4.0/3.0*(diamepar/2.0)**3  
tpulse1=tpulse/periode
```

```

write(6,21)

1  write(6,*) 'Choose the time step (advice:0.1 sec):'
   read(5,*) dt
   write(6,*)
2  write(6,*) 'Do you want to reach the steady-state'
   write(6,*) '(The steady-state is said to be reached'
   write(6,*) 'when the temperature increase at any'
   write(6,*) 'point is less than 0.1%)?'
   read(5,*) steady

   if ((steady.eq.'y').or.(steady.eq.'Y')) then
       go to 3
   else if ((steady.eq.'n').or.(steady.eq.'N')) then
       write(6,*) 'Number of steps:'
       read(5,*) numbersteps
       write(6,*) 'The transient temperature distribution'
       write(6,*) 'will be stopped after '
       write(6,*) numbersteps*dt,'sec'
       timelimit=numbersteps*dt
       go to 3
   else
       go to 2
   endif

3  write(6,21)
   write(6,*) 'Do you want the temperature distribution'
   write(6,*) 'inside a pellet?'
   read(5,*) TempDist

   if ((TempDist.eq.'y').or.(TempDist.eq.'Y')) then
       write(6,*) 'At what time'
       read(5,*) TimeDist
       write(6,*) 'At what location'
       read(5,*) LocaDist
   endif

4  rewind 7
   rewind 15
   rewind 16
   rewind 17

   do 5 i=0,pty-1
       tetam(i)=0.0d+0
       tgas(i)=0.0d+0
       tpel(i)=0.0d+0
5  continue

   do 6 i=1,5
       tpel1(i)=tpel(writ(i))
       tgas1(i)=tgas(writ(i))
6  continue

```

```

time=0.0d+0
open(unit=15,file='gastemperature')
write(15,*) tgas
open(unit=16,file='pellettemperature')
write(16,*) tpel

c....Load the electric field for the case where the user wants the temperature
c....evolution of z-modified electric field
  if (mode.eq.'2') then
    rewind 19
    open(unit=19,file='electricfield')
    read(19,*) field
    else
    do 7 i=0,pty-1
      field(i)=abs(magn)
7      continue
    endif

    decision=1
    step=0

    call coordi(pty,dy)
    open(unit=14,file='filecoordinates')
    read(14,*)coord,dy

    do 8 i=0,pty-1
      if ((coord(i).le.LocaDist).and.(coord(i+1).gt.LocaDist)) then
        x1=coord(i)
        x2=coord(i+1)
      endif
8      continue
      interloc=(LocaDist-x1)/(x2-x1)

      time=0.0d0
      do 9 i=0,numbersteps
        if ((time.le.TimeDist).and.(time+dt.gt.TimeDist)) then
          ti1=time
          ti2=time+dt
          endif
          time=time+dt
9          continue
          intertime=(TimeDist-ti1)/(ti2-ti1)
          time=0.0d0
          rewind 26

10         if ((decision.eq.1).or.(step.lt.numbersteps)) then

c....'localize' the point where the temperature distribution inside
c....a pellet should be done
          if ((TempDist.eq.'y').or.(TempDist.eq.'Y')) then
            if (time.lt.TimeDist) then
              if (LocaDist.eq.1.0) then
                open(unit=26,file='pelldistfile')

```

```

        write(26,*) time,tgas(pty-1),tpel(pty-1)
        go to 12
    endif
    do 11 i=0,40
        x=coord(i)
        if ((x.le.LocaDist).and.(x+dy-ee.gt.LocaDist)) then
            markgas=(tgas(i+1)-tgas(i))*interloc+tgas(i)
            markpel=(tpel(i+1)-tpel(i))*interloc+tpel(i)
            open(unit=26,file='pelldistfile')
            write(26,*) time,markgas,markpel
        endif
11        continue
    endif
endif
c....End "localization"

12        time=time+dt

c....Determines the temperature distribution in the bed
        do 14 j=1,inner
            do 15 i=0,pty-1
                magn=field(i)
                tpel(i)=tetam(i)+kuttasolid(ipulse,time,dt,
&                tgas(i),tpel(i),coord(i))
                if (i.lt.pty-1) then
                    tgas(i+1)=tgas(i)+kuttagas(dy,tgas(i),tpel(i))
                endif
15                continue
14                continue
c....End temperature determination

c.....Pick up the datas necessary for the temperature distribution
c.....within a pellet
        if ((TimeDist.gt.time-ee).and.(TimeDist.lt.time+ee)) then
            if (LocaDist.gt.1.0-ee) then
                open(unit=26,file='pelldistfile')
                write(26,*) time,tgas(pty-1),tpel(pty-1)
            endif
        endif
        if ((time.gt.TimeDist).and.(time-dt.le.TimeDist)) then
            do 16 i=0,40
                x=coord(i)
                if ((x.le.LocaDist).and.(x+dy-ee.gt.LocaDist)) then
                    markgasbis=(tgas(i+1)-tgas(i))*interloc+tgas(i)
                    markpelbis=(tpel(i+1)-tpel(i))*interloc+tpel(i)
                    markgas=(markgasbis-markgas)*intertime+markgas
                    markpel=(markpelbis-markpel)*intertime+markpel
                    open(unit=26,file='pelldistfile')
                    write(26,*) TimeDist,markgas,markpel
                endif
16                continue
            endif
c.....End "pick up"

```

```

        decision=0

c....Determines if steady-state is reached
        if ((steady.eq.'y').or.(steady.eq.'Y')) then
        do 17 i=0,pty-1
        test1(i)=(tpel(i)-tetam(i))/tpel(i)
        if (abs(test1(i)).gt.(1.0d-6)) then
        decision=1
        endif
17      continue
        if (decision.eq.0) then
        return
        endif
        endif
c....End "steady-state"

c....Prepares the next iteration; print some datas on the screen
        do 18 i=0,pty-1
        tetam(i)=tpel(i)
18      continue
        do 19 i=1,5
        tpel1(i)=tpel(writ(i))
        tgas1(i)=tgas(writ(i))
19      continue

c....Uncomment to check the calculation
c          write(6,106) tgas1
c          write(6,106) tpel1,time
c 106      format(1x,5(F10.3,2x),2x,F5.2)
c          write(6,107)
c 107      format (/)

        open(unit=15,file='gastemperature')
        write(15,*) tgas
        open(unit=16,file='pellettemperature')
        write(16,*) tpel
        if ((steady.eq.'y').or.(steady.eq.'Y')) then
        numbersteps=numbersteps+1
        endif

        if((time-int(time+ee)).lt.(1.0d-4)) then
        write(6,*) time
        endif
        step=step+1
    else
        return
    endif
    go to 10

c....Saves the temperature profile
        do 20 i=0,pty-1
        open(unit=17,file='temperatureevolution')

```



```

        write(17,*) tpel(i),tgas(i),tpel(i)-tgas(i)
20    continue
        write(6,21)
21    format(/)
        rewind 7
        end

```

```

c-----
        program model
c.....the program is set up to calculate the gas and pellet temperature

```

```

        implicit double precision(a-h,o-z)
        double precision coord(0:40),tpel(0:40)
        double precision tetam(0:40),tgas(0:40)
        double precision diff(0:40),field(0:40)
        double precision fixtem(0:40)
        double precision test1(0:40)
        double precision magn,pty1
        double precision kuttagas,kuttasolid
        double precision tgas1(14),tpel1(14)
        integer pty,vpulse,writ(5),decision,step
        double precision r(0:32),a(0:32,1)
        double precision fl,ee,t0,tf,x
        double precision LocaDist,TimeDist
        double precision radius(0:19),dist(0:19)
c.....interpolations variables
        double precision inter1,inter2,inter3
        double precision markgasloc1,markgasloc2
        double precision markgasloc3,markgasloc4
        double precision markpelloc1,markpelloc2
        double precision markpelloc3,markpelloc4
        double precision markgas1,markgas2,markpel1
        double precision markpel2,markgas,markpel
        double precision markgasbis,markpelbis
        double precision intertime,interloc
        character*1 mode,transient,steady,kind,run
        character*1 TempDist
        character*5 modif
        character*16 parameter

```

```

c----- dimensions de tgas et tpel: cv1+2

```

```

        common/Block1/ dt,numbersteps,inner
        common/Block2/ frac
        common/Block3/ diamereac,diamepar,emf,epsilon,
&fl,velocity,rhoal,troom
        common/Block4/ freq,epsi0,pi,magn,ivar
        common/Block5/ dpt,cppt,rhopt,fpt
        common/Block6/ tshell,sapel,volpel
        common/Block8/ ial,imix,ipt
        common/Block9/ tpulse,periode,tpulse1

```

```

        data writ/0,10,20,30,40/

```

```

c.....ial=1: alpha alumina
c.....imix=1 : Rayleigh formula
c.....imix=2 : Maxwell-Garnet Theory
c.....ipt=1 : Pt conductivity evaluated a the bulk value
c.....ipt=2 : Pt conductivity compensated for size dependance
c.....ipulse=1 : Electric field is pulsed
c.....ivar=1 : Electric field is modified by means of a function
c.....mode=1: The electric field is already set
c.....mode=2: the electric is to be determined

```

```

epsi0=8.8542d-12
pi=3.1415965352d+0
ee=1.0d-6

```

```

rewind 14
rewind 15
rewind 16
rewind 17
rewind 18
rewind 19

```

```

c.....Read the parameters from the "parameters" file
open(unit=18,file='parameters')

```

```

  read(18,*)parameter,ial
  read(18,*)parameter,imix
  read(18,*)parameter,ipt
  read(18,*)parameter,ipulse
  read(18,*)parameter,ivar
  read(18,*)parameter,inner
  read(18,*)parameter,troom
  read(18,*)parameter,tpulse
  read(18,*)parameter,periode
  read(18,*)parameter,dt
  read(18,*)parameter,numbersteps
  read(18,*)parameter,frac
  read(18,*)parameter,freq
  read(18,*)parameter,emf
  read(18,*)parameter,epsilon
  read(18,*)parameter,tshell
  read(18,*)parameter,dpt
  read(18,*)parameter,rhopt
  read(18,*)parameter,fpt
  read(18,*)parameter,magn
  read(18,*)parameter,diamereac
  read(18,*)parameter,diamepar
  read(18,*)parameter,velocity
  read(18,*)parameter,rhoal
  read(18,*)parameter,fl

```

```

sapel=4*(diamepar/2.0)**2*pi
volpel=pi*4.0/3.0*(diamepar/2.0)**3
tpulse1=tpulse/periode

```

```

c.....Select the modes
1  write(6,*) 'In which mode do you want to work?'
   write(6,*) 'Mode 1: electric field is set'
   write(6,*) 'Mode 2: determination of electric field'
   read(5,*) mode

   if ((mode.ne.'1').and.(mode.ne.'2')) then
     go to 1
   endif

c..... Print the variables used .....
write(6,*) '-----'
write(6,2)
2  format(' ---- Default parameters ----')
   write(6,*) '-----'
   write(6,*) 'Room temperature      (C): ',troom
   write(6,*) 'Bed height          (inch): ',fl/0.0254d0
   write(6,*) 'Inlet gas velocity (m/s): ',velocity
   write(6,*) 'Pellet diameter      (m): ',diamepar
   write(6,*) 'Bed radius          (m): ',diamereac
   write(6,*) 'Electric field      (V/m): ',magn
   if(ipulse.eq.1) then
     write(6,*) 'Duty cycle value      : ',tpulse1
     write(6,*) 'Periode              (sec): ',periode
   endif
   write(6,*) 'Pellets density (kg/m3): ',rhoal
   write(6,*) '-----'

3  if (ial.eq.1) then
     write(6,*) 'Alpha-alumina'
   elseif (ial.eq.2) then
     write(6,*) 'Gamma-alumina'
   else
     go to 3
   endif

4  if (imix.eq.1) then
     write(6,*) 'Rayleigh mixture formula'
   else if (imix.eq.2) then
     write(6,*) 'Maxwell-Garnet theory'
   else
     go to 4
   endif

5  if(ipt.eq.1) then
     write(6,*) 'Bulk conductivity'
   else if (ipt.eq.2) then
     write(6,*) 'Size dependent conductivity'
   else
     go to 5
   endif

6  if(ipulse.eq.1) then
     write(6,*) 'Unsteady electric field'
   else if (ipulse.eq.2) then

```

```

        write(6,*) 'Steady electric field'
        else
            go to 7
        endif
7    if(ivar.eq.1) then
        write(6,*) 'The electric field is modified by '
        write(6,*) 'means of a function'
    endif

    pty=41
    call coordi
    open(unit=14,file='filecoordinates')
    read(14,*)coord,dy

c....Initialization of the temperatures
    t=0.0d+0
    do 8 i=0,pty-1
        tetam(i)=0.0d+0
        tgas(i)=0.0d+0
        tpel(i)=0.0d+0
8    continue

    if (mode.eq.'2') then
        call fielddeter(pty,field)
        write(6,*) field
9    write(6,*) 'Do you want the transient evolution'
        write(6,*) 'of this computed electric field (y/n)'
        read(5,*) transient
        if ((transient.eq.'y').or.(transient.eq.'Y')) then
            go to 10
        else if ((transient.eq.'n').or.(transient.eq.'N')) then
            go to 23
        else
            go to 9
        endif
    else
10    write(6,22)
        call profiletemp(pty,mode,steady,tgas,tpel,time,TempDist,
            &TimeDist,LocaDist)
    endif

c.....The next statements print the results .....

11    if ((steady.eq.'y').or.(steady.eq.'Y')) then
        write(6,*) 'The steady-state has been reached'
        write(6,*) 'after ', time, ' sec.'
        write(6,*) 'The temperature distribution is:'
        go to 14
    endif

12    write(6,13) time
13    format(/'The temperature distribution, at t=',F5.2,'sec, is:')
14    write(6,15)

```

```

15  format(69('-'))
    write(6,16)
16  format('|','Dimensionless coordinates','|',
& 'Gas temperature (C)'
& '|','Solid temperature (C)','|'/'|',25('-'),
& '|',19('-'),'|',21('-'),'|')
    do 18 i=0,pty-1
    write(6,17) coord(i),tgas(i)+troom,tpel(i)+troom
17  format('|',10x,F5.3,10x,'|',7x,F6.2,6x,'|',8x,
& F6.2,7x,'|')
18  continue
    write(6,15)

    if ((TempDist.eq.'y').or.(TempDist.eq.'Y')) then
    write(6,22)
    write(6,*) 'At t=',TimeDist,'sec, the temperature'
    write(6,*) 'distribution inside a pellet'
    write(6,*) 'located at x=',LocaDist,' is:'

    call pelletdistribution(dist,LocaDist,TimeDist,nb)
    write(6,22)
    write(6,21)
21  format(28('-')/'|',' Distance ', '|', ' Solid ',
& '| ' /'|', ' from the ', '|', 'temperature ', '|'/'|',1x,
& 'center (m)',2x,'|',12x,'|',/ 28('-'))
    do 20 i=0,nb-1
    open(unit=27,file='pellettemperature')
    read(27,*) radius(i),dist(i)
    write(6,19) radius(i),dist(i)+troom
19  format('|',2x,F9.7,2x,'|',3x,F6.2,3x,'|')
20  continue
    rewind 27
    endif

    write(6,22)
22  format(/)
    write(6,*) 'Do you want to do another run'
    read(5,*) run

23  if ((run.eq.'y').or.(run.eq.'Y')) then
    go to 1
    else if ((run.eq.'n').or.(run.eq.'N')) then
    go to 24
    else
    go to 23
    endif

24  end

```

Vita

Florent B. Faucher was born on January 1, 1975, in Guérande, (Loire-Atlantique) France. He attended high school in Guérande, where he earned a Baccalauréat C (Mathematics - Physics) in 1992. He entered the Institut Universitaire de Saint-Nazaire, and graduated in 1995 with a degree in Chemical Engineering. He then entered the Université de Technologie de Compiègne (UTC), and through an exchange program with the Virginia Polytechnic Institute and State University (VPI&SU), got simultaneously a Chemical Engineering diploma and a Master of Science in Mechanical Engineering in the fall of 1998.

Permanent Address: 16, rue de la Maisonneuve
44350 Guérande
FRANCE

This thesis was typeset with L^AT_EX 2_ε¹ by the author.

¹L^AT_EX 2_ε is an extension of L^AT_EX. L^AT_EX is a collection of macros for T_EX. T_EX is a trademark of the American Mathematical Society. The macros used in formatting this thesis were written by Greg Walker, Department of Mechanical Engineering, Virginia Tech.